Integrated Photovoltaic and Photothermal Strategies for Continuous Energy Harvesting from Sunlight and Indoor LED Lighting in Buildings

Materials Science and Engineering Conference, July 8, 2026, Boston, MA

Dr. Donglu Shi
The Materials Science and Engineering Program

Dept. of Mechanical and Materials Engineering
College of Engineering and Applied Science
University of Cincinnati

Collaborators

Meher Saketh Gandharapu, Anudeep Katepalli, Thiraj Mohankumar, Sagar Shrestha, Yuxin Wang, Jou Lin, Mengyao Lyu, Brent Webster

The Materials Science and Engineering Program
Dept. Mechanical Materials Industrial Engineering
College of Engineering and Applied Science
University of Cincinnati

Anton Harfmann
College of Design, Architecture, Art and Planning,
University of Cincinnati, Cincinnati, OH 45221, USA

Prof. John Krupczak
Dept. of Engineering,
Hope College

Mathias Bonmarin
Institute of Computational Physics
Zurich University of Applied Science
Switzerland

Outline

- Current critical issues in solar harvesting
- Efficiency limitations in PV energy generation
- Spectral selective solar harvesting via porphyrin and iron oxide compounds
- Photothermal heating with plasmonic nanoparticles
- Transparent thin films for 3D solar harvesting and energy generation
- Photon recycling via indoor LED lights

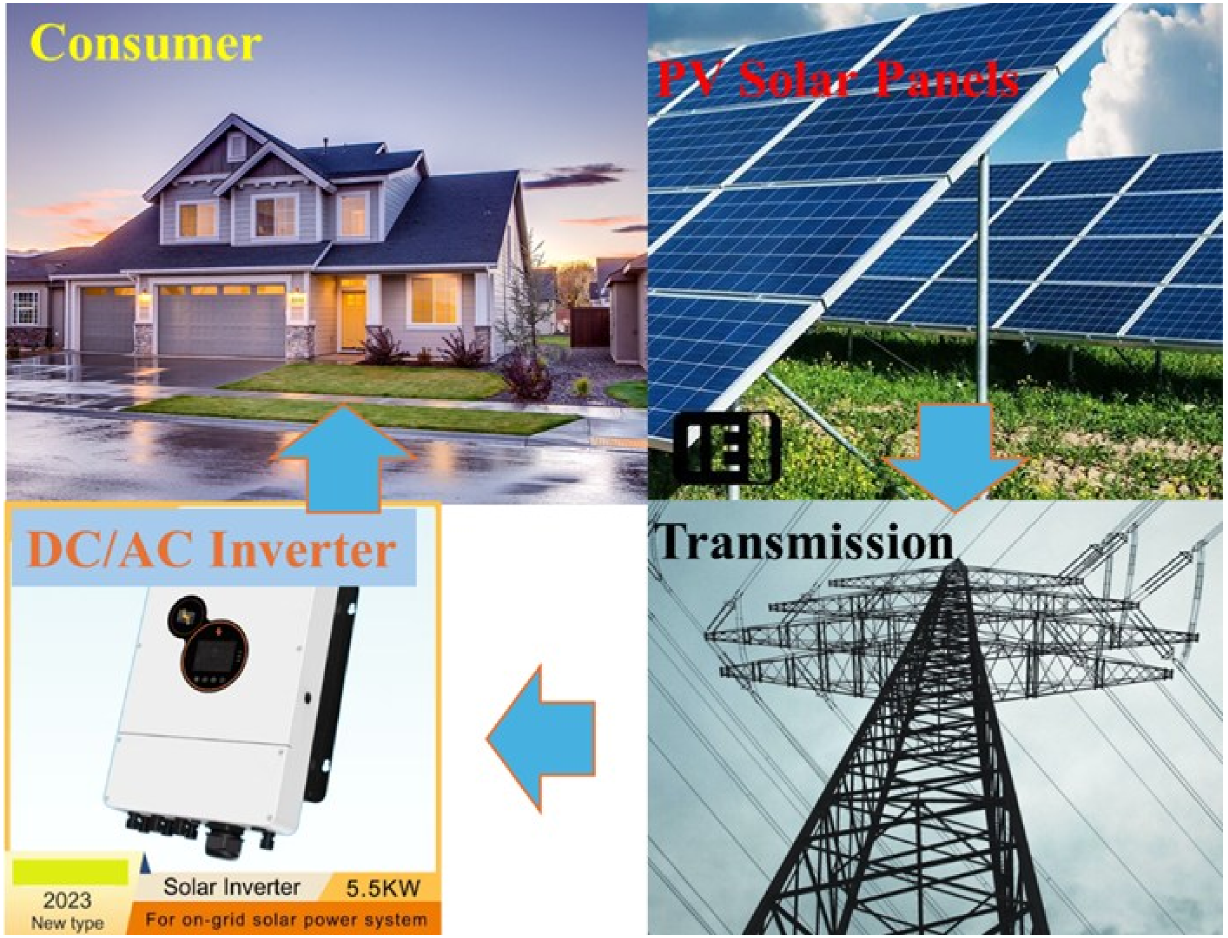

The terms “utility-scale solar” refers to solar power facilities designed to produce electricity at a capacity sufficient to supply many customers rather than a single home or business

Utility-Scale Solar Photovoltaics

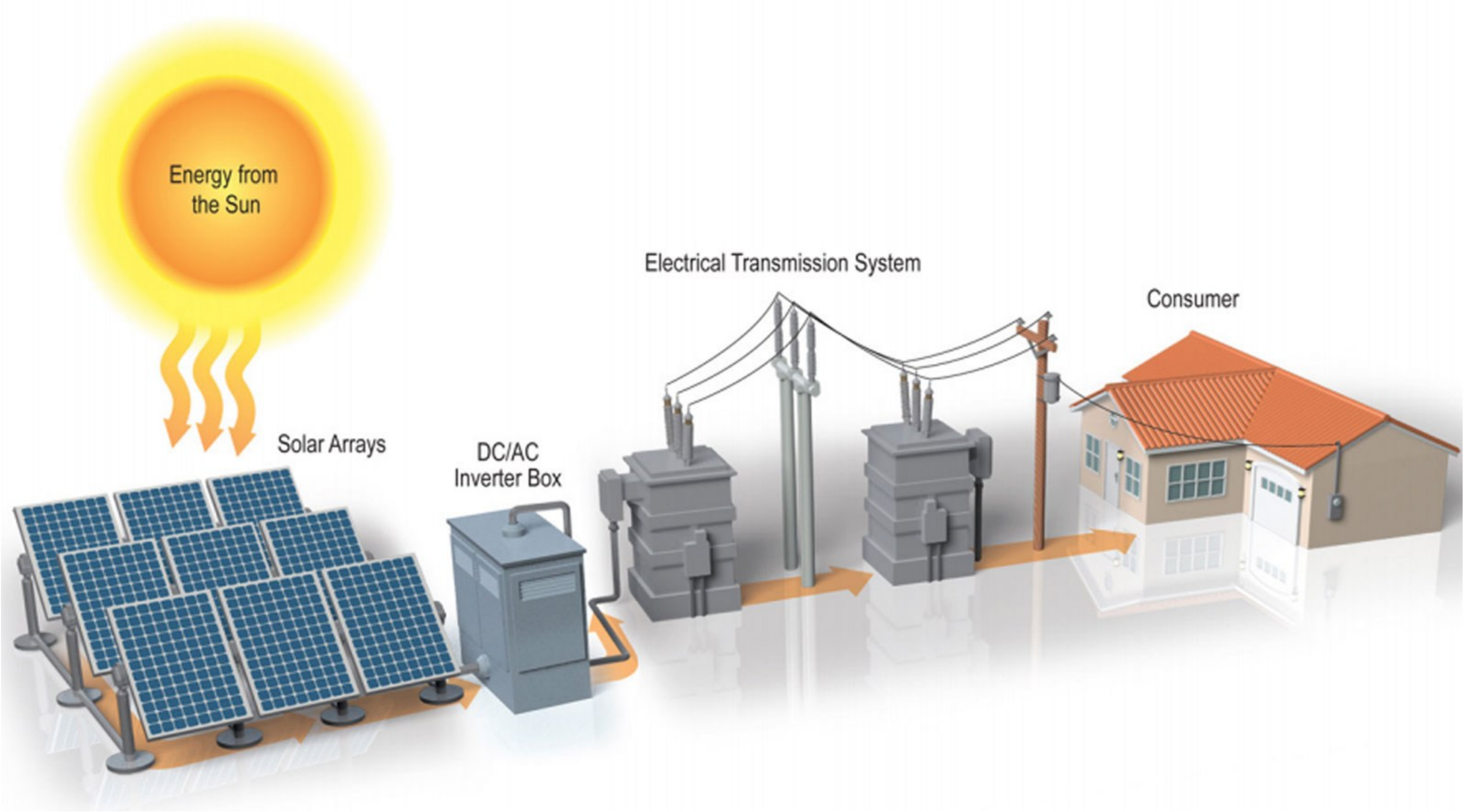

Solar hot water systems

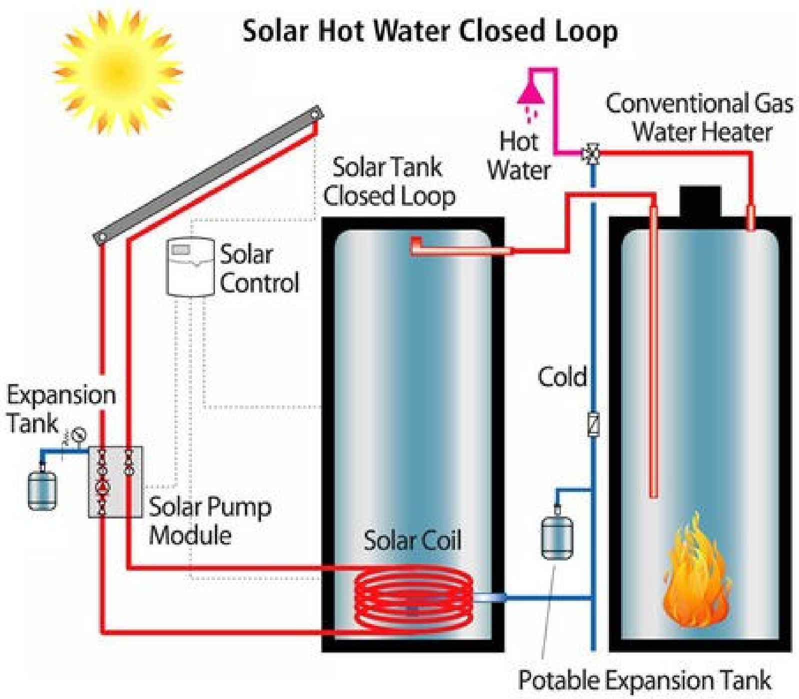

Conventional solar hot water systems are complex due to their reliance on multiple components like pumps, heat exchangers, and controllers, each of which adds to maintenance needs and introduces potential points of failure; pump malfunctions or controller inaccuracies can impact system reliability.

Source	Acre/Megawatts
Coal	12.21
Natural gas	12.41
Nuclear	12.71
Solar	43.50
Wind	70.64

Solar energy is 8 times more expensive than primary energy

Solar harvesting via multiple transparent photothermal films

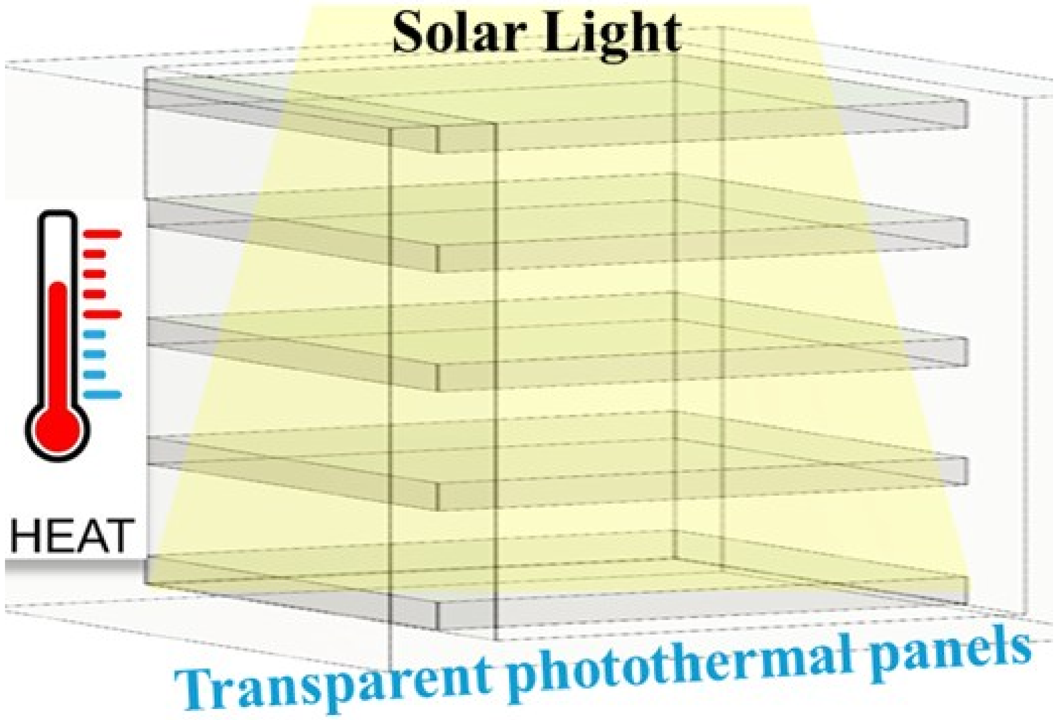

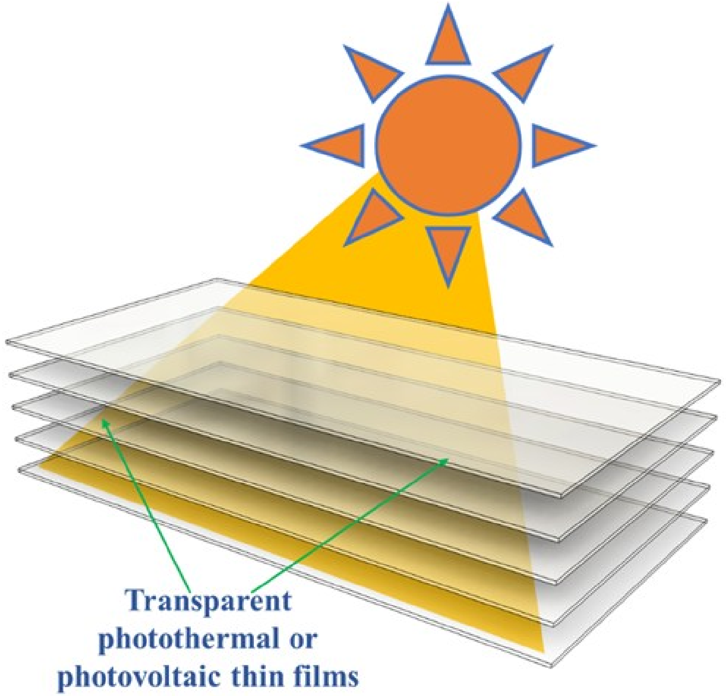

Mengyao Lyu, Jou Lin, John Krupczak, and Donglu Shi, "Solar harvesting through multilayer spectral selective iron oxide and porphyrin transparent thin films for photothermal energy generation," Advanced Sustainable Systems,(2021) https://doi.org/10.1002/adsu.202100006

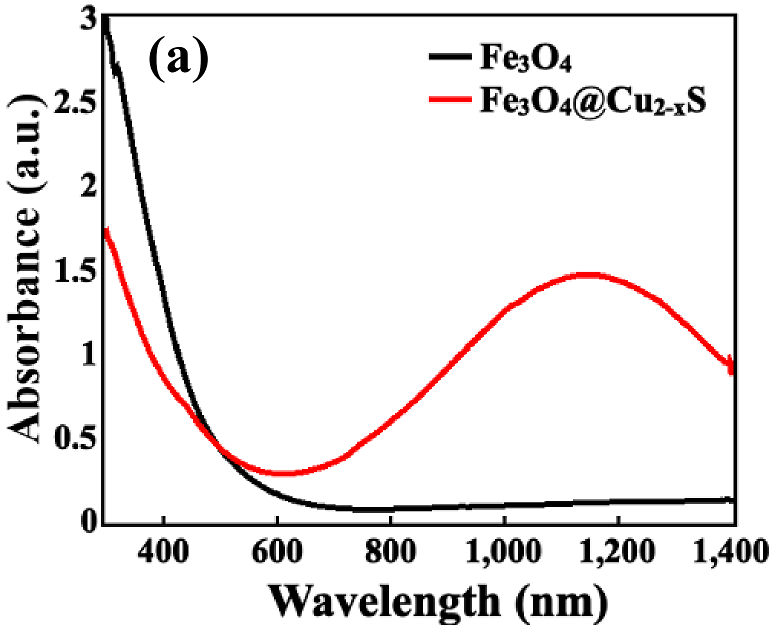

(a)
Fe3O4
Fe3O4@Cu2-xS
Absorbance (a.u.)
Wavelength (nm)
0
0.5
1
1.5
2
2.5
3
400
600
800
1,000
1,200
1,400
(b)
Transparent photothermal panels

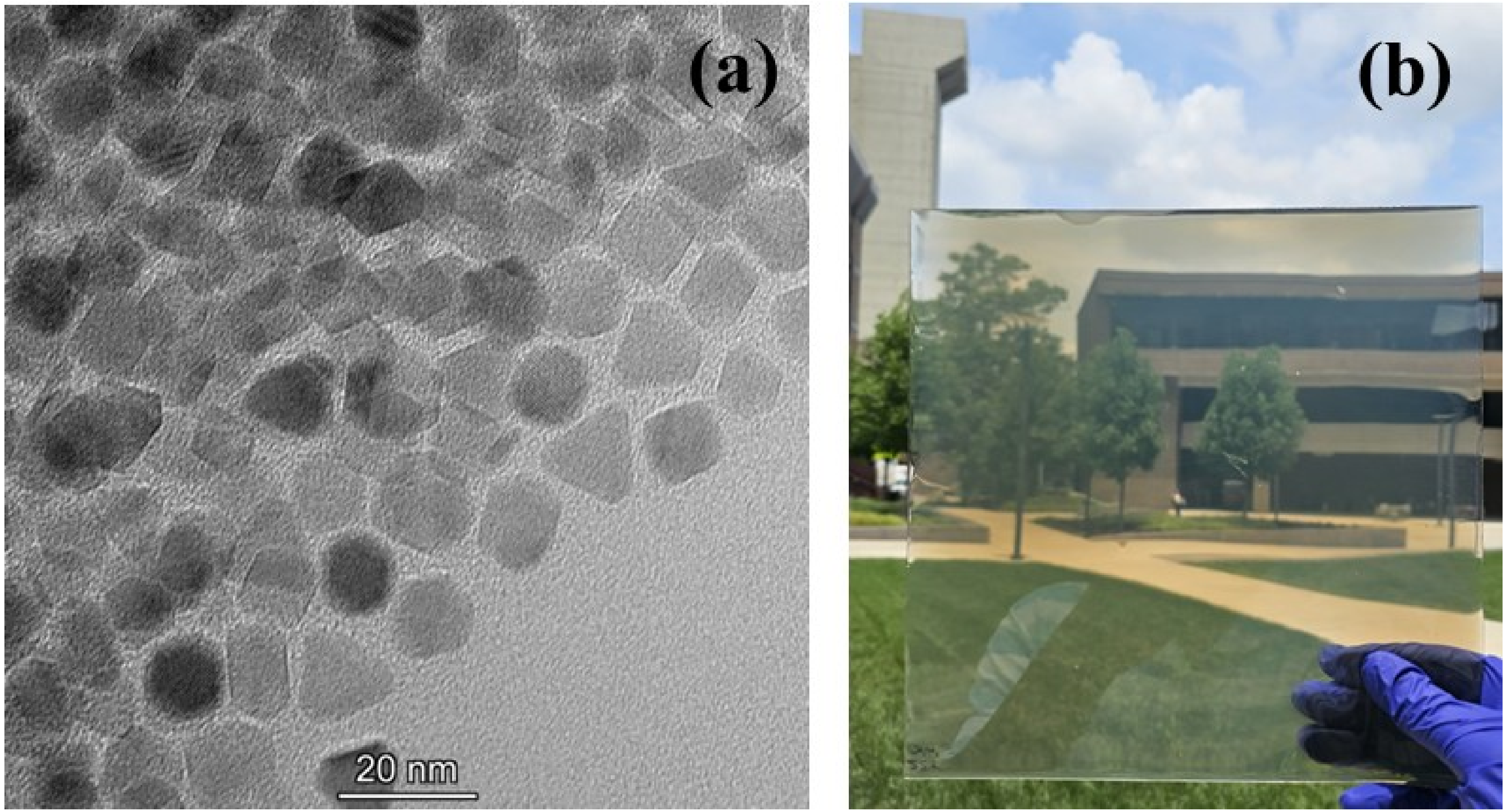

(a) TEM image Fe_3O_4@$Cu_{2-x}S$ nanoparticles and (b) photograph of the Fe_3O_4@$Cu_{2-x}S$ thin film.

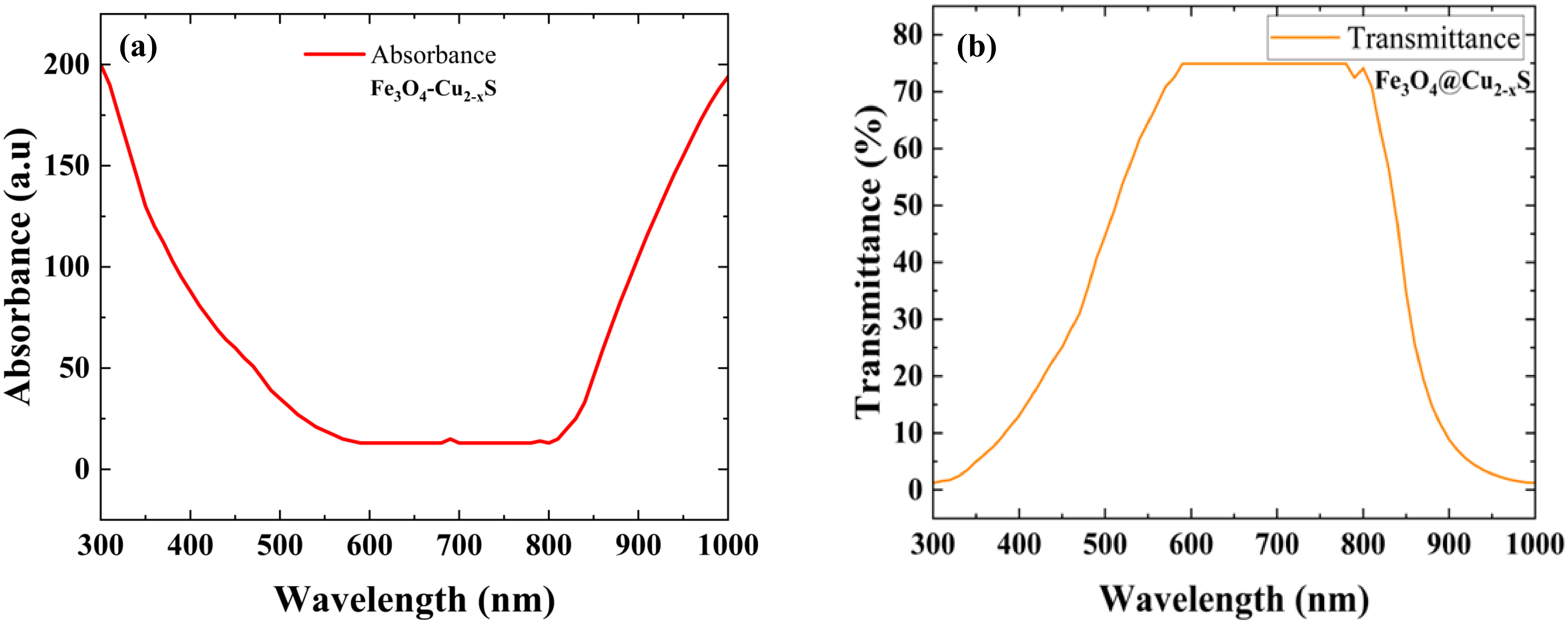

Fig. (a) UV-Vis spectrum of TPGP (b) Transmittance of TPGP

Modulating solar spectrum via porphyrins and iron oxides

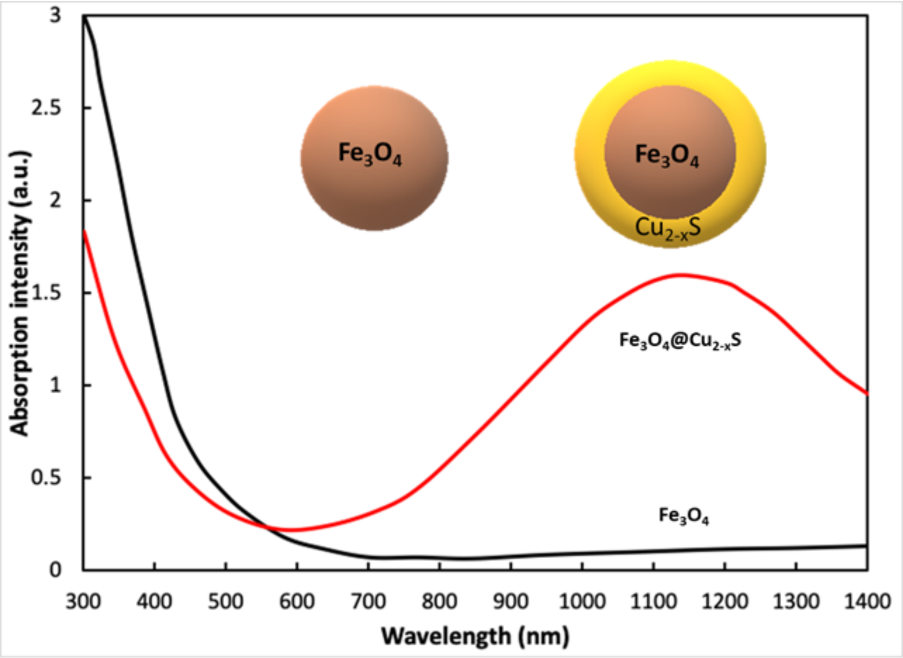

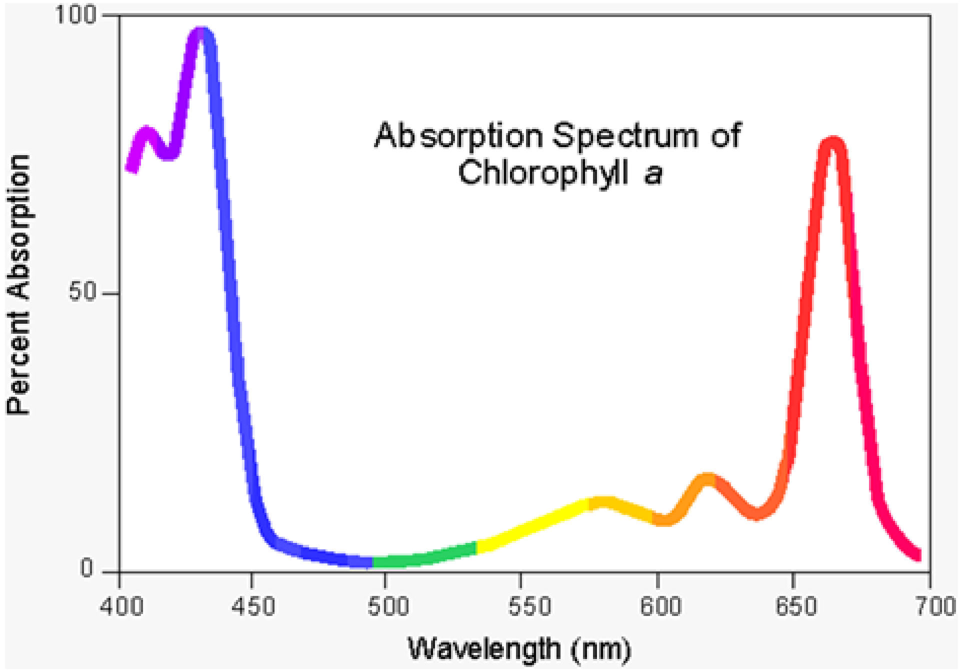

1. Lin, J.; Lyu, M.; Shi, D. 3D Solar Harvesting and Energy Generation via Multilayers of Transparent Porphyrin and Iron Oxide Thin Films. Energies 2023, 16, 3173. https://doi.org/10.3390/en16073173
2. Jou Lin, Yuxin Wang, Mengyao Lyu, Donglu Shi, Transparent porphyrin-based hybrid films for spectral selective solar harvesting and energy generation, Solar Energy Materials and Solar Cells, 243 15 (2022)
3. Jou Lin and Donglu Shi," Photothermal and photovoltaic properties of transparent thin films of porphyrin compounds for energy applications," Applied Physics Reviews, 8, 011302 (2021);
4. Yuan Zhao, Andrew Dunn, Donglu Shi, Effective reduction of building heat loss without insulation materials via the photothermal effect of a chlorophyll thin film coated "Green Window," MRS Communications: doi:10.1557/mrc.2019.52 (2019)

Transparent photothermal thin films

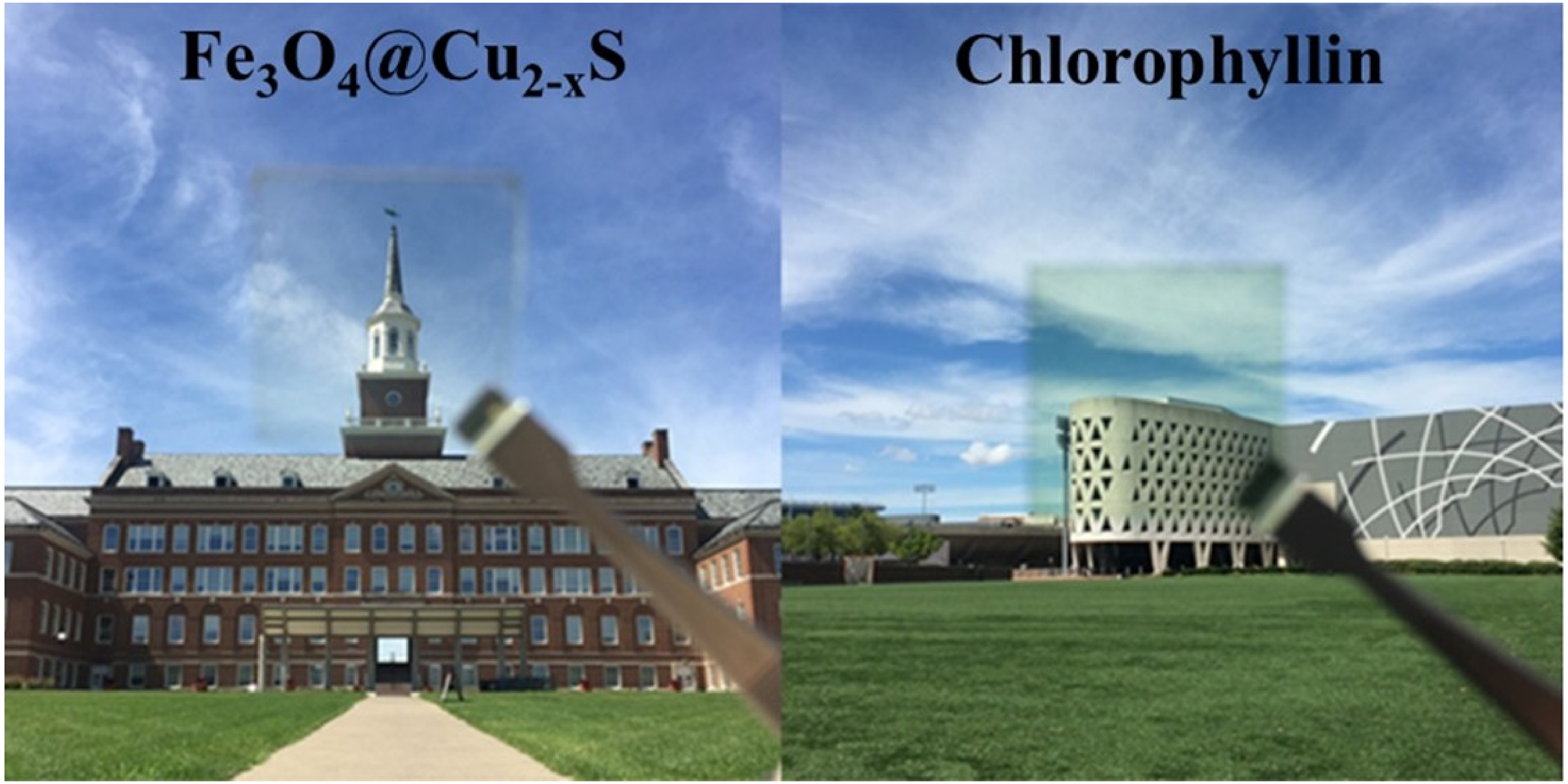

The $Cu_{2-X}S$ nanocrystal has a tunable localized surface plasmon resonance (LSPR) in the NIR region.

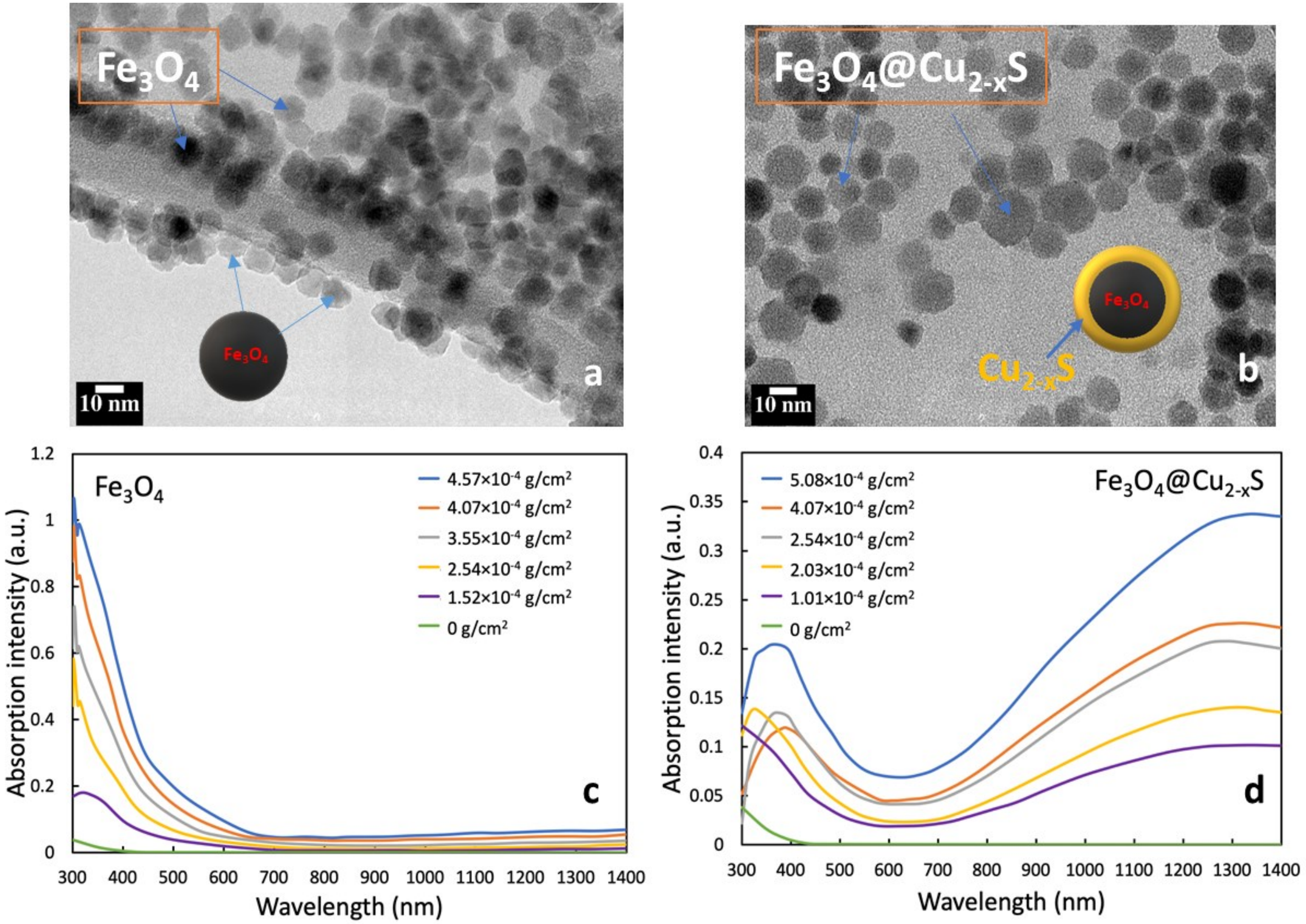

Optical thermal insulation via the photothermal effects of Fe3O4 and Fe3O4@Cu2−xS thin films for energy-efficient single-pane windows, Jou Lin, Yuan Zhao, and Donglu Shi, MRS Communications Volume 10, Issue 1, pp. 155-163 (2020)

Fe_3O_4

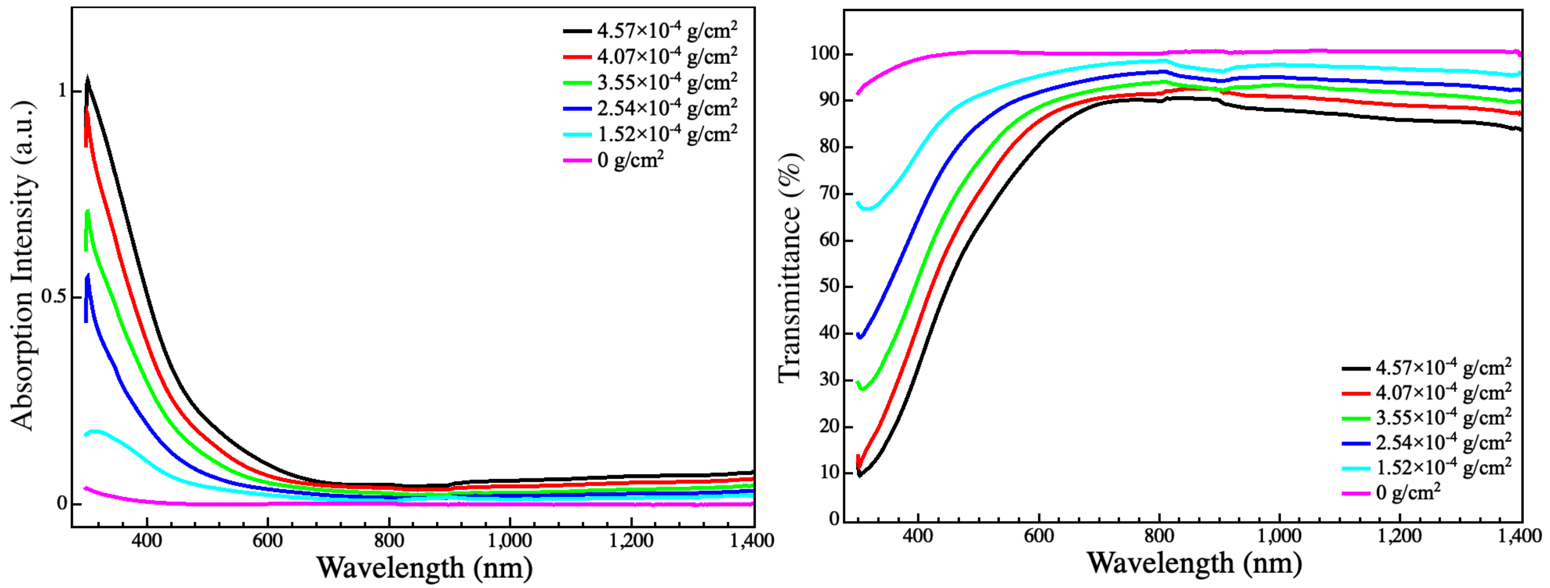

$Fe_3O_4@Cu_{2-x}S$

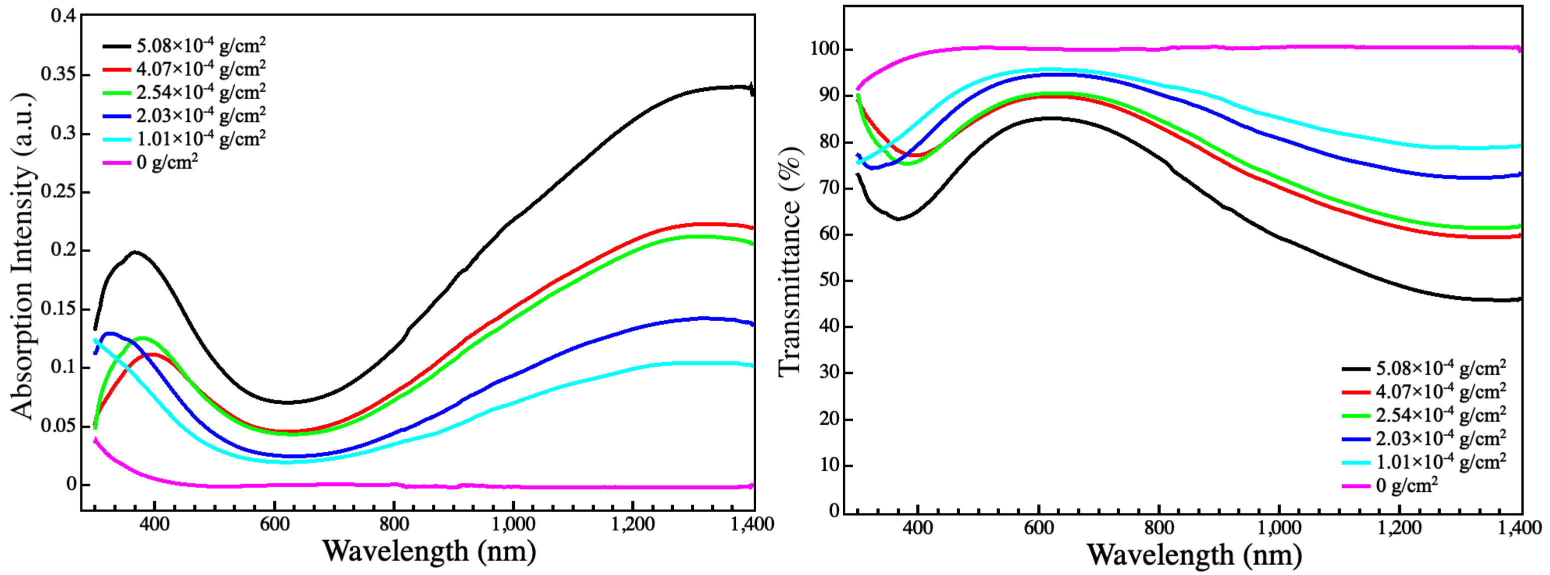

Photothermal Effect of Fe3O4 Nanoparticles

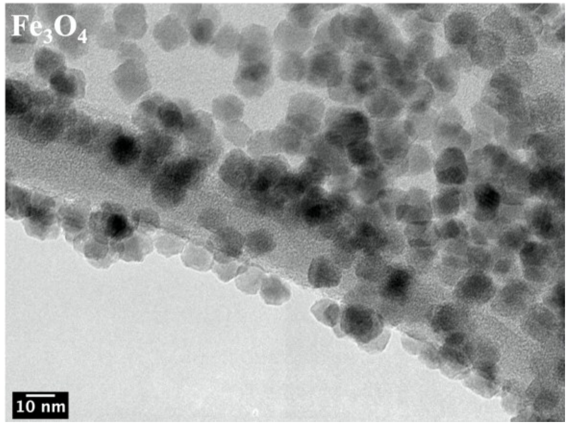

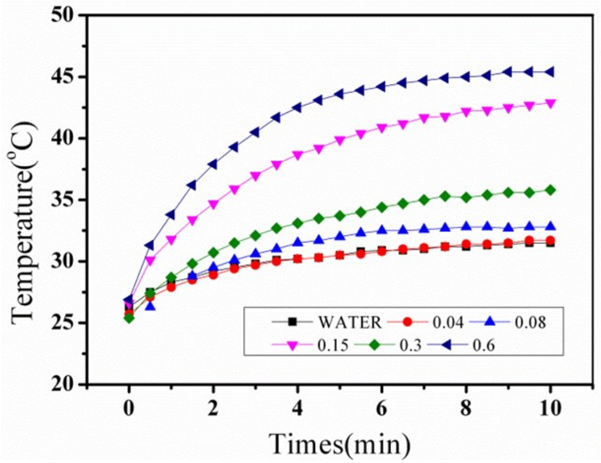

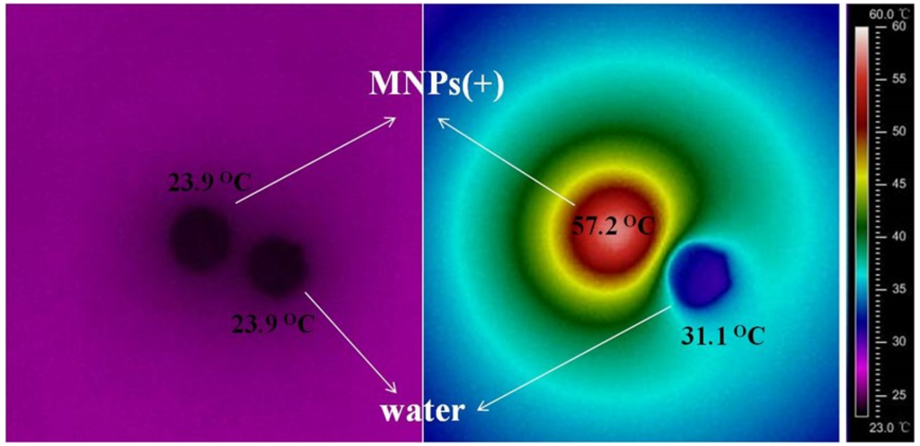

In vivo Imaging and Drug Storage by Quantum-Dot-Conjugated Carbon Nanotubes, Y. Guo et al with D. Shi, *Adv. Funct Mater*, 18, 1-9, 2008

Biomarkerless targeting and photothermal cancer cell killing by surface-electrically-charged superparamagnetic Fe3O4 composite nanoparticles, Xiao Han et al with Donglu Shi,
Nanoscale 2017, 9, 1457-1465

The Photothermal Effect (PT): Localized Surface Plasmon Resonance

- A localized surface plasmon resonance (LSPR) is the result of the confinement of a surface plasmon in a nanoparticle smaller than the wavelength of the incident light.
- A nanoparticle's response to the oscillating electric field can be described by the so-called dipole approximation of Mie theory.
- The oscillation frequency is determined by the density of electrons, the effective electron mass,

and the size and shape of the charge distribution.

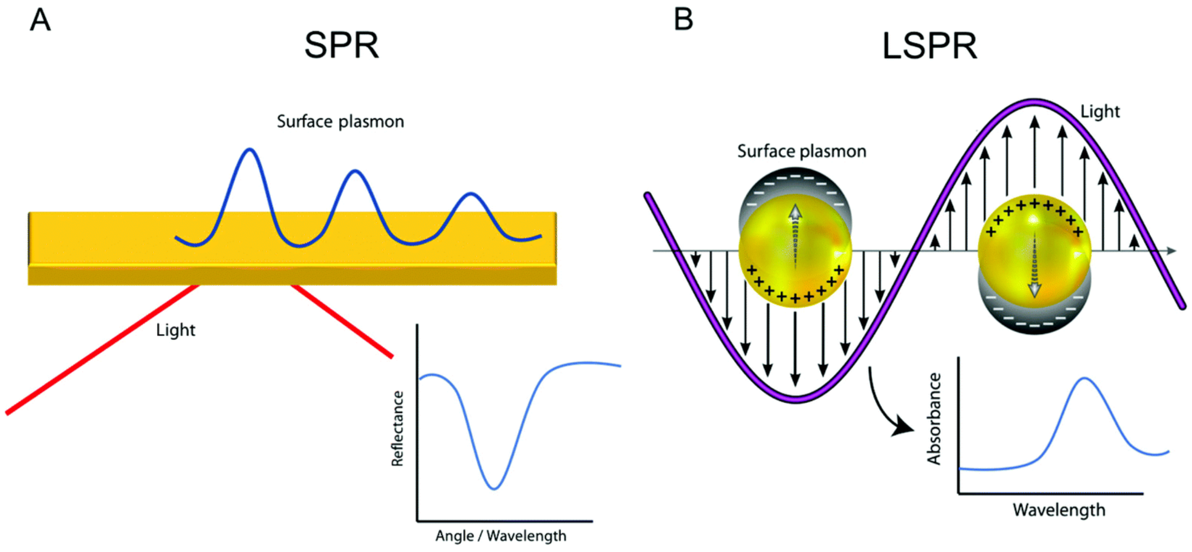

Jean-Francois Masson, *Analyst*, 2020, https://doi.org/10.1039/D0AN00316F

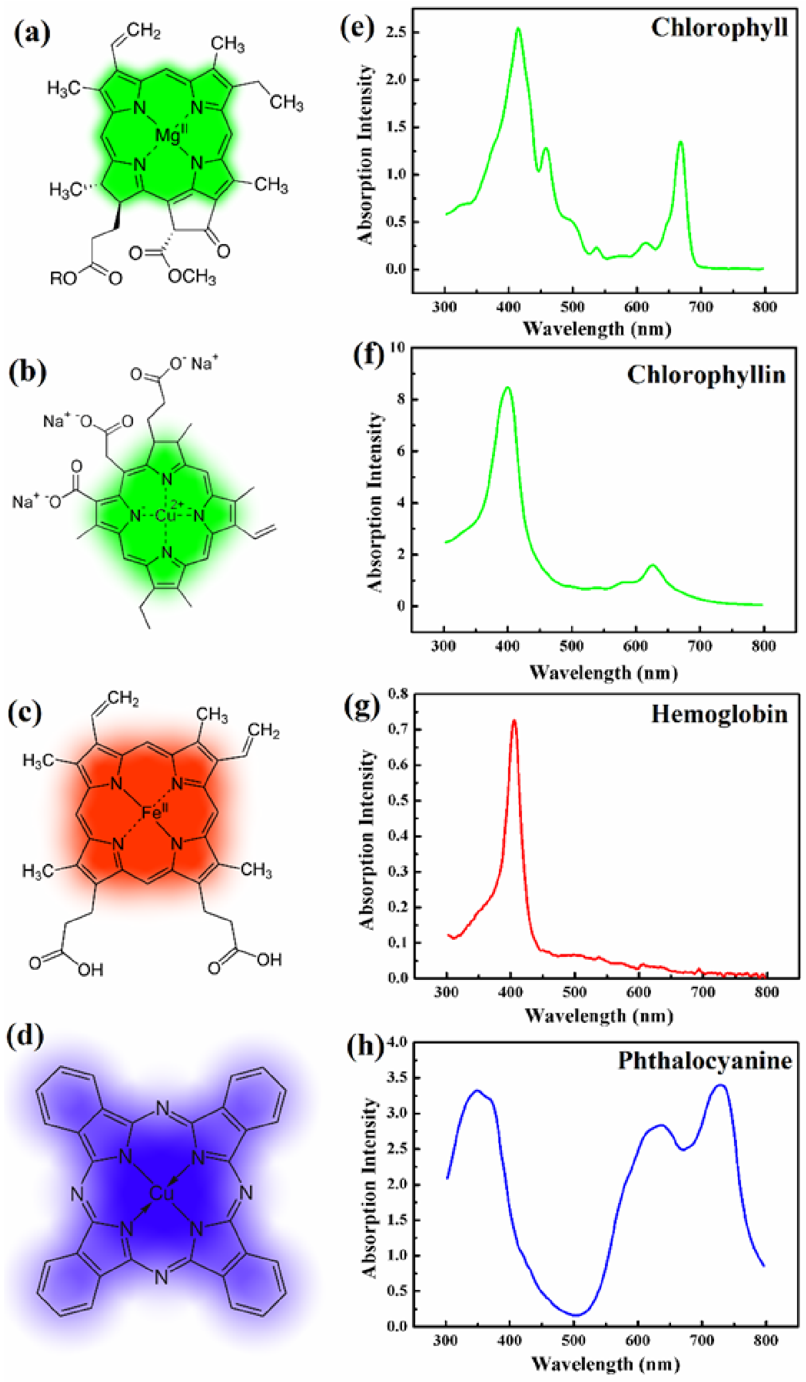

The porphyrin compounds

An organic compounds shares a common structural feature, namely, porphyrin, composed of four modified subunits bounded with carbon atoms forming a “ring-like” structure, therefore also known as “porphyrin rings.”

A porphyrin is a large ring molecule consisting of 4 pyrroles, which are smaller rings made from 4 carbons and 1 nitrogen. These pyrrole molecules are connected together through a series of single and double bonds which forms the molecule into a large ring.

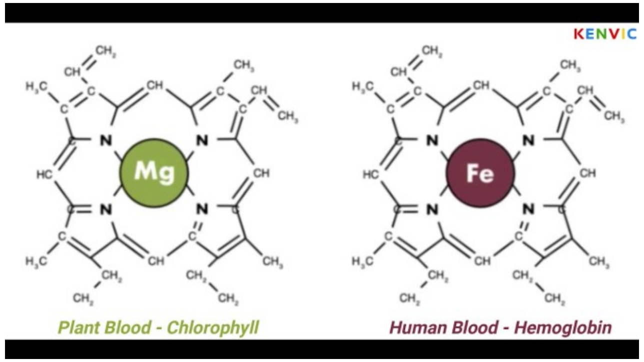

Zhao Y., Lin J., Kundrat D. M., Bonmarin M., Krupczak J. Jr., Thomas S. V., Lyu M., and Shi D., “Photonically-Activated Molecular Excitations for Thermal Energy Conversion in Porphyrinic Compounds,” *J. Phys. Chem. C*, 124, 2, 1575–1584, (2020)

Porphyrin Compounds: Chlorophyll

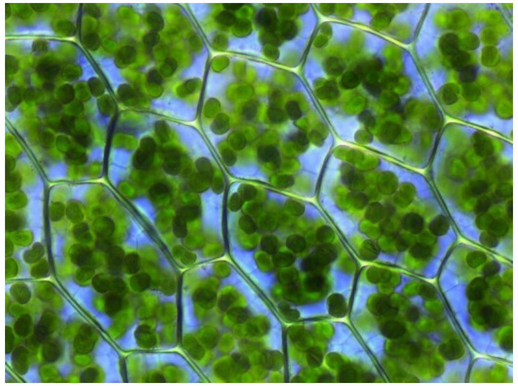

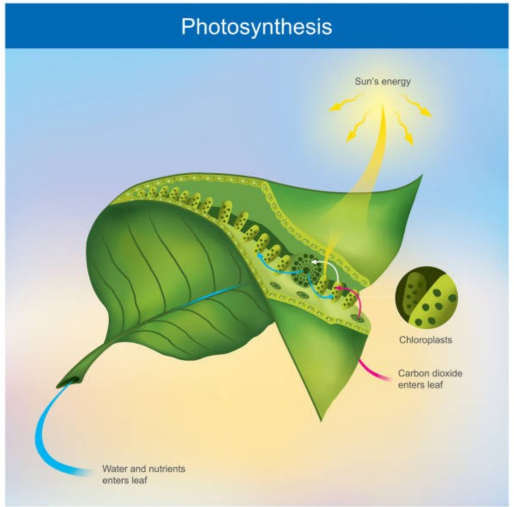

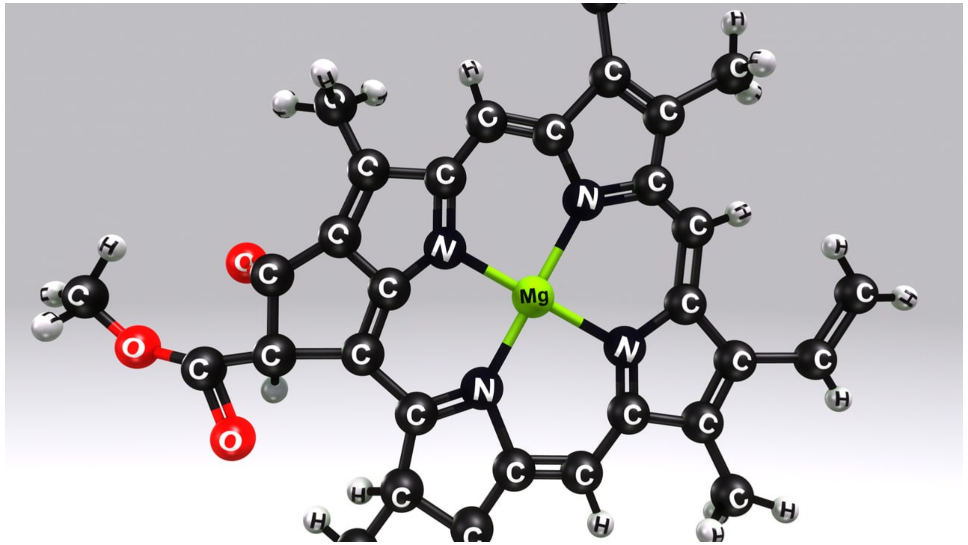

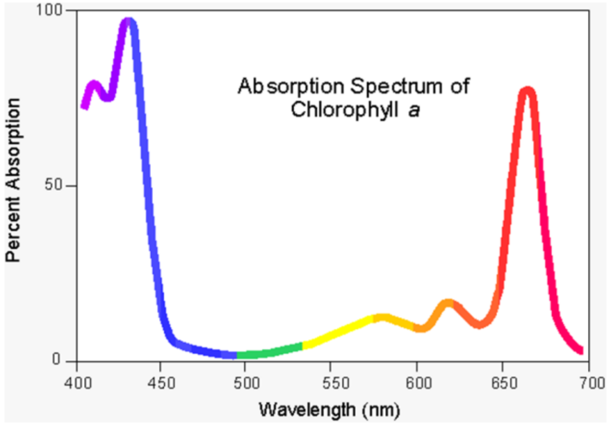

The chlorophyll molecule consists of a central magnesium atom surrounded by a nitrogen-containing structure called a porphyrin ring; attached to the ring is a long carbon–hydrogen side chain, known as a phytol chain.

Solutions of porphyrin compounds:
Chlorophyll, Chlorophyllin, Hemoglobin, Phthalocyanine

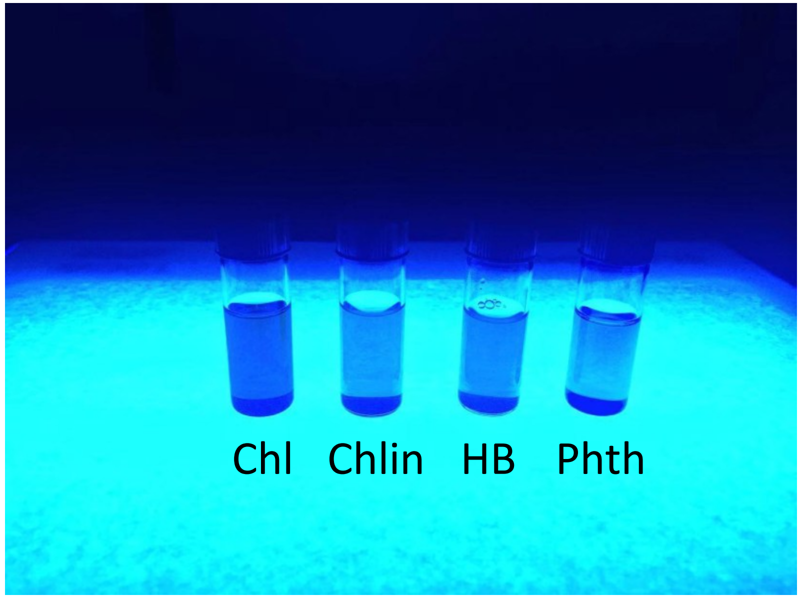

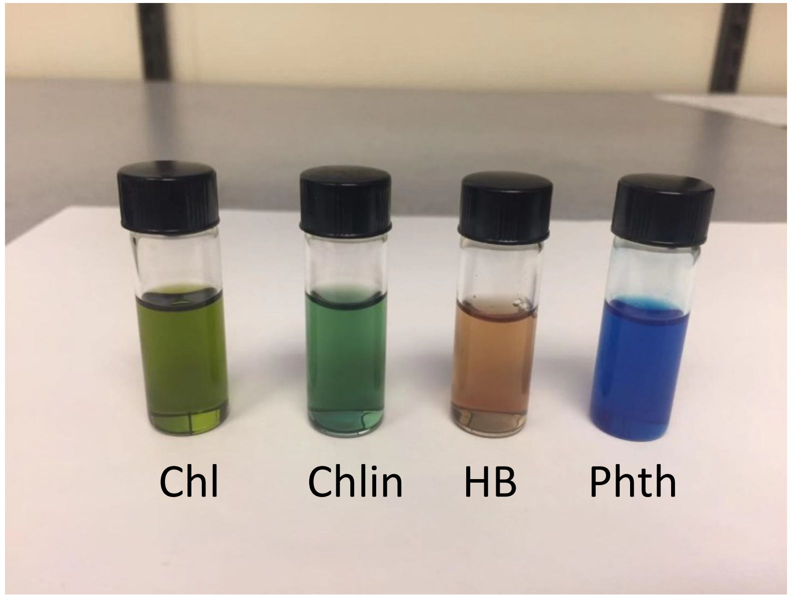

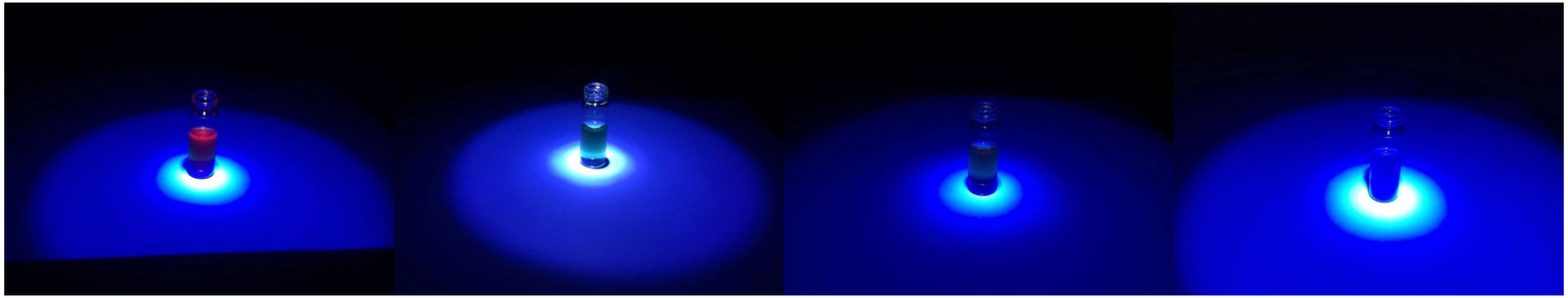

Y. Zhao et al with D. Shi, *J. Phys. Chem. C*, 124, 2, 1575–1584, (2020)

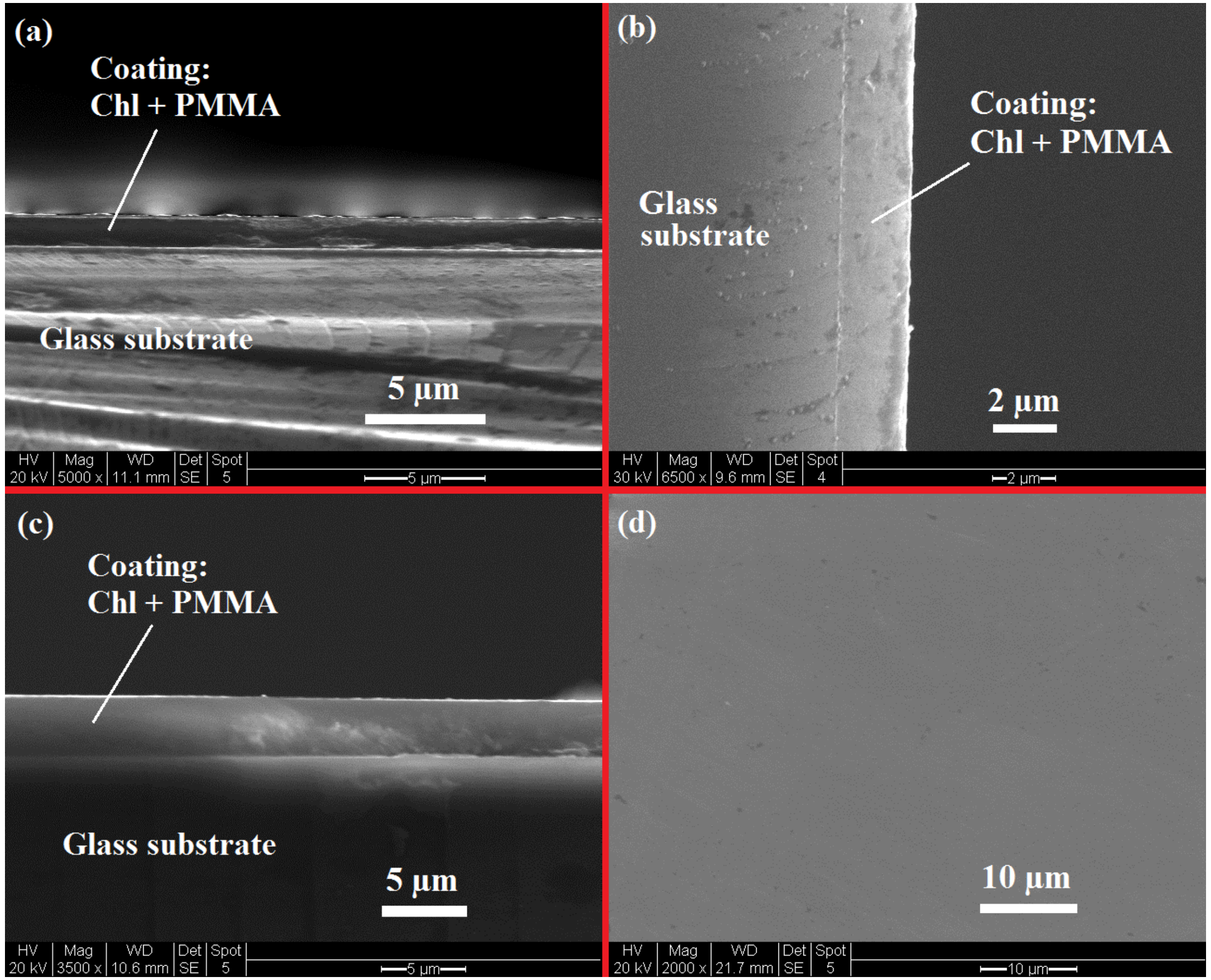

Zhao Y., Dunn A., Shi. D., “Effective reduction of building heat loss without insulation materials via the photothermal effect of a chlorophyll thin film coated “Green Window,”
MRS Communications: Volume 9, Issue 2, pp. 675-681 (2019)

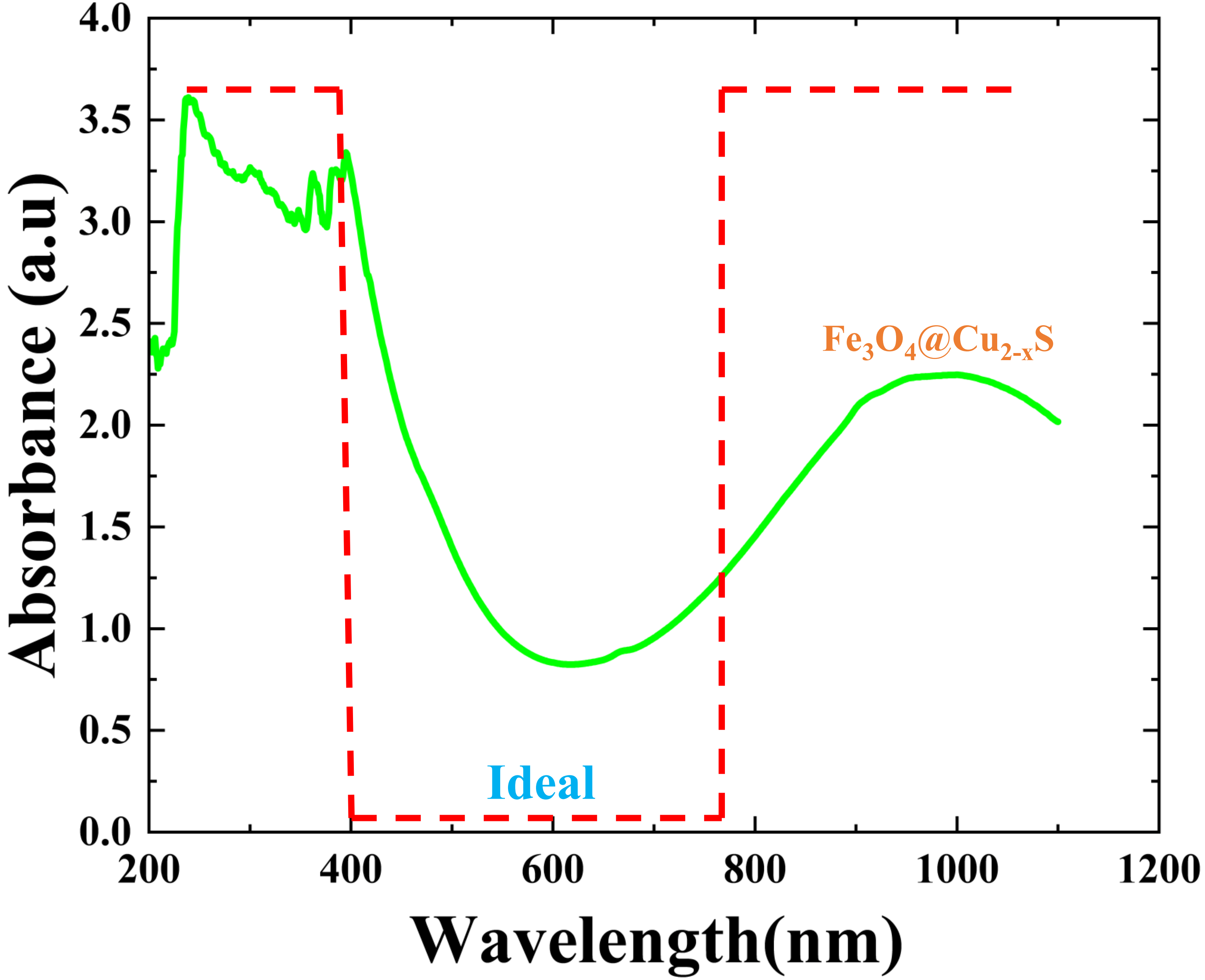

Absorbance (a.u)
4.0
3.5
3.0
2.5
2.0
1.5
1.0
0.5
0.0
200
400
600
800
1000
1200
Wavelength(nm)
Fe_3O_4@$Cu_{2-x}S$
Ideal

Nano Hybrids

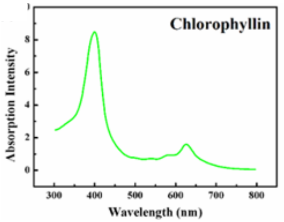

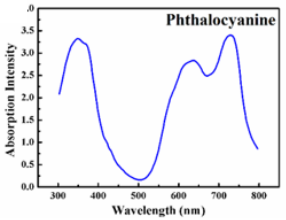

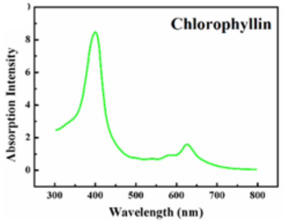

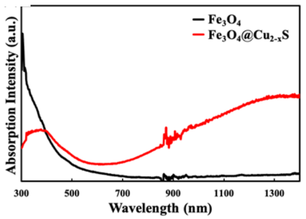

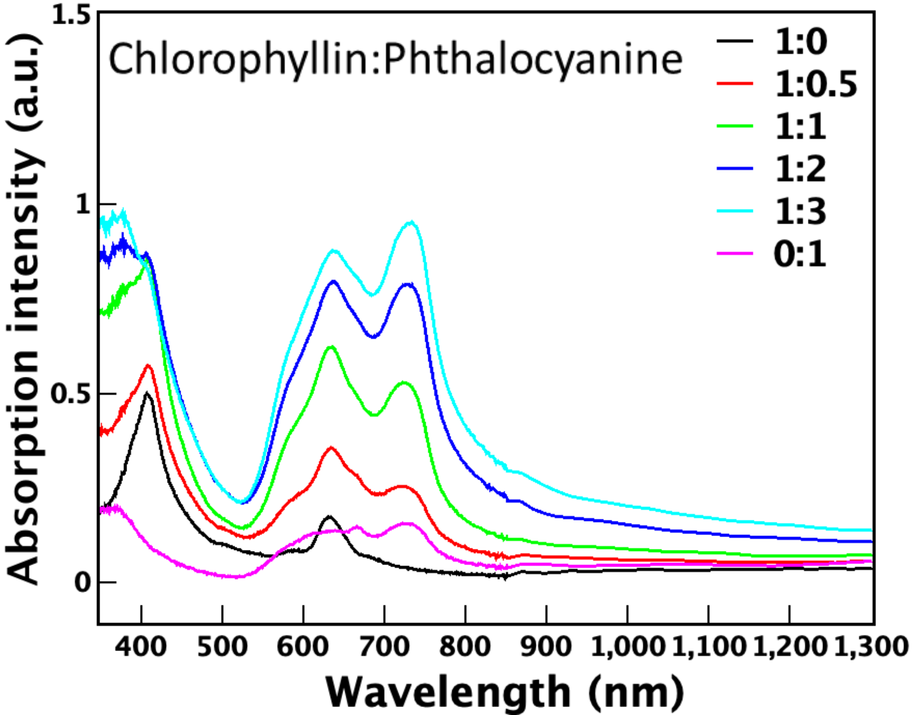

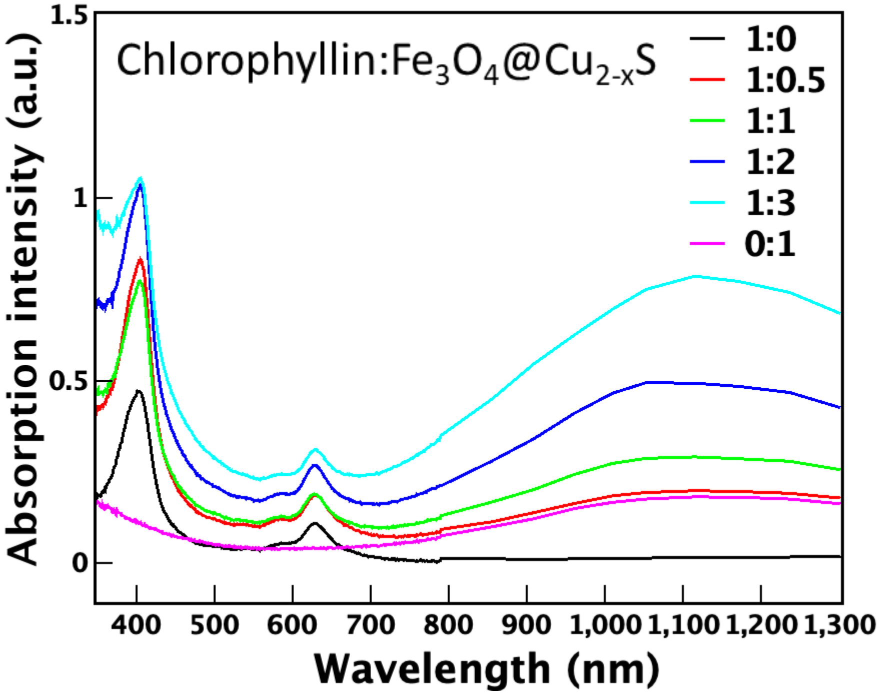

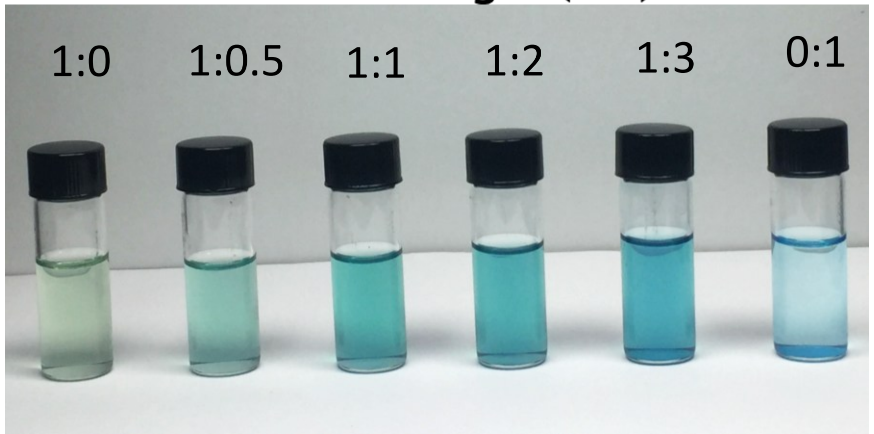

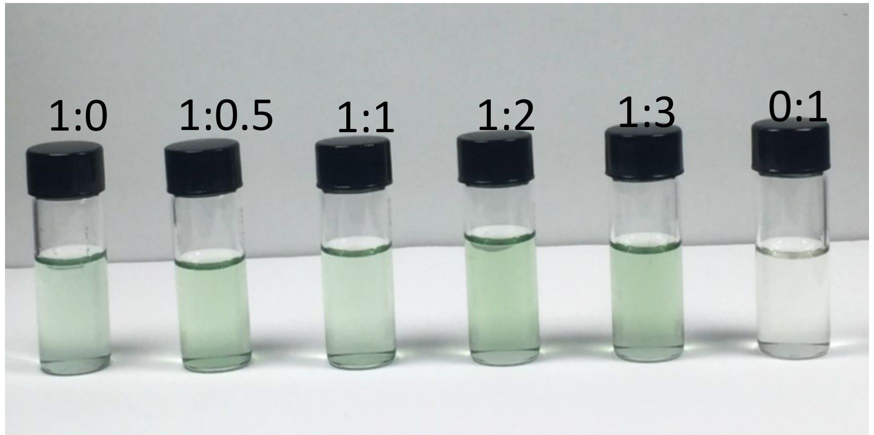

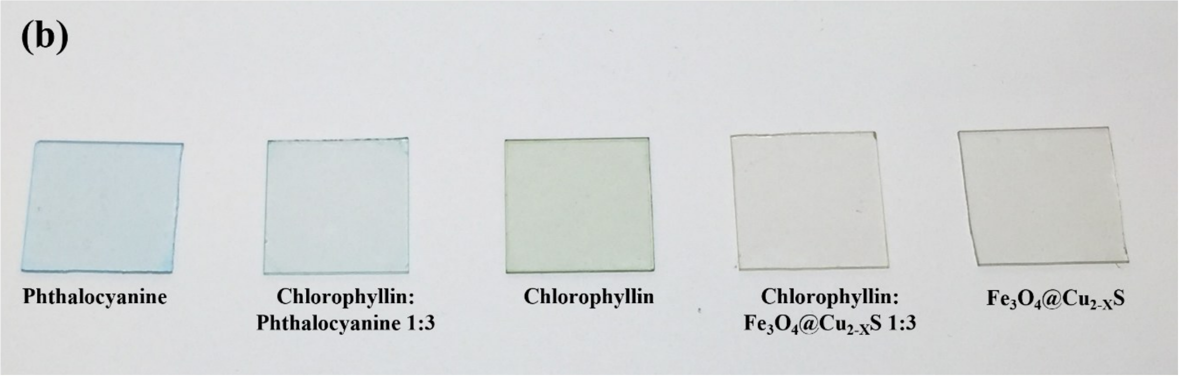
(b)
Phthalocyanine
Chlorophyllin:
Phthalocyanine 1:3
Chlorophyllin
Chlorophyllin:
Fe_3O_4@$Cu_{2-X}S$ 1:3
Fe_3O_4@$Cu_{2-X}S$

(c)


Chlorophyllin
Chloroyphllin:Phthalocyanine
1:0.5
Phthalocyanine
Chlorophyllin:Fe_3O_4@$Cu_{2-x}S$
1:3
Fe_3O_4@$Cu_{2-x}S$

Photothermal Generator (PTG)

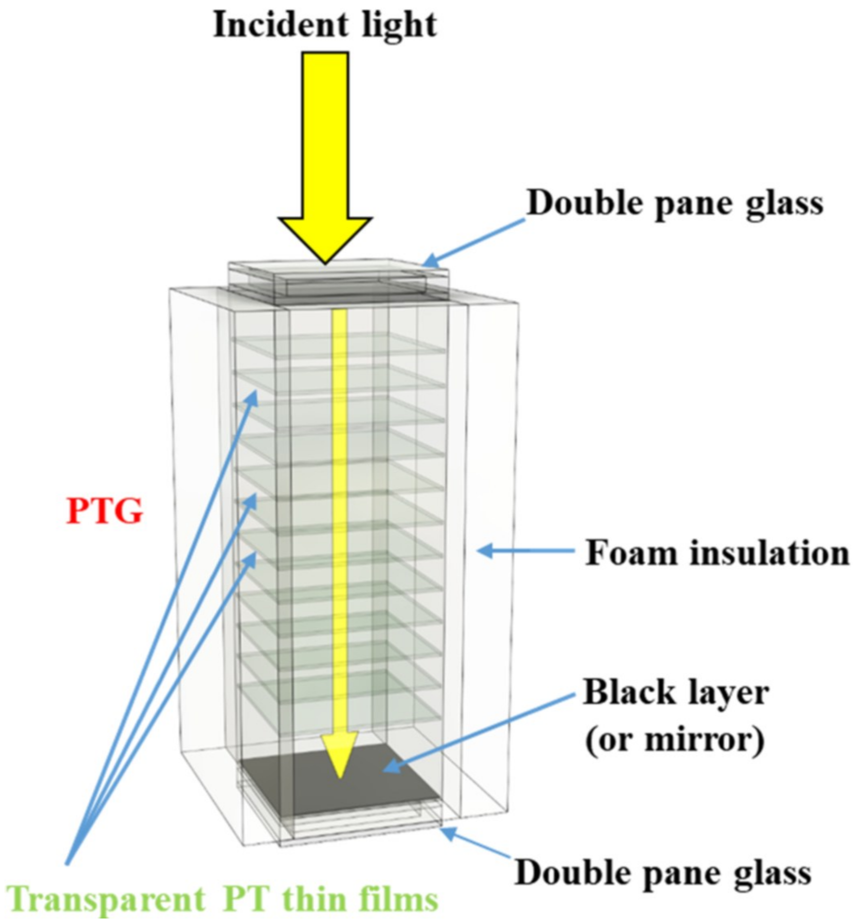

Infrared thermal photographs of the photo-thermal generator with 10 layers of $Fe_3O_4@Cu_{2-x}S$ films (85% AVT) illuminated by solar simulator (0.4 W·cm^{-2} power density) for different times.

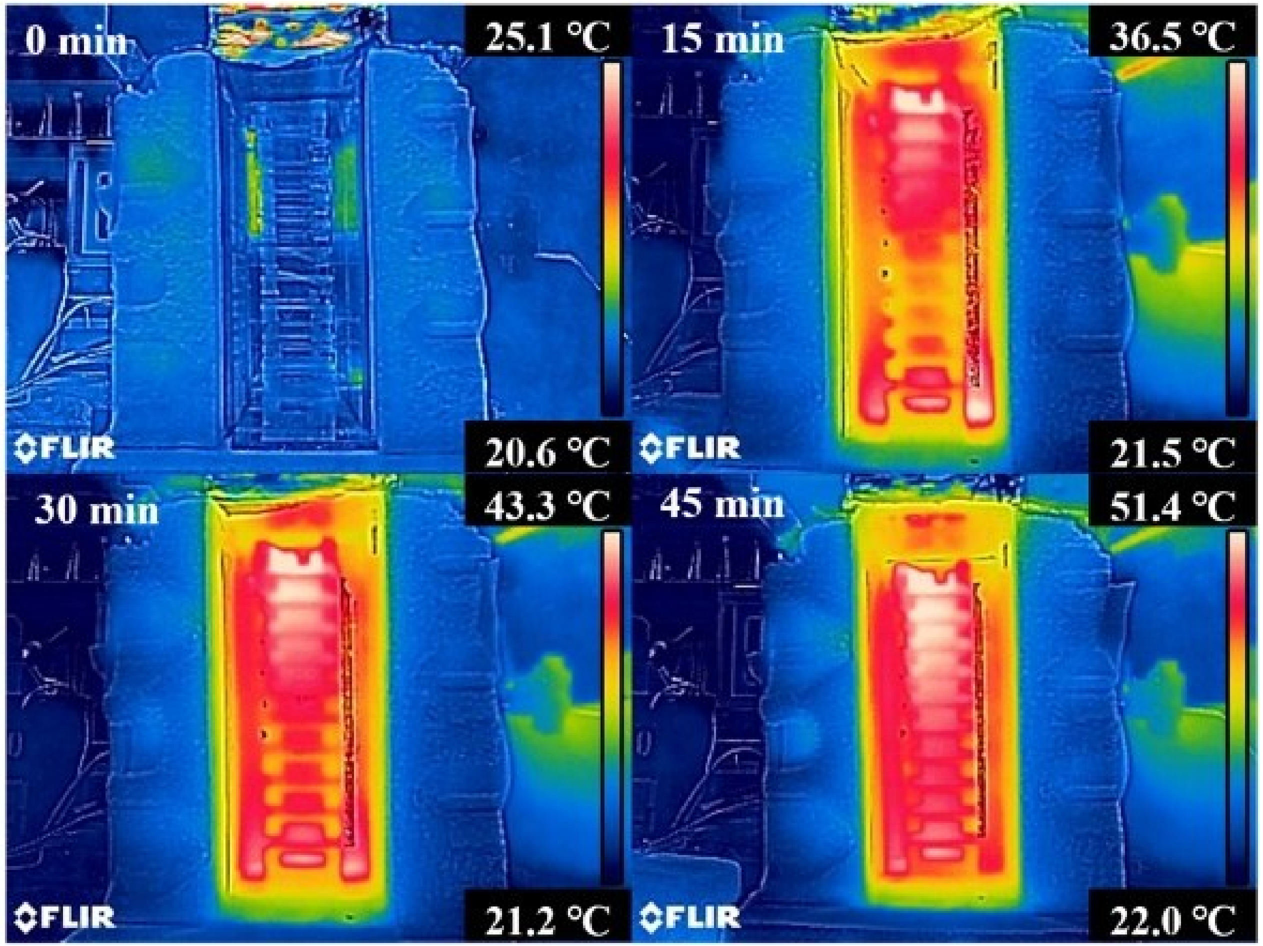

Heating Curves with insulation

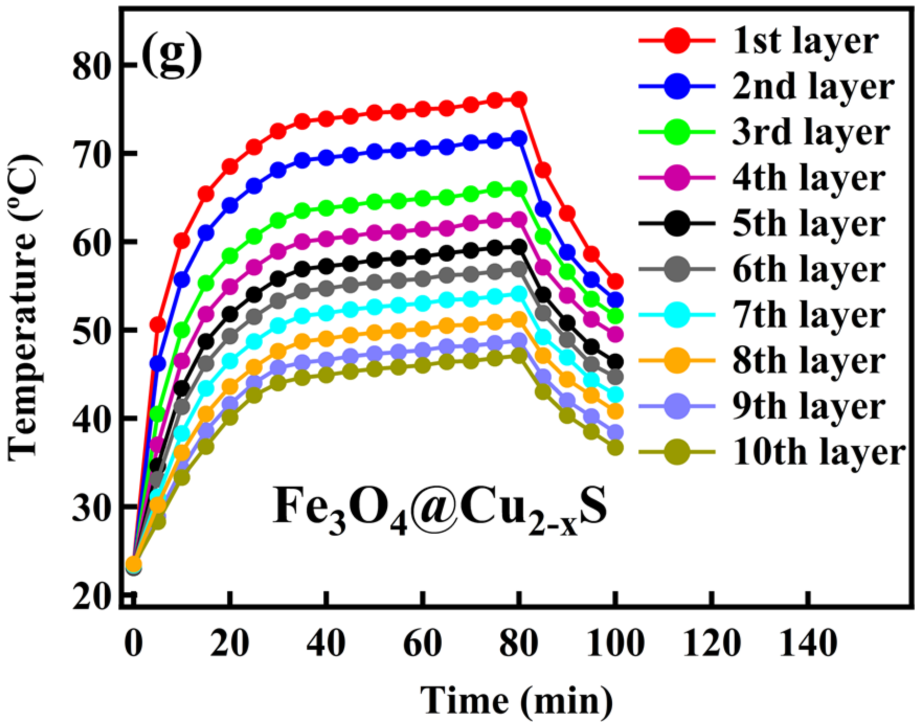

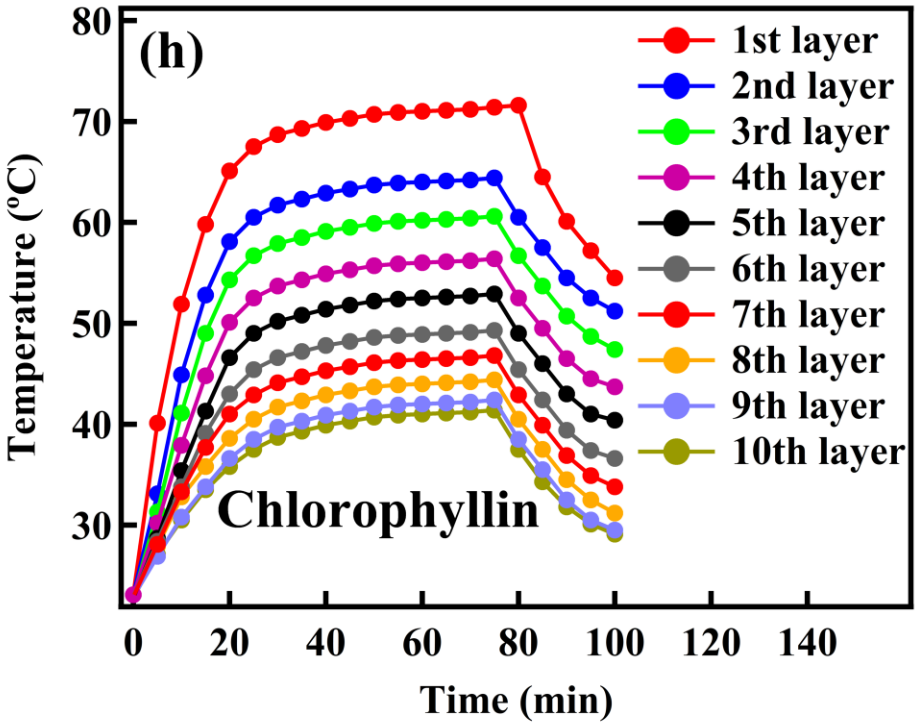

The photothermal conversion efficiency, η, is defined as the ratio of the thermal energy generated by the sample to the incident photon energy.

$$\eta = \frac{(C_{glass} m_{glass} + C_{PT\ material} m_{PT\ material} + C_{polymer} m_{polymer})\Delta T_{max}}{IA\Delta t} \approx \frac{C_{glass} m_{glass} \Delta T_{max}}{IA\Delta t} \quad \textbf{(3)}$$

where c is the specific heat capacity (J/g·℃), m is mass (g), ΔT_{max} is the maximum change in temperature increase of the sample (℃), I is the power density (W/cm^2), A is the surface area of the sample, and Δt is the time for sample to achieve the maximum temperature (sec). In this research, the specific heat of glass is 0.84 J/g·℃, and mass of the substrate is 1.75 g, the power density is 0.1 W/cm^2, and the surface area of substrate is 2.54 x 2.54 cm^2.

Table S1. The photothermal efficiencies of the photothermal generator with different number of layers calculated for both Fe3O4@Cu2-xS and chlorophyllin thin films

- The solar photothermal efficiency (η) is defined as the ratio of the energy increase inside the cuboid to the incident simulated solar radiation.
- $\dot{Q}$ is the heat produced by the photothermal effect in unit of (J/s).
- $\dot{Q}_{in}$ is the input energy from light source in unit of (J/s).
- $\eta = \frac{\dot{Q}}{Q_{in}}$

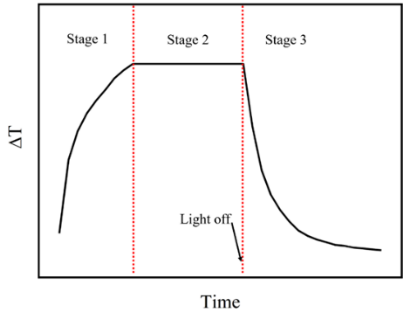

Number of layers	1	2	3	4	5	6	7	8	9	10
Fe_3O_4@$Cu_{2-x}S$: η (%)	40.9	42.9	44.2	46.3	48.0	49.6	57.2	58.2	60.6	63.4
Chlorophyllin: η (%)	30.9	43.7	46.4	52.4	53.5	56.9	57.7	58.9	60.7	61.6

Photonically-Activated Molecular Excitations for Thermal Energy Conversion in Porphyrinic Compounds
Yuan Zhao, Jou Lin, David M. Kundrat, Mathias Bonmarin, John Krupczak Jr., Som V. Thomas, Mengyao Lyu, and Donglu Shi
J. Phys. Chem. C 2020, 124, 2, 1575–1584

Photothermal Energy Generation

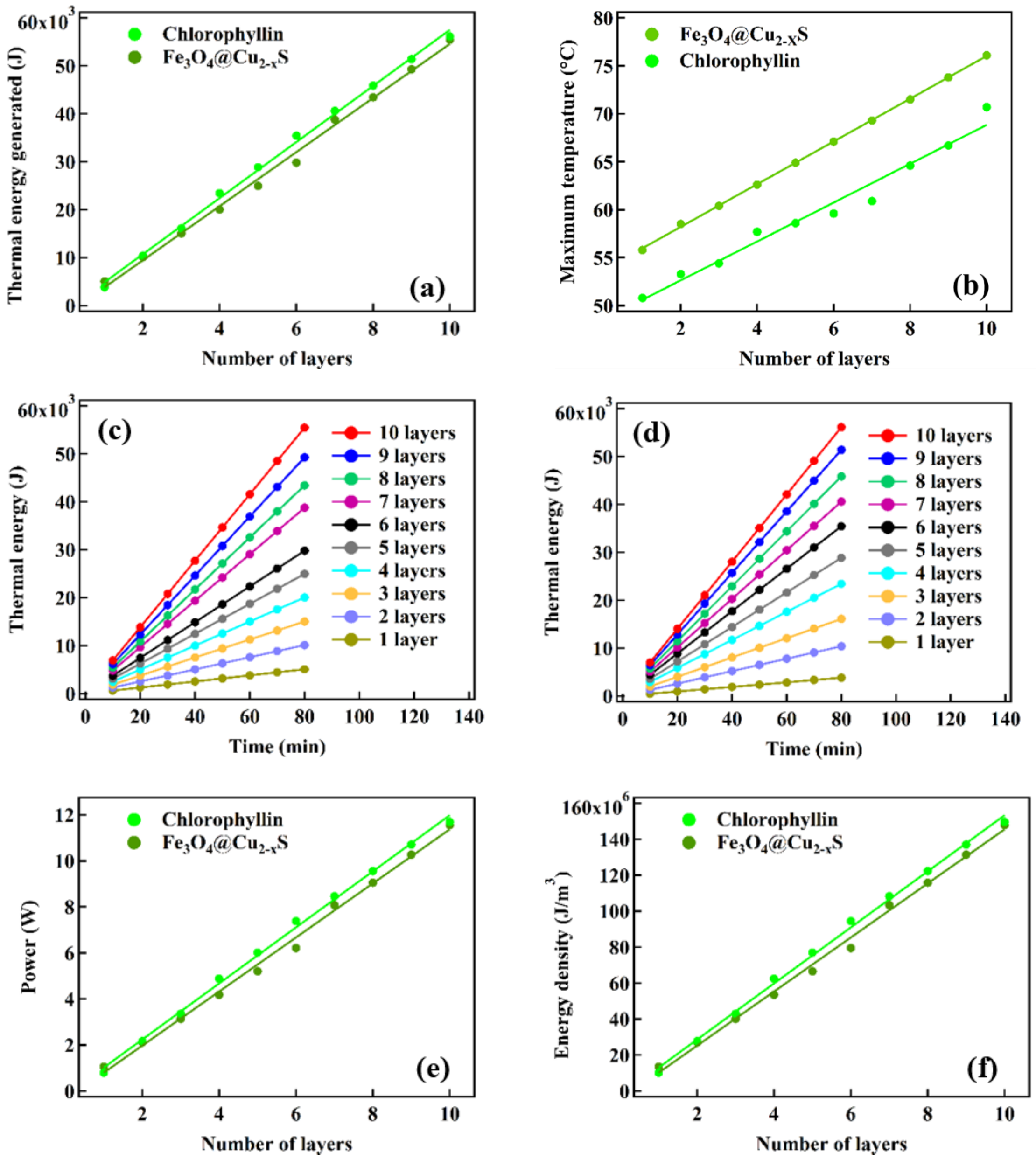

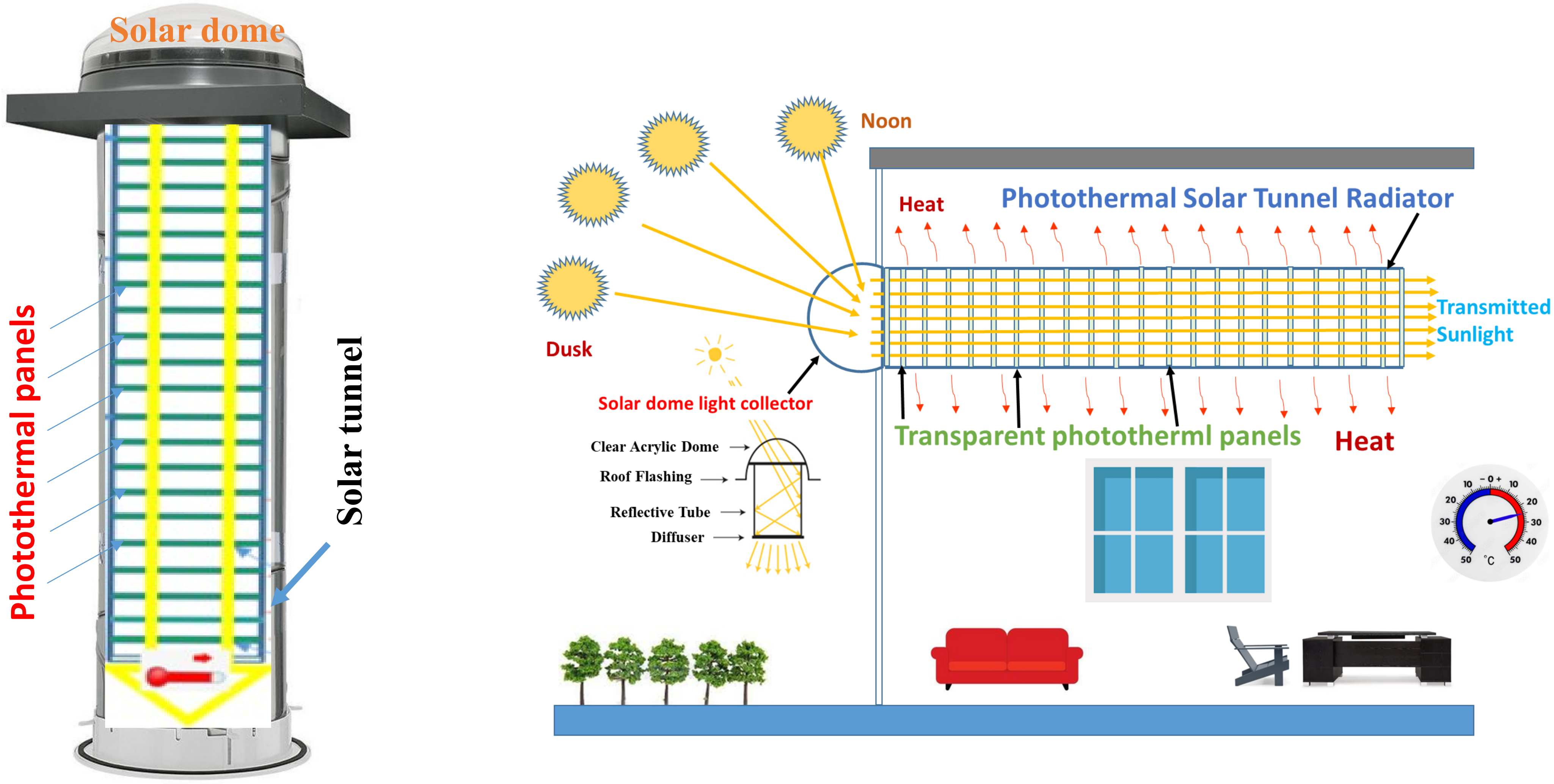

Solar dome
Photothermal panels
Solar tunnel
Noon
Dusk
Heat
Photothermal Solar Tunnel Radiator
Transmitted
Sunlight
Solar dome light collector
Clear Acrylic Dome
Roof Flashing
Reflective Tube
Diffuser
Transparent phototherml panels
Heat

Photothermal utility heating

Solar dome and solar tunnel

Solar dome lighting

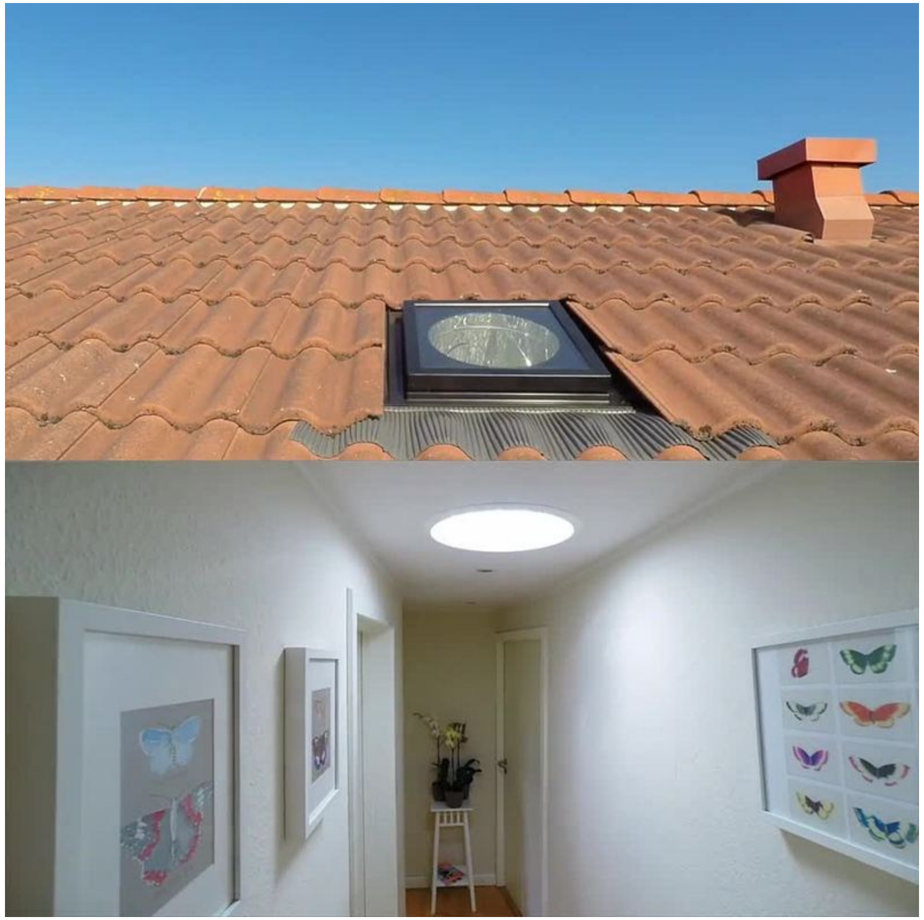

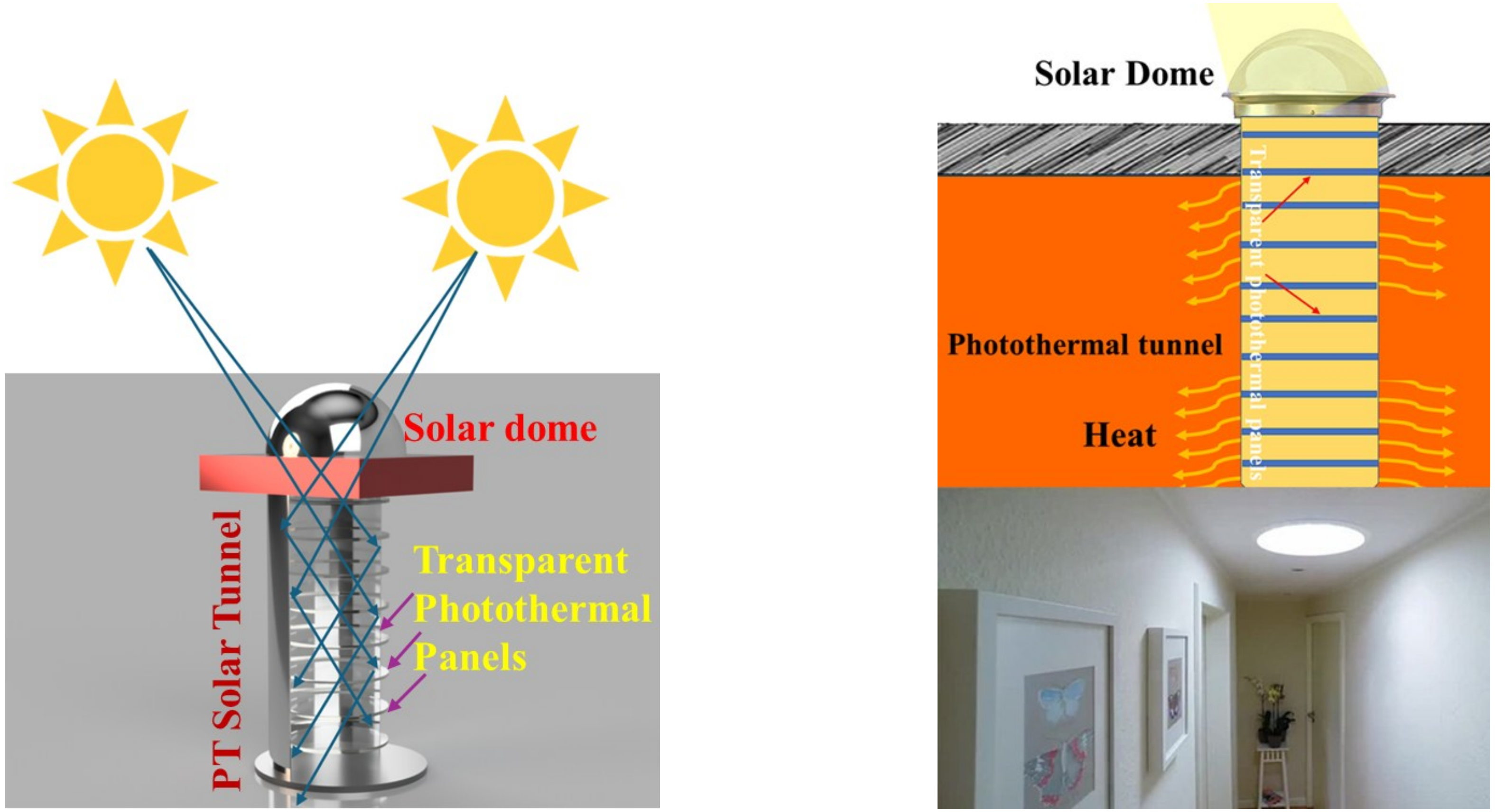

Diagram showing the Photothermal Solar Tunnel Radiator (PSTR) concept.

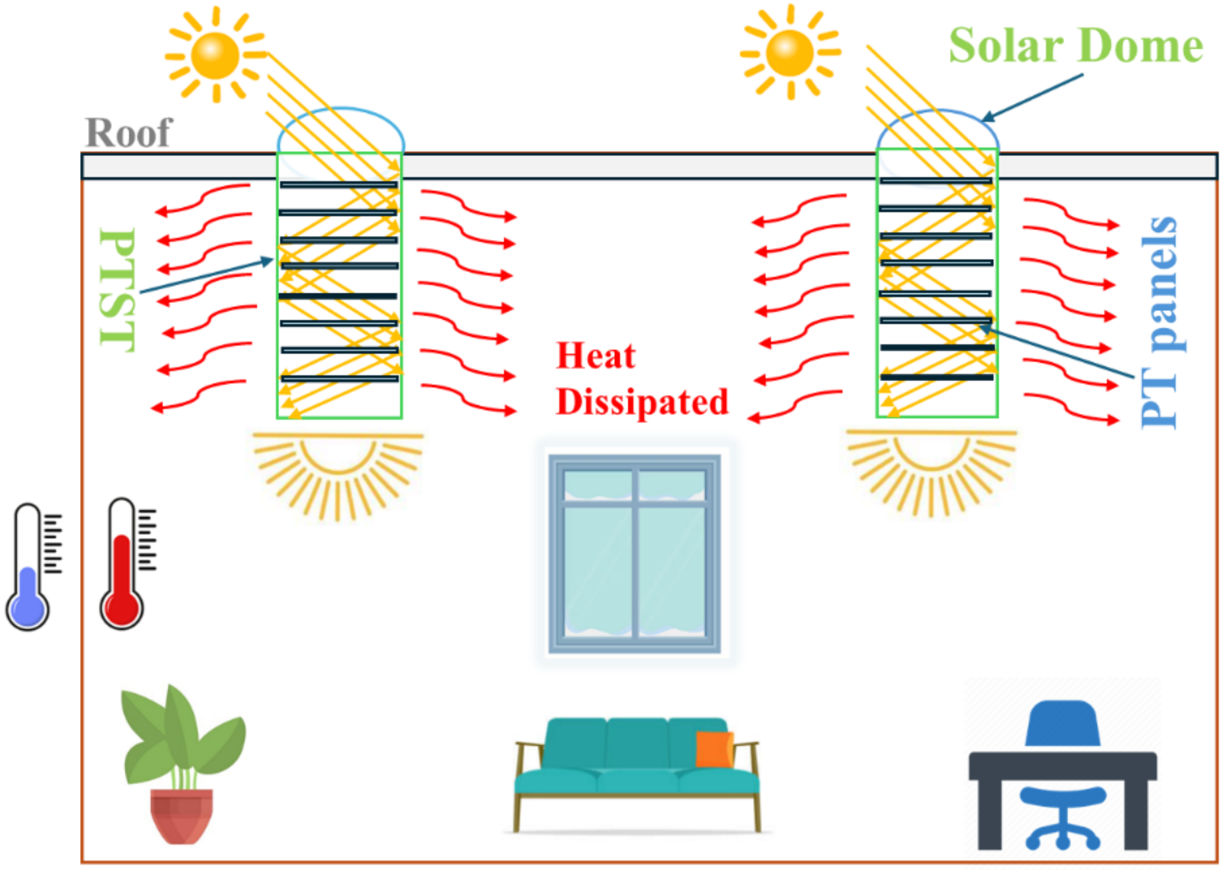

Schematic diagram showing the concept of the utility heating with the Photothermal Solar Tunnel (PTST) and the photothermal (PT) panels.

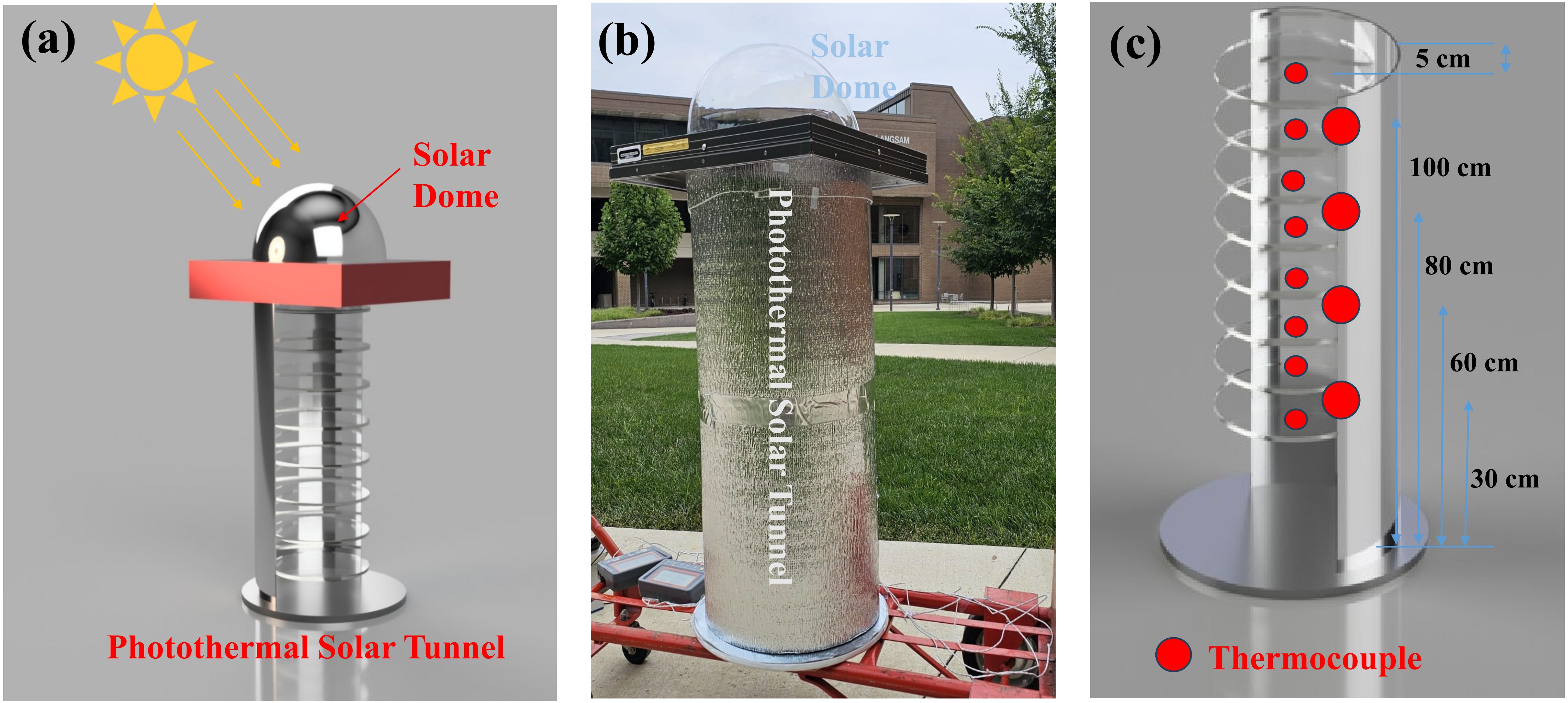

Figure 2: (a) Schematic diagram of the Photothermal Solar Tunnel (PTST) system, (b) Photograph of the solar dome connected with the PTST, and (c) The positions of thermocouples within the PTST as indicated by the red spots. The small red dots are located right on the top of each PT panel in the center and the larger red circles are located right inside the PTST at heights of 100cm, 80 cm, 60 cm, and 30 cm from the bottom of the tunnel, respectively.

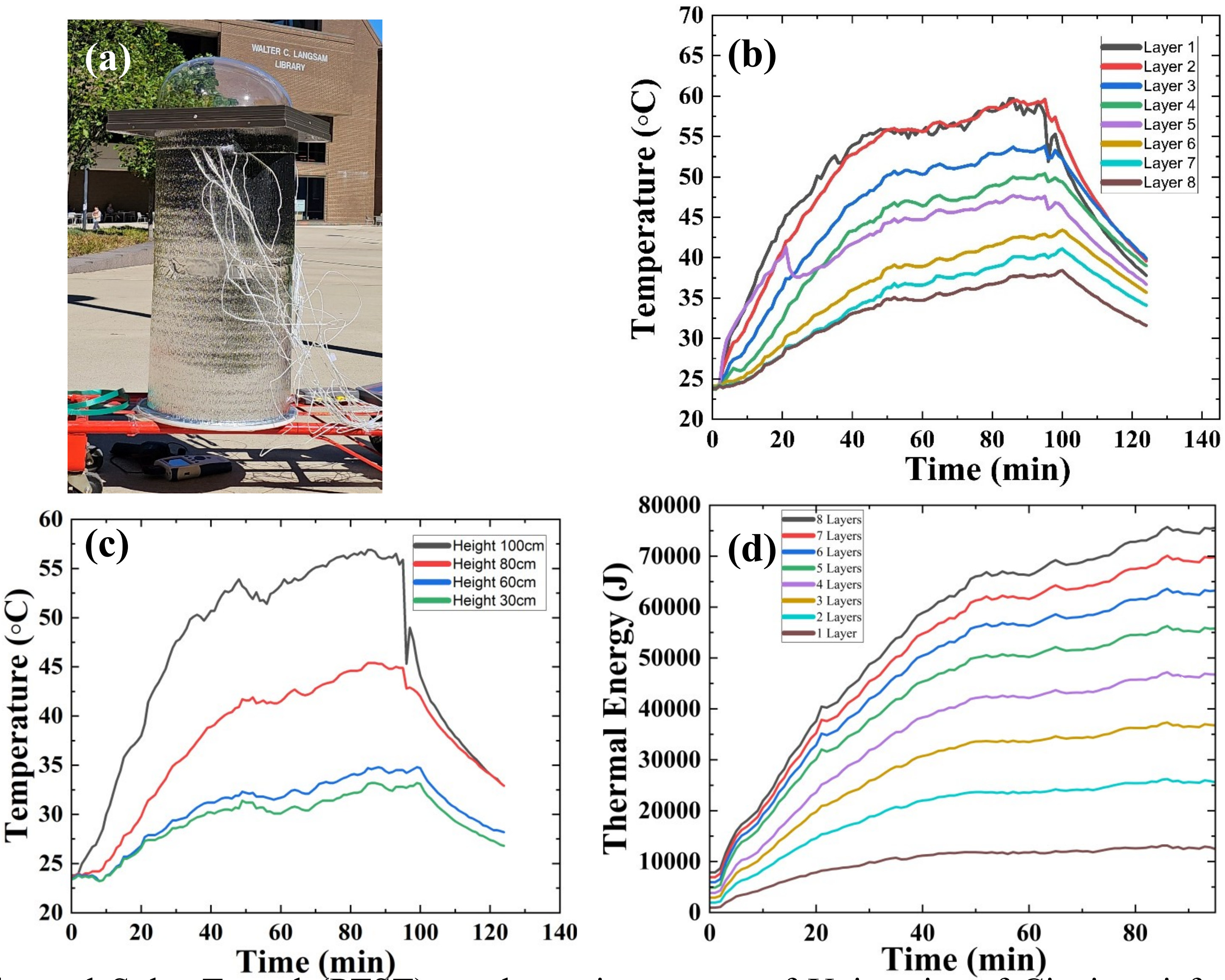

(a)Photograph of Photothermal Solar Tunnel (PTST) on the main campus of University of Cincinnati for solar harvesting experiments. The experiments were conducted on October 2nd,2024 at 2PM. Ambient temperature was 21 ∘C. (b) Temperature vs time heating curves obtained from the thermocouples located on each photothermal panels as indicated by the red spots as shown in Figure 2c (c) Temperature vs time heating curves obtained from the thermocouples located inside the wall of PTST at heights of 100cm,80cm,60cm,and 30cm from the bottom of the tunnel, respectively. (d) Thermal energy vs time calculated from the heating curves shown in Figure 4b.

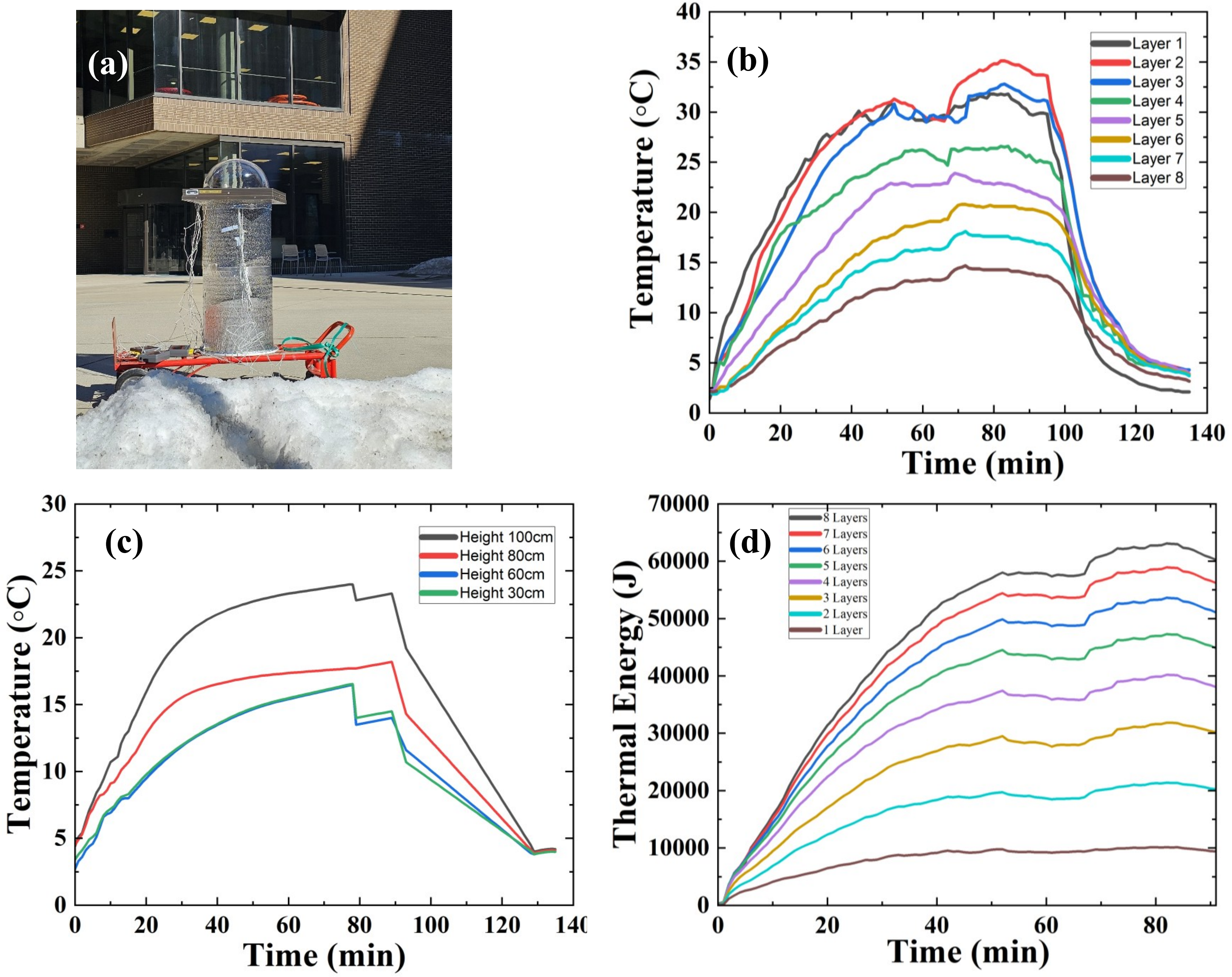

(a)Photograph of Photothermal Solar Tunnel (PTST) on the main campus of University of Cincinnati for solar harvesting experiments. The experiments were conducted on February 1st,2024 from 12Noon to 2.20PM. **Ambient temperature was 5◦C.** (b) Temperature vs time heating curves obtained from the thermocouples located on each photothermal panels as indicated by the redspots as shown in Figure 2c (c)Temperature vs time heating curves obtained from the thermocouples located inside the wall of PTST at heights of 100,80cm,60cm, and 30cm from the bottom of the tunnel, respectively. (d)Thermal energy vs time calculated from the heating curves shown in Figure 4b.

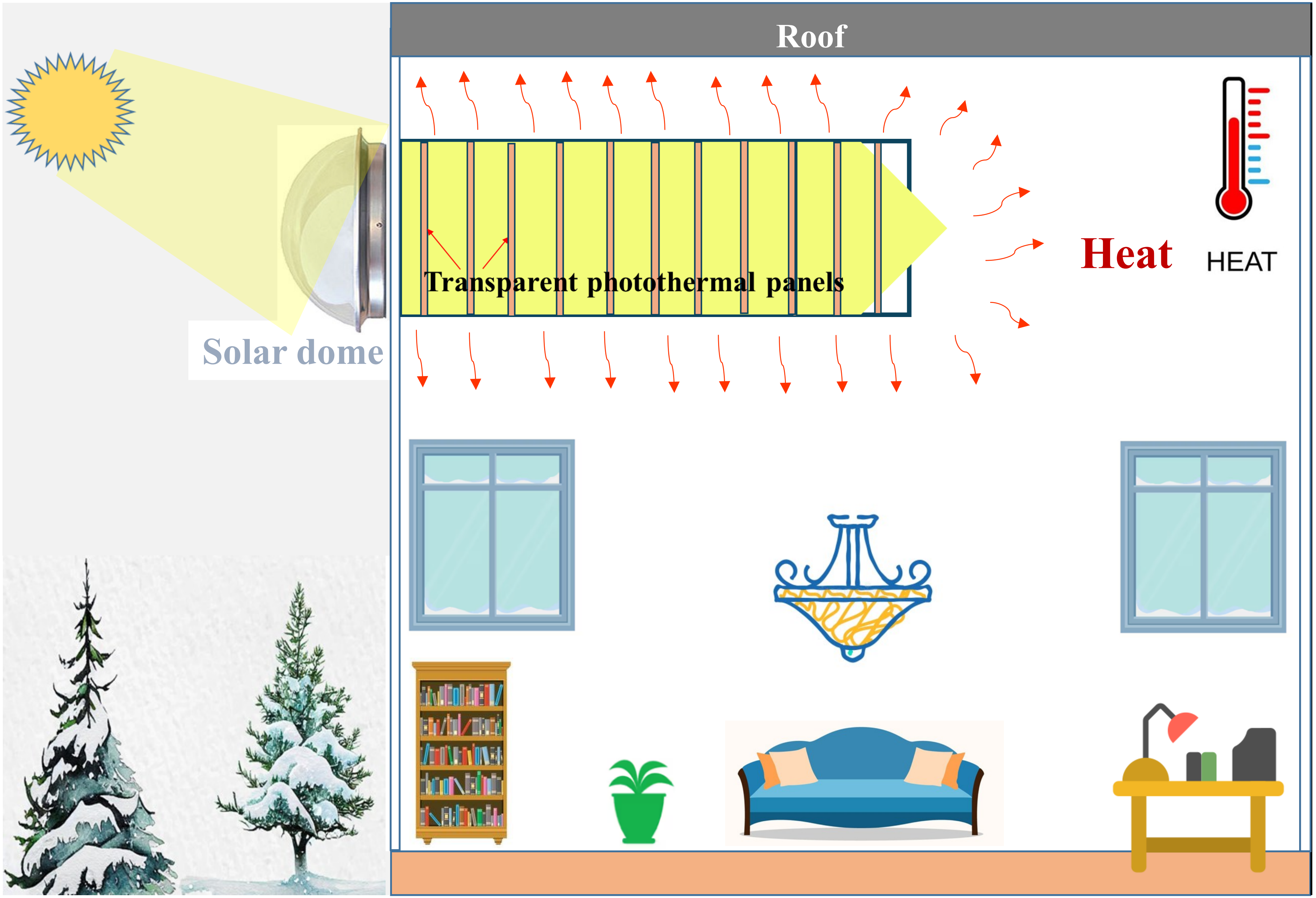
Roof
Solar dome
Transparent photothermal panels
Heat
HEAT

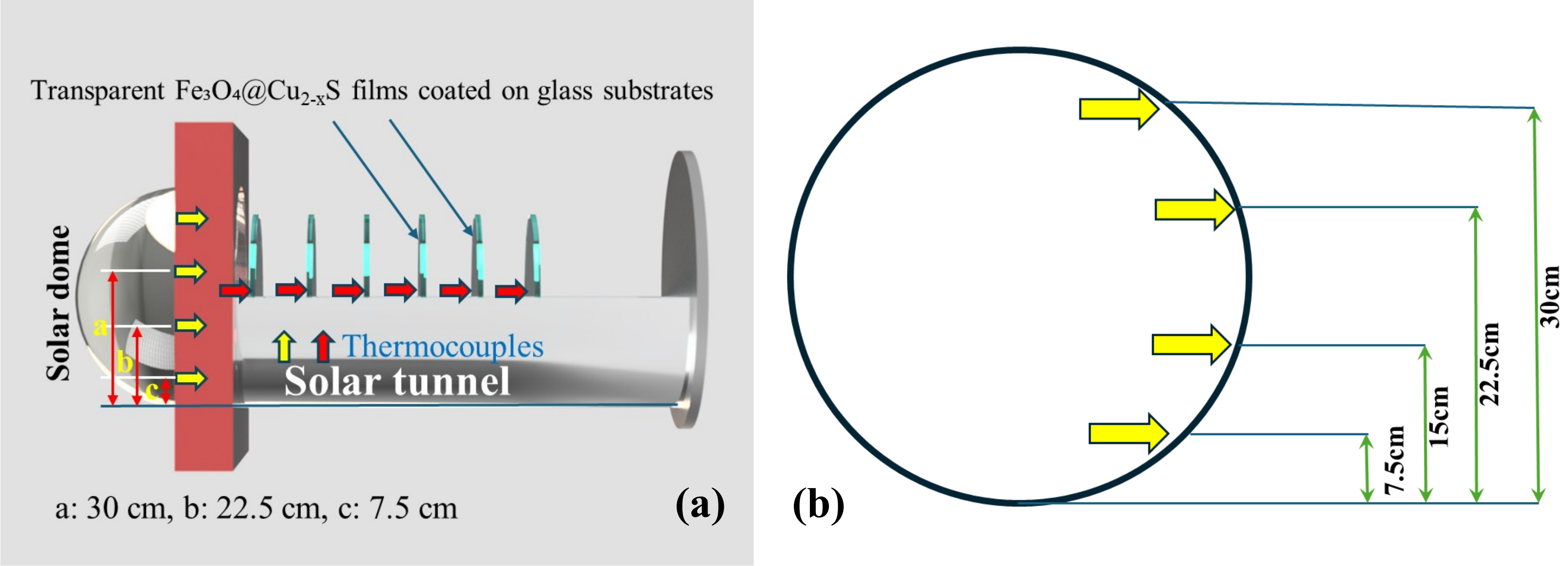
Transparent Fe3O4@Cu2-xS films coated on glass substrates
Solar dome
Thermocouples
Solar tunnel
a
b
c
a: 30 cm, b: 22.5 cm, c: 7.5 cm
(a)
(b)
30cm
22.5cm
15cm
7.5cm

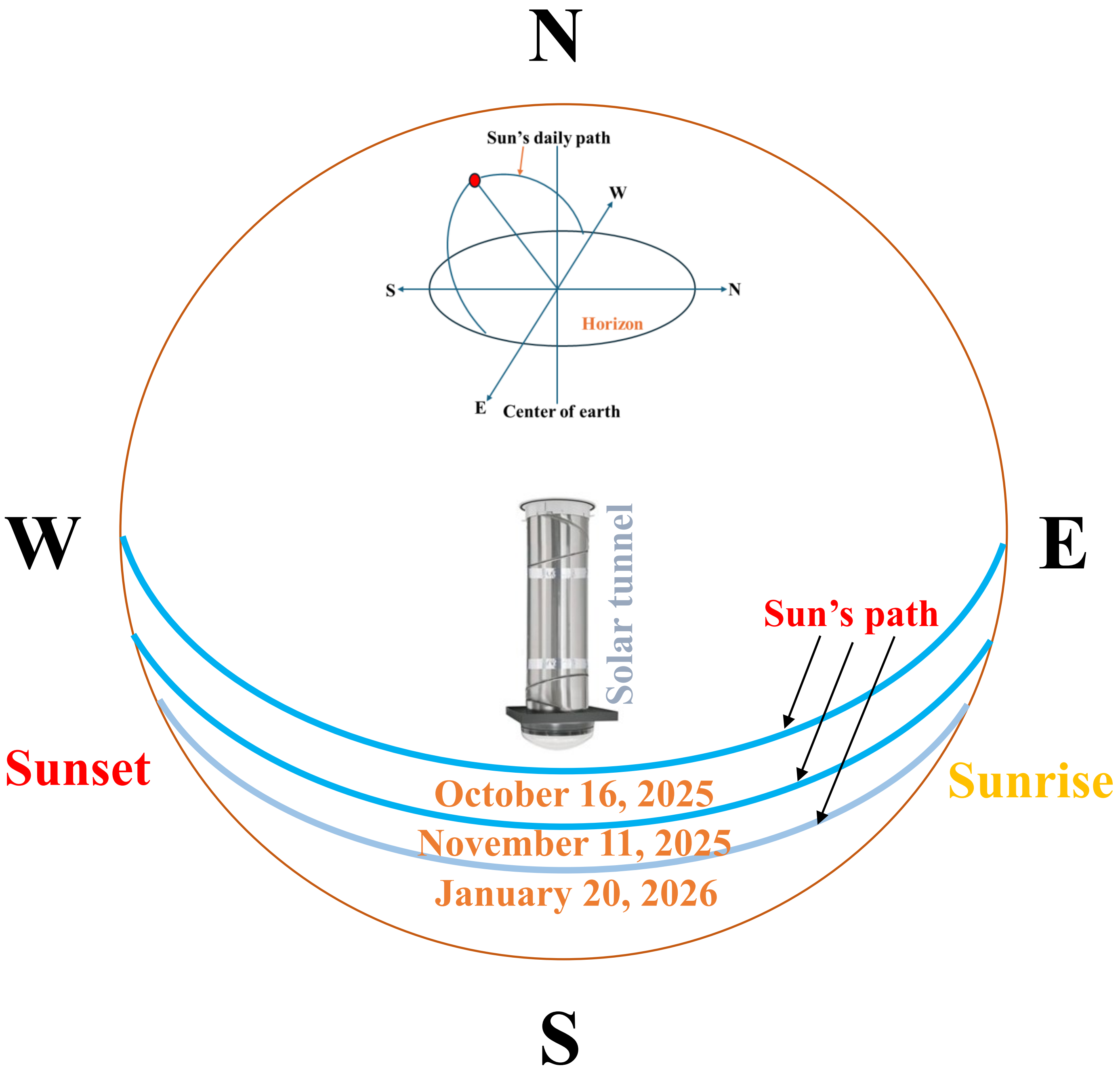
N
Sun's daily path
W
S
N
Horizon
E
Center of earth
W
E
Solar tunnel
Sun's path
Sunset
Sunrise
October 16, 2025
November 11, 2025
January 20, 2026
S

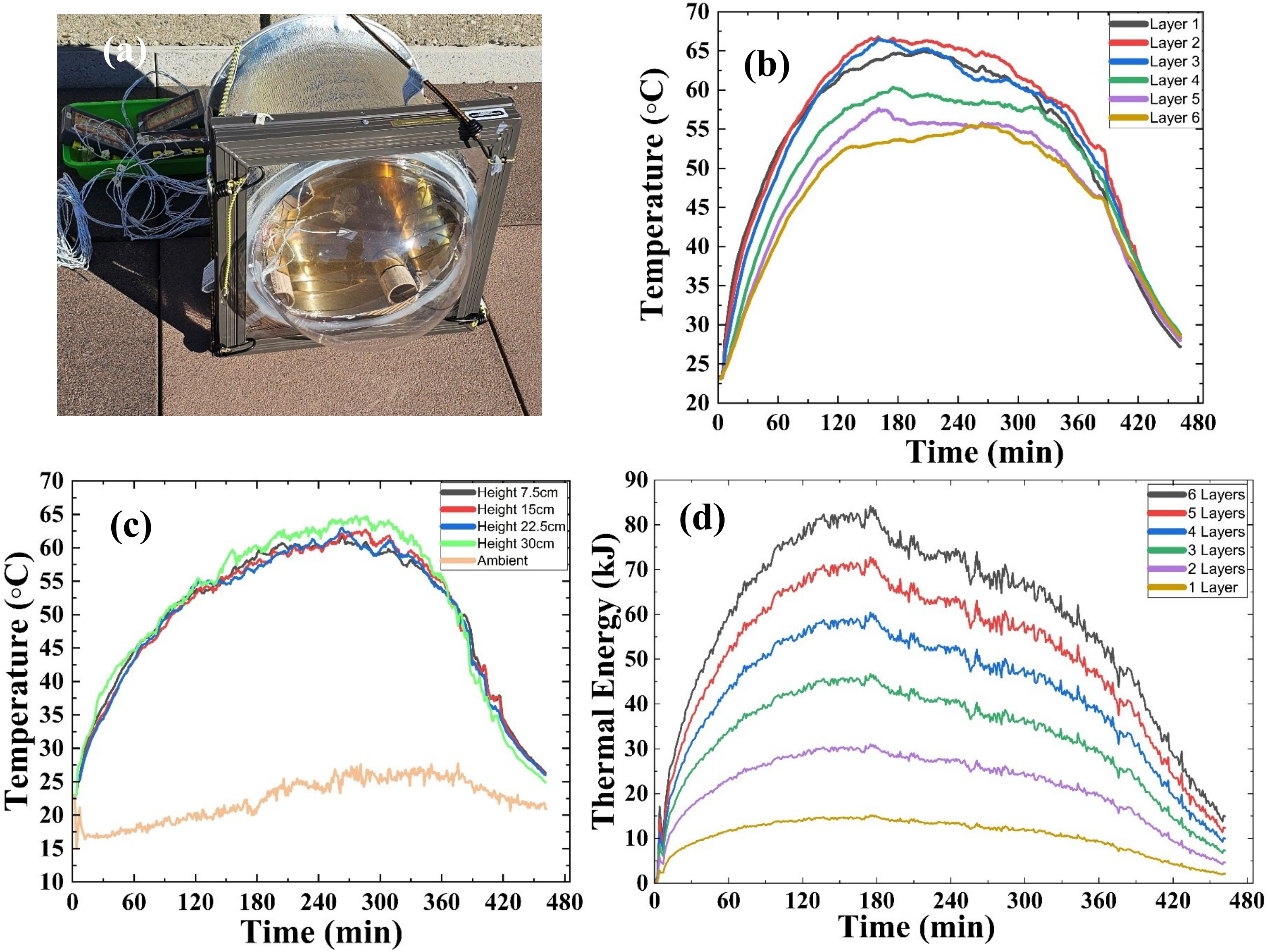

Figure 7: (a)Photograph of Photothermal Solar Tunnel Radiator(PTSTR) on the main campus of University of Cincinnati for solar harvesting experiments. The experiments were conducted on October 16th,2025 from 10AM to 5:30PM with an ambient temperature varying between 15 to 25 ◦C. (b) Temperature vs time heating curves obtained from the thermocouples located on each photothermal

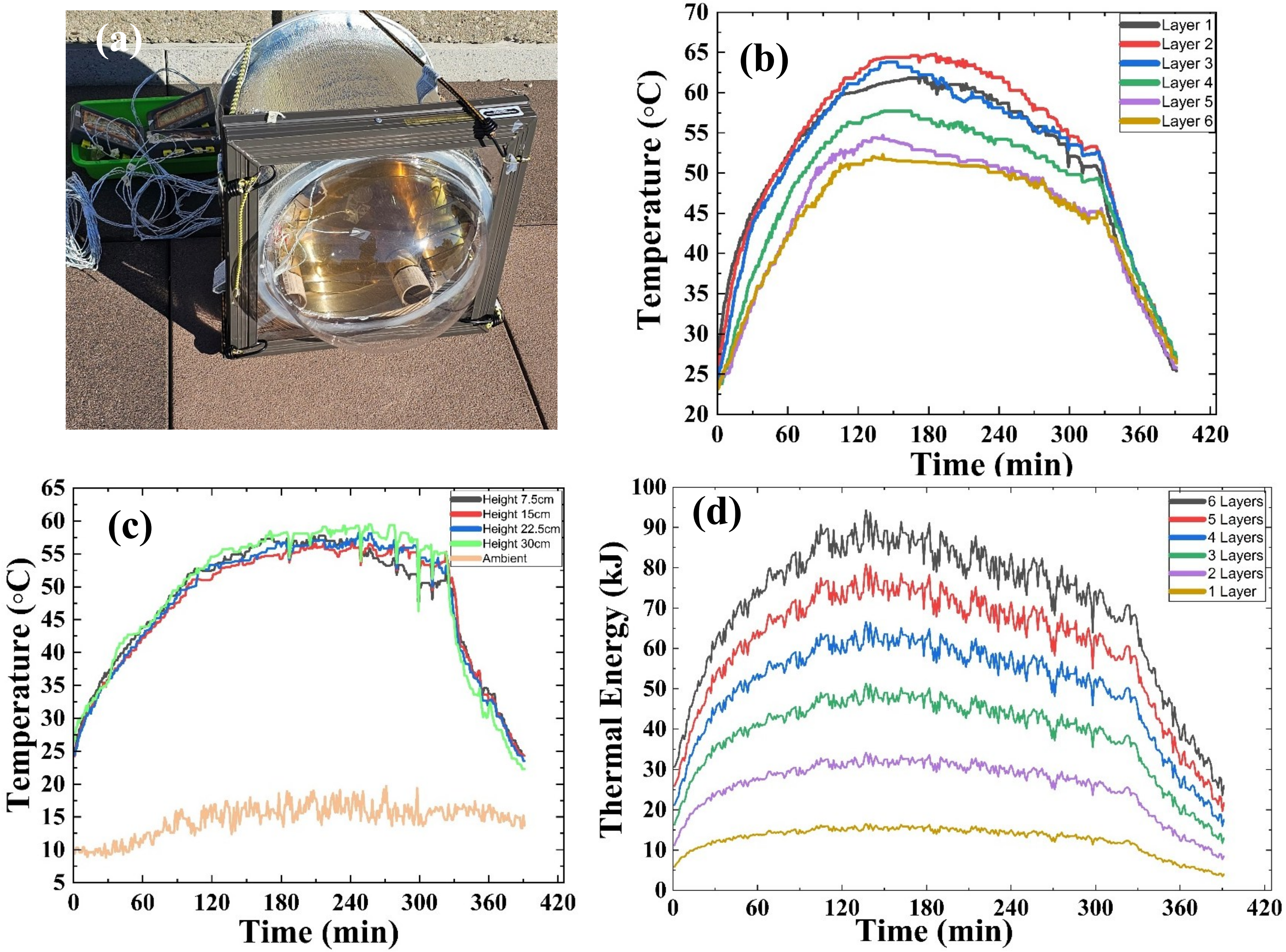

Figure 8: (a)Photograph of Photothermal Solar Tunnel Radiator(PTSTR) on the main campus of University of Cincinnati for solar harvesting experiments. The experiments were conducted on October 23rd,2025 from 10:30AM to 5PM with an ambient temperature varying between 10 to 16 ∘C. (b) Temperature vs time heating curves obtained from the thermocouples located on each photothermal panels (c) Temperature vs time heating curves obtained from the thermocouples bottom of the tunnel. (d) Thermal energy vs time calculated from the heating curves.

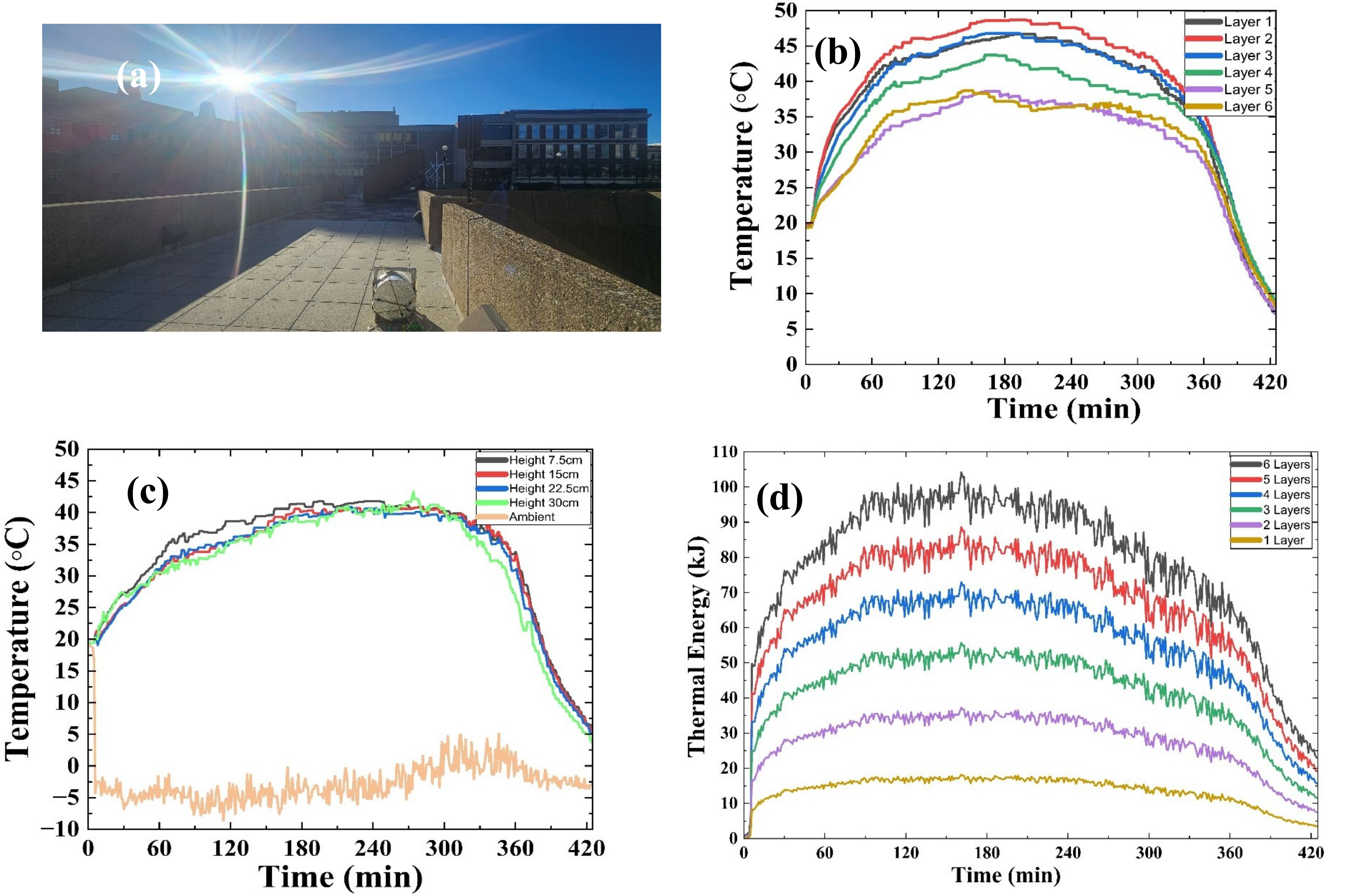

Figure 10: (a)Photograph of Photothermal Solar Tunnel Radiator(PTSTR) on the main campus of University of Cincinnati for solar harvesting experiments. The experiments were conducted on January 20th,2026 from 9:30AM to 5:00PM with an ambient temperature varying between -6 to -2◦C. (b) Temperature vs time heating curves obtained from the thermocouples located on each photothermal panels (c) Temperature vs time heating curves obtained from the thermocouples located at varied heights in the PTSTR. (d) Thermal energy vs time calculated from the heating curves.

The Photothermal Solar Tunnel (PTST): Transparent Solar Heating

- **Innovative Architecture:** Replaces traditional opaque collectors with a sequence of transparent panels in a tunnel geometry, allowing for cumulative, gradual light absorption.
- **Advanced Materials:** Utilizes plasmonic **$Fe_3O_4@Cu_{2-x}S$** core-shell nanoparticles that directly and instantly convert UV and infrared light into thermal energy.
- **Dual Functionality:** Delivers immediate, reliable thermal gain while allowing most visible light to pass through, preserving natural daylighting for building interiors.
- **Seamless Integration:** The system is lightweight, low-complexity, and modular, making it easy to incorporate into both new constructions and existing building infrastructures.
- **Practical Validation:** Advances previous lab-scale proofs into a commercially viable, building-integrated technology, supported by detailed photon-to-thermal analysis and numerical simulations.
- **Future Development:** Ongoing improvements focus on enhancing spectral selectivity, increasing thermal insulation for better heat retention, and scaling the architecture for larger-area applications.





Harvesting "wasted light" – photon recycling

Advantages of Harvesting Indoor Lights for Energy Generation

- **1. Energy Efficiency & Sustainability**
- **Utilization of Existing Light Sources**: Converts artificial lighting into usable energy, reducing energy waste., **Renewable Energy Source**: Complements traditional solar energy and decreases reliance on fossil fuels. **Reduced Carbon Footprint**: Lowers greenhouse gas emissions by generating electricity from ambient light. **Highrise Lighting Utilization**: Lights in high-rise buildings often remain on continuously and can be harnessed for energy recovery.
- **2. Economic & Cost-Effectiveness**
- **Energy Savings**: Offsets power consumption in small electronics, reducing electricity bills. **Extended Battery Life**: Reduces the need for frequent battery replacements in low-power devices. **Lower Maintenance Costs**: Indoor light harvesting solutions require minimal upkeep compared to large-scale renewable energy systems.
- **3. Technological & Application Benefits**
- **Works in Low-Light Conditions**: Unlike traditional solar panels, indoor photovoltaics (PVs) operate efficiently under artificial light. **Powering Smart Devices & IoT**: Enables self-sustaining sensors, smart home devices, and wearable electronics. **Integration with Transparent & Flexible Electronics**: Can be implemented in windows, displays, and flexible surfaces.
- **4. Improved Energy Recovery**
- **Higher Utilization of Light Spectrum**: Indoor PVs can be optimized to harvest light from LED and fluorescent sources. **Reduced Energy Loss**: Converts ambient light that would otherwise be wasted into functional energy. **Indoor Photothermal & Photovoltaic Energy Generation**: During cloudy and rainy days, indoor lighting can drive both photovoltaic and photothermal energy generation, ensuring continuous power production.
- **5. Environmental & Practical Advantages**
- **Supports Off-Grid Applications**: Useful in locations with unreliable power sources. **No Need for Outdoor Exposure**: Operates without weather constraints, unlike traditional solar panels. **Enhances Energy-Neutral Buildings**: Contributes to sustainable building designs by integrating energy generation within interior spaces.

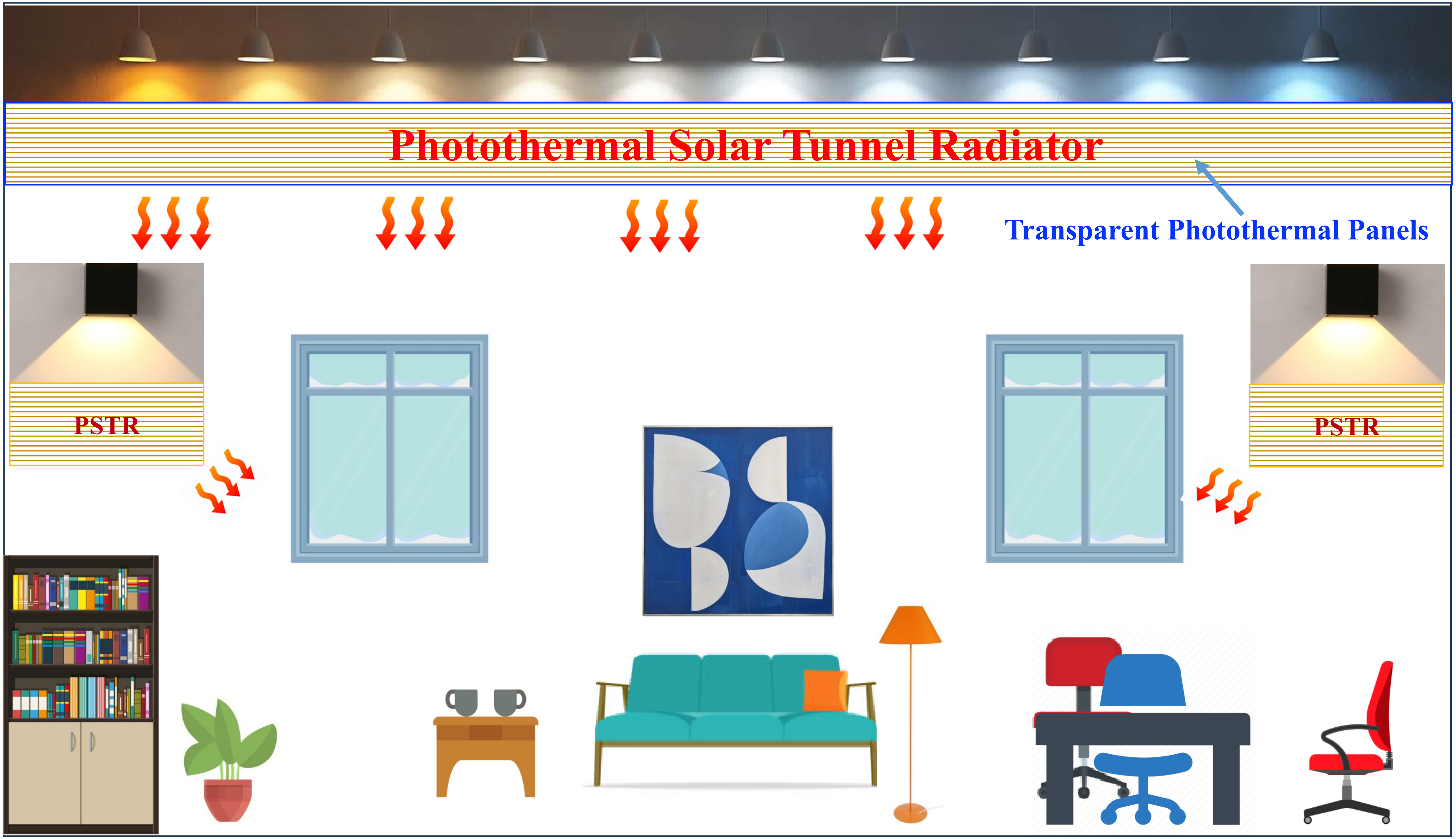
Photothermal Solar Tunnel Radiator
Transparent Photothermal Panels
PSTR
PSTR

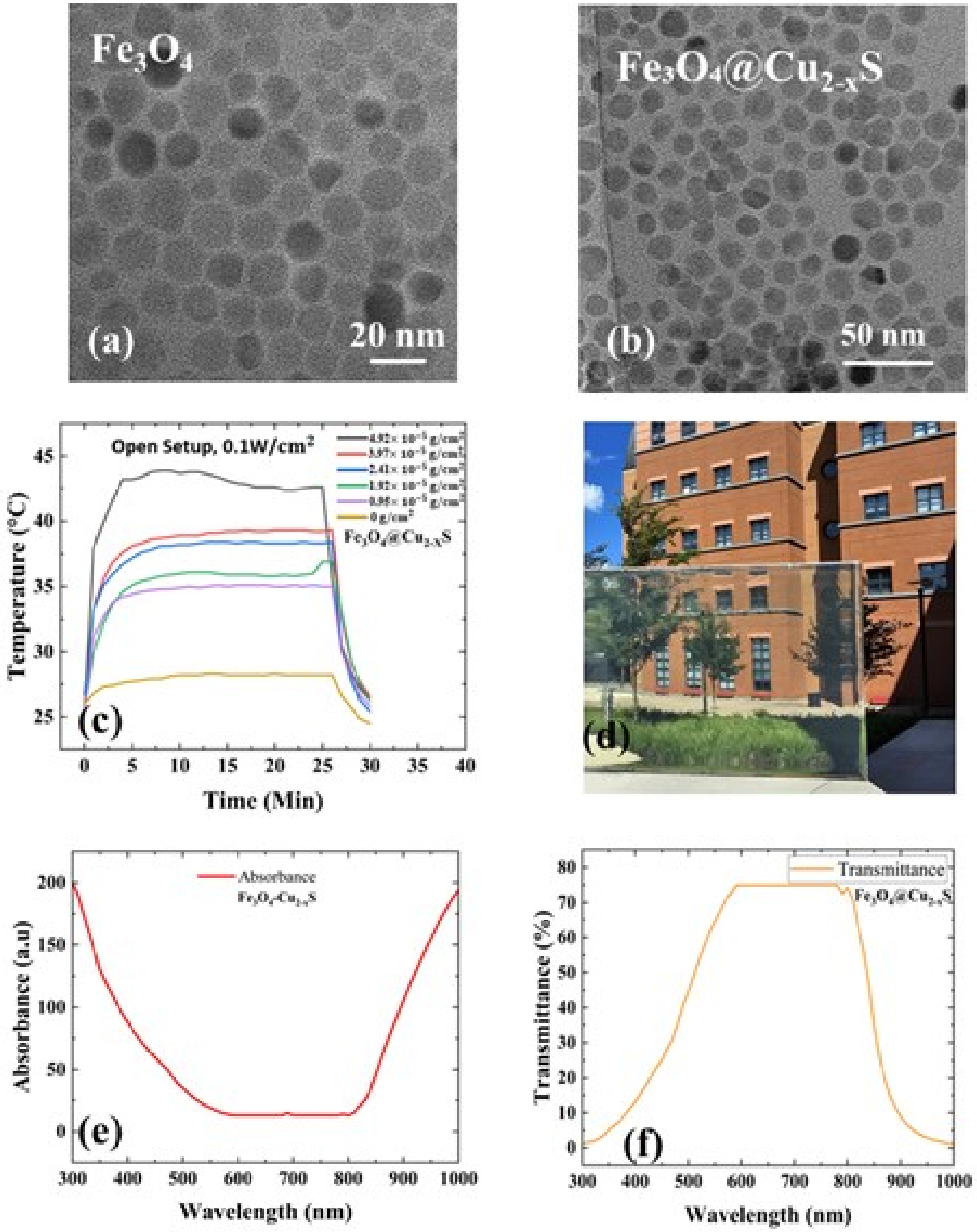

Fe3O4
20 nm
(a)
Fe3O4@Cu2-xS
50 nm
(b)
Open Setup, 0.1W/cm2
4.92× 10-5 g/cm2
3.87× 10-5 g/cm2
2.41× 10-5 g/cm2
1.92× 10-5 g/cm2
0.95× 10-5 g/cm2
0 g/cm2
Fe3O4@Cu2-xS
Temperature (°C)
Time (Min)
(c)
(d)
Absorbance
Fe3O4-Cu2-xS
Absorbance (a.u)
Wavelength (nm)
(e)
Transmittance
Fe3O4@Cu2-xS
Transmittance (%)
Wavelength (nm)
(f)

Experimental set up

- To simulate indoor conditions and investigate the heating effectiveness under diffused light, a Diffused Light Photothermal Box (DLPB) was custom-built.
- The transparent photothermal panels (TPTP) used in the experiment were coated with the $Fe_3O_4@Cu_{2-x}S$ thin films.
- The design of the DLPB was tailored to mimic building environments, featuring a vertical photothermal tunnel encased within a transparent PMMA box measuring 50 cm (length) × 37 cm (width) × 50 cm (height).
- Within this photothermal tunnel, eight removable TPTPs were arranged horizontally in parallel for efficient photon collection.
- To enhance energy harvesting, the interior of the tunnel was lined with mirrors to effectively reflect photons.
- Each TPTP utilized in the experiment was crafted with dimensions of 18 cm (length) × 13 cm (width) × 3 mm (height), ensuring a uniform heating surface area throughout the study.

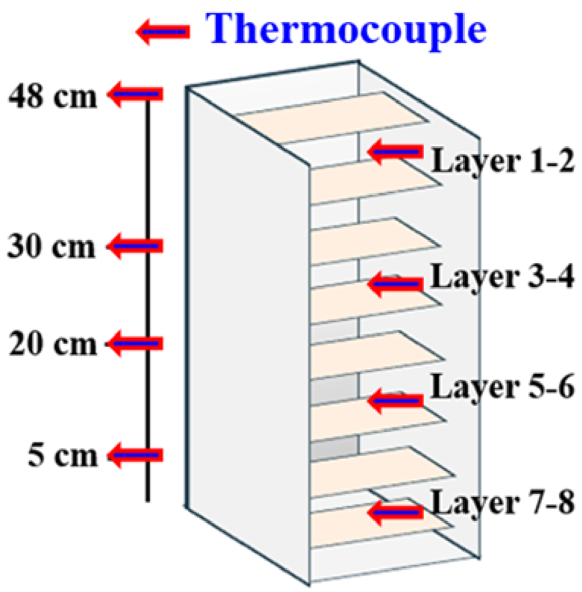

Experimental details

- The average visible transmittance (AVT) of the photothermal panels was precisely maintained at 75%, while that of the polymethyl methacrylate (PMMA) box enclosing the setup was maintained at 93%.
- Both IR and UV lamps are utilized to simulate diffused lights.
- The NIR lamp: 850 nm and UV lamp: 380 nm.
- The light power density (LPD) for all lighting conditions is controlled at 15 mW/cm^2.
- LPD measurements are obtained using the Newport Optical Power Meter Model 1600-R.

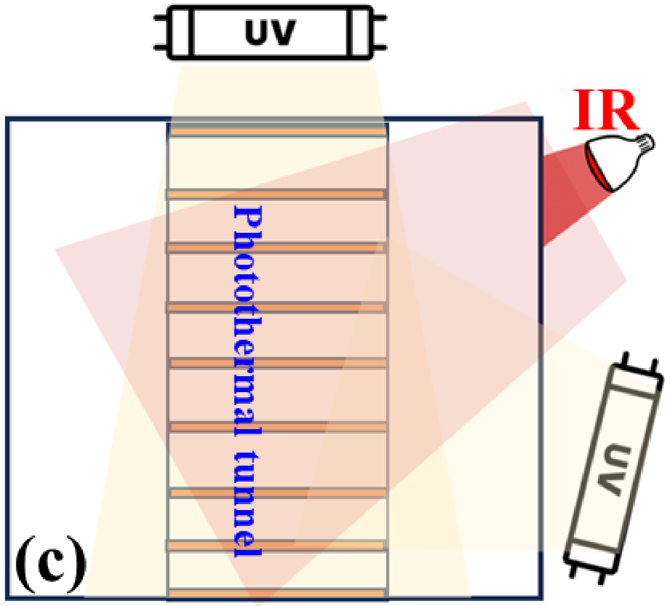

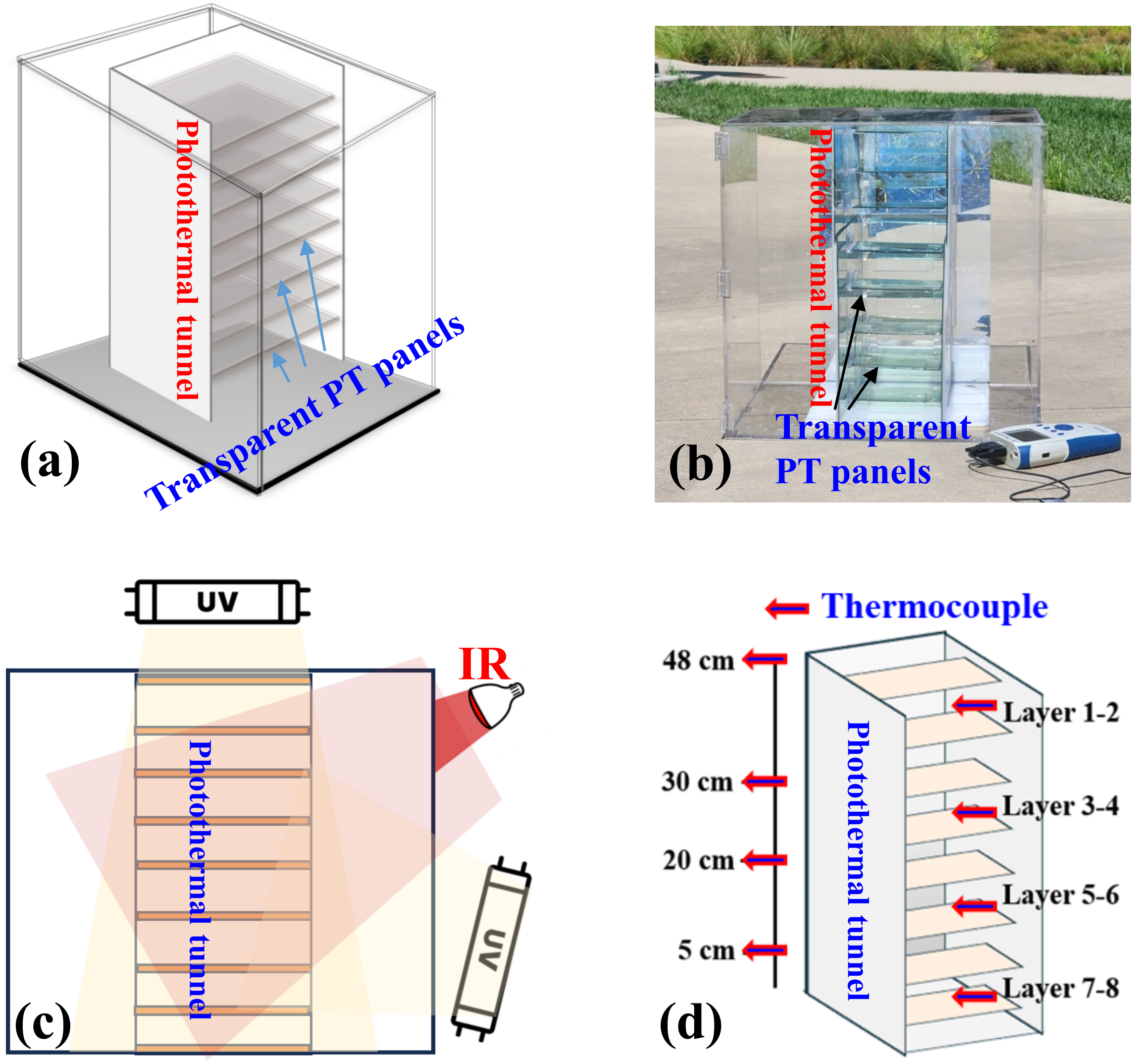

Photothermal Utility Heating with Diffused Indoor Light via Multiple Transparent Fe3 O4 @Cu2− x S Thin Films, Katepalli, Anudeep | Tene, Neshwanth Kumar | Wang, Yuxin | Harfmann, Anton | Bonmarin, Mathias | Krupczak, John | Shi, Donglu, *Energy Technology, volume 12, issue 8 (2024).* 10.1002/ente.202400703

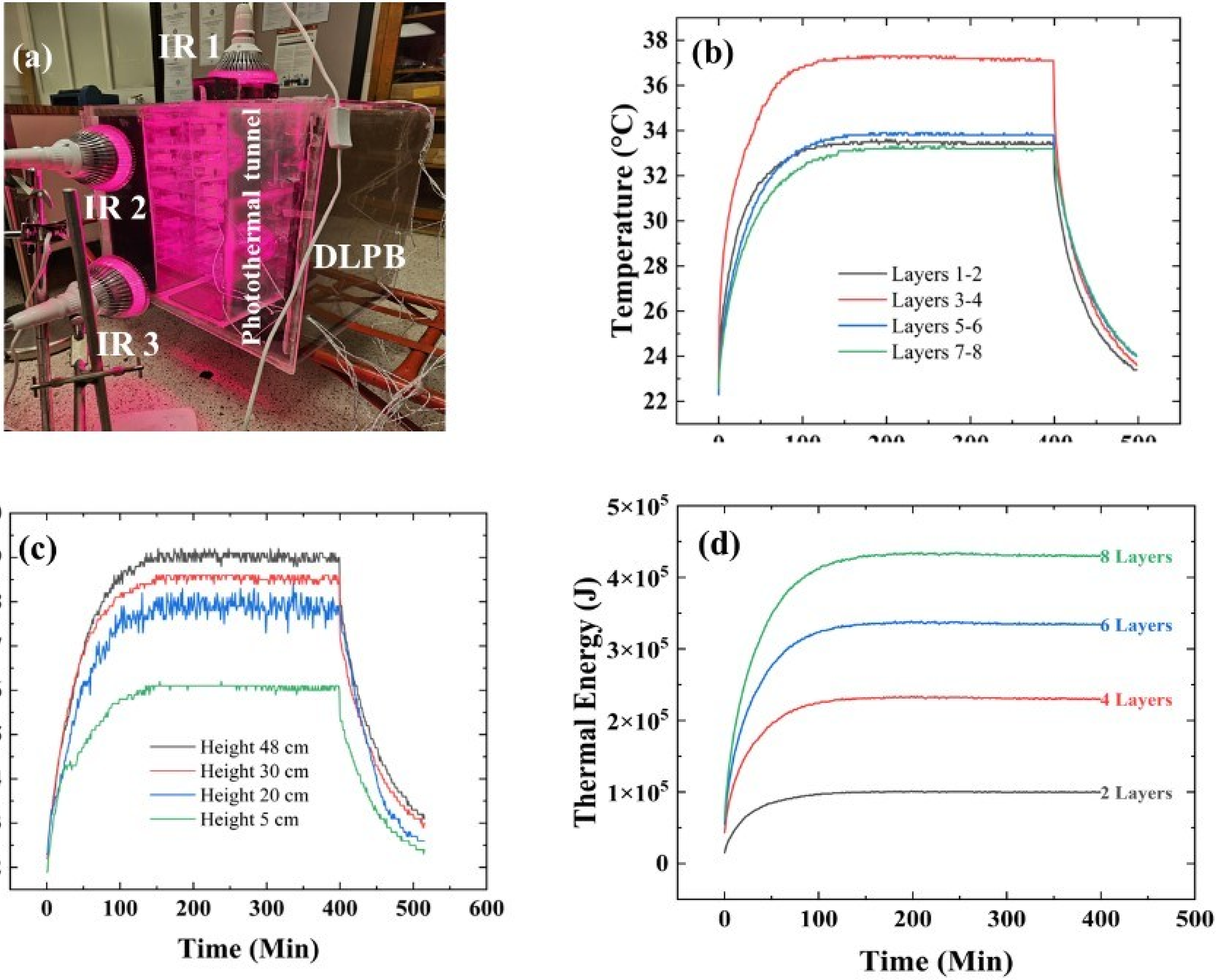
(a)
IR 1
IR 2
IR 3
Photothermal tunnel
DLPB
(b)
Temperature (°C)
38
36
34
32
30
28
26
24
22
Layers 1-2
Layers 3-4
Layers 5-6
Layers 7-8
(c)
Temperature (°C)
30
29
28
27
26
25
24
23
22
Height 48 cm
Height 30 cm
Height 20 cm
Height 5 cm
0
100
200
300
400
500
600
Time (Min)
(d)
Thermal Energy (J)
5×10^5
4×10^5
3×10^5
2×10^5
1×10^5
0
8 Layers
6 Layers
4 Layers
2 Layers
0
100
200
300
400
500
Time (Min)

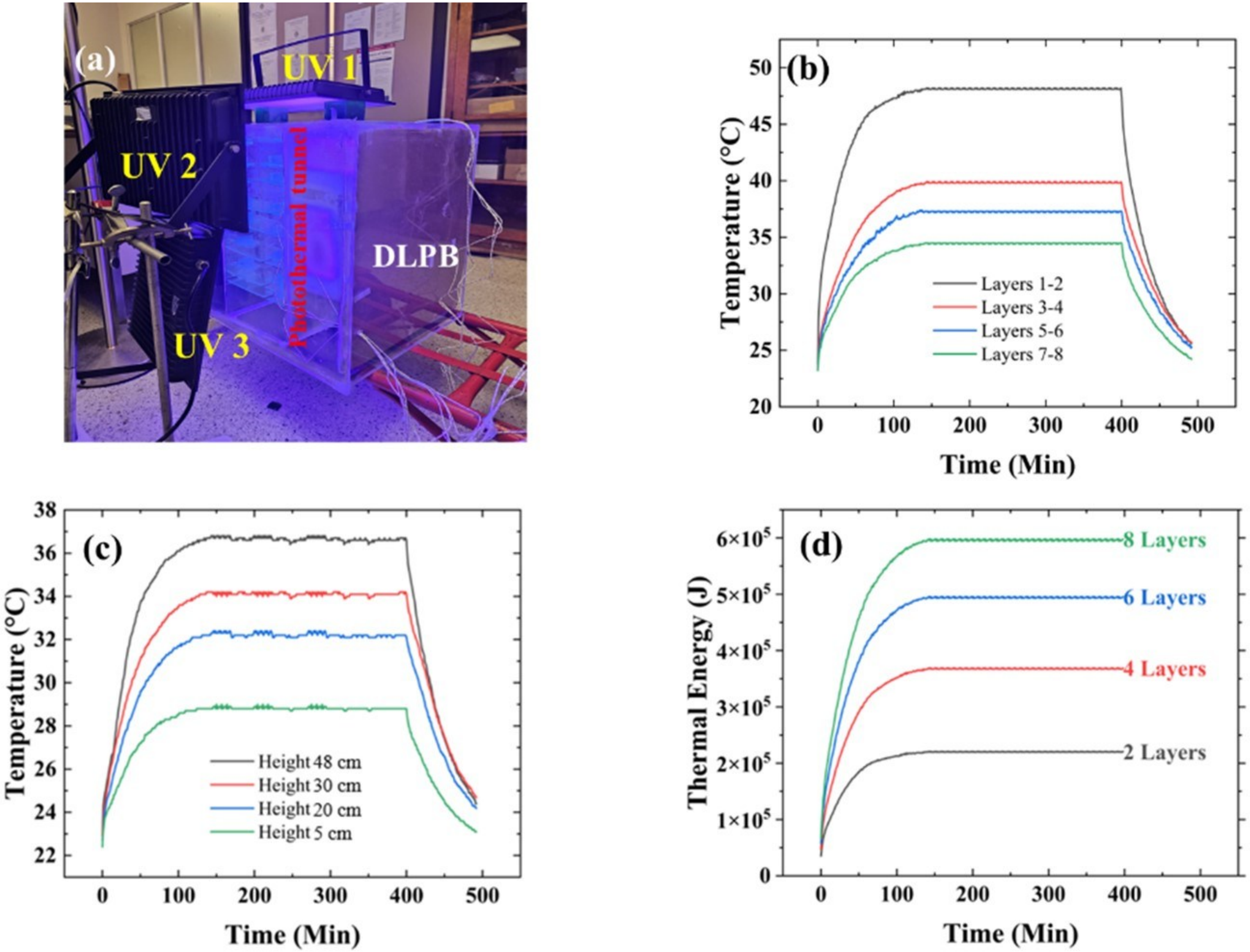
(a)
UV 1
UV 2
UV 3
Photothermal tunnel
DLPB
(b)
Temperature (°C)
Time (Min)
Layers 1-2
Layers 3-4
Layers 5-6
Layers 7-8
(c)
Temperature (°C)
Time (Min)
Height 48 cm
Height 30 cm
Height 20 cm
Height 5 cm
(d)
Thermal Energy (J)
Time (Min)
8 Layers
6 Layers
4 Layers
2 Layers

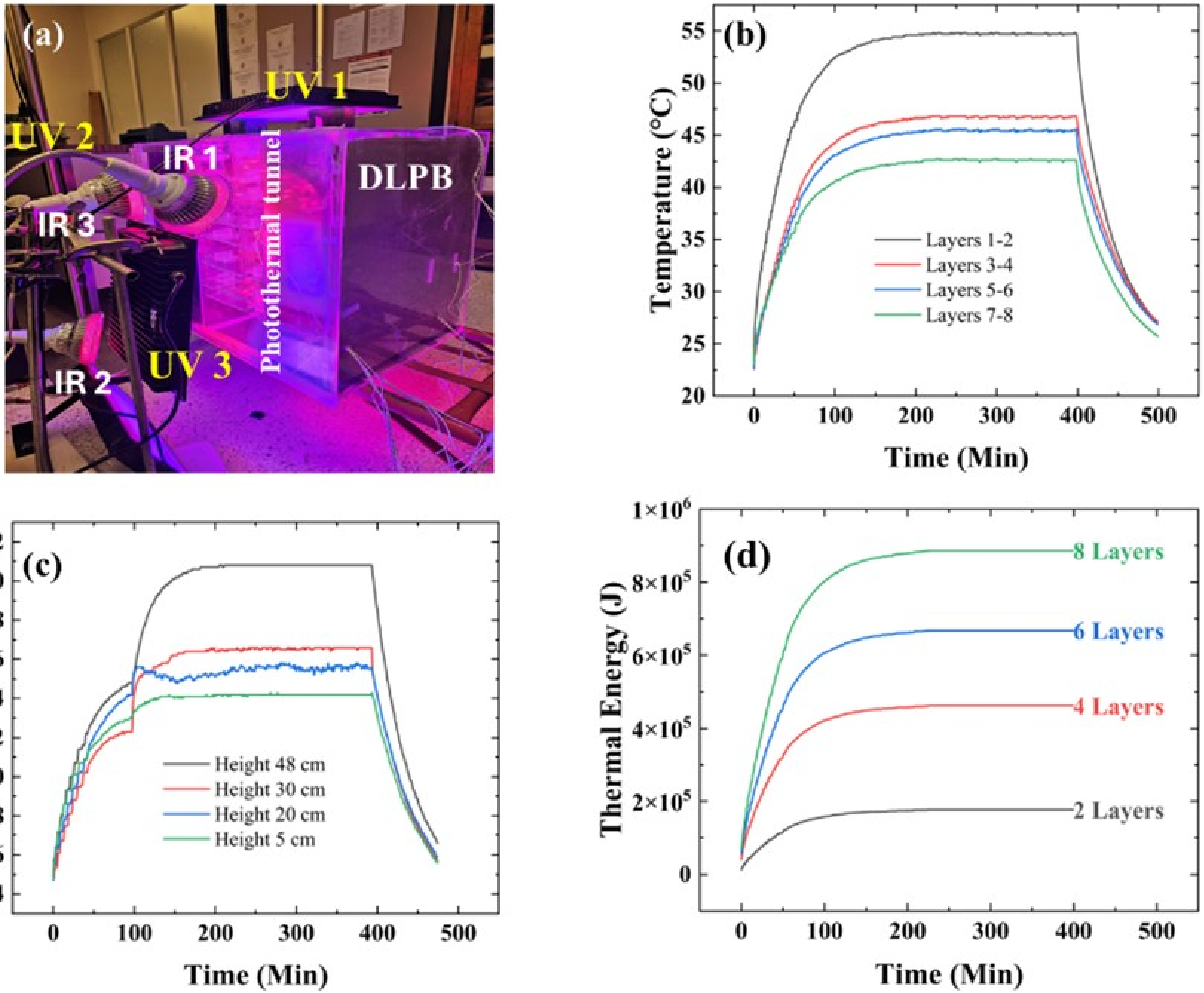
(a)
UV 1
UV 2
IR 1
IR 3
IR 2
UV 3
Photothermal tunnel
DLPB
(b)
Temperature (°C)
Time (Min)
Layers 1-2
Layers 3-4
Layers 5-6
Layers 7-8
(c)
Temperature (°C)
Time (Min)
Height 48 cm
Height 30 cm
Height 20 cm
Height 5 cm
(d)
Thermal Energy (J)
Time (Min)
8 Layers
6 Layers
4 Layers
2 Layers

Conclusions

- Synthesized spectral selective plasmonic particles with strong UV and IR absorptions.
- The photothermal thin films are highly transparent.
- Demonstrated solar and indoor light harvesting via multiple panels.
- Utilized a solar tunnel for spectral selective photon harvesting and efficient Photothermal energy generation.
- Novel Photothermal Solar Tunnel (PTST): Introduces an innovative solar harvesting system for direct and efficient conversion of sunlight into thermal energy.
- Superior Thermal Performance: Demonstrates significant heating capability, raising internal tunnel temperatures from subzero ambient conditions (-5°C to -7°C) to
- above 30.9°C on panel surfaces and 22.8°C within the tunnel interior.
- Sustainable and Cost-Effective: Offers a scalable and low-cost alternative to conventional photovoltaic (PV)-based heating systems, reducing reliance on fossil fuels.
- Strong Heat Retention and Stability: Exhibits excellent temperature stabilization even under intermittent sunlight exposure, making it suitable for various environmental
- conditions.

 

•**Inefficient land use:** 2D PV farms require vast surface areas that could otherwise support food production, forestry, or natural ecosystems.

•**Limited availability:** Suitable open fields are scarce, especially in urban and densely populated regions, restricting large-scale deployment.

Intrinsic Limitations of PV

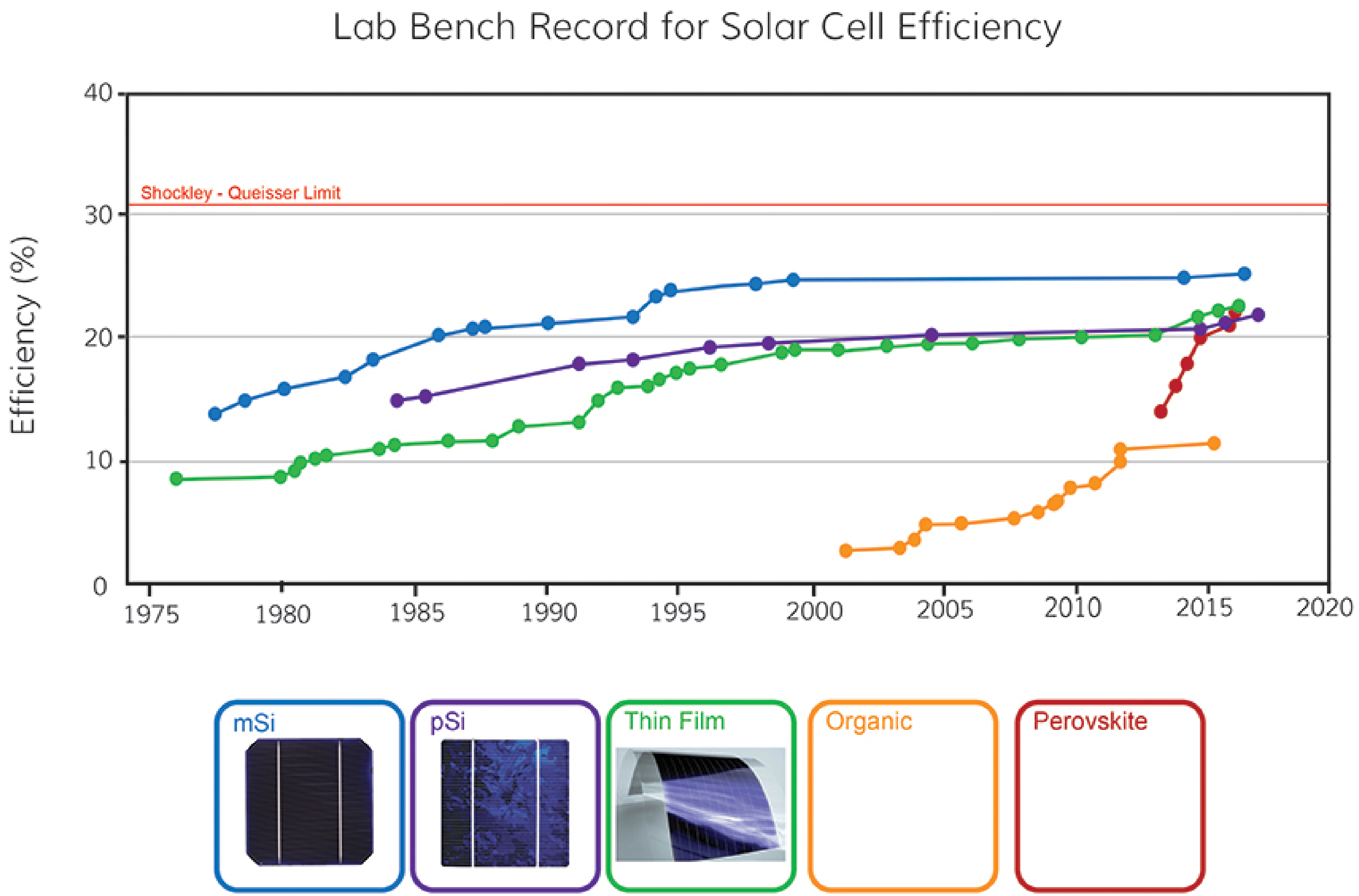

Source: NREL

https://www.viridiansolar.co.uk/resources-4-2-1-solar-cell-efficiencies.html

Spectrum losses – Spectral Efficiency

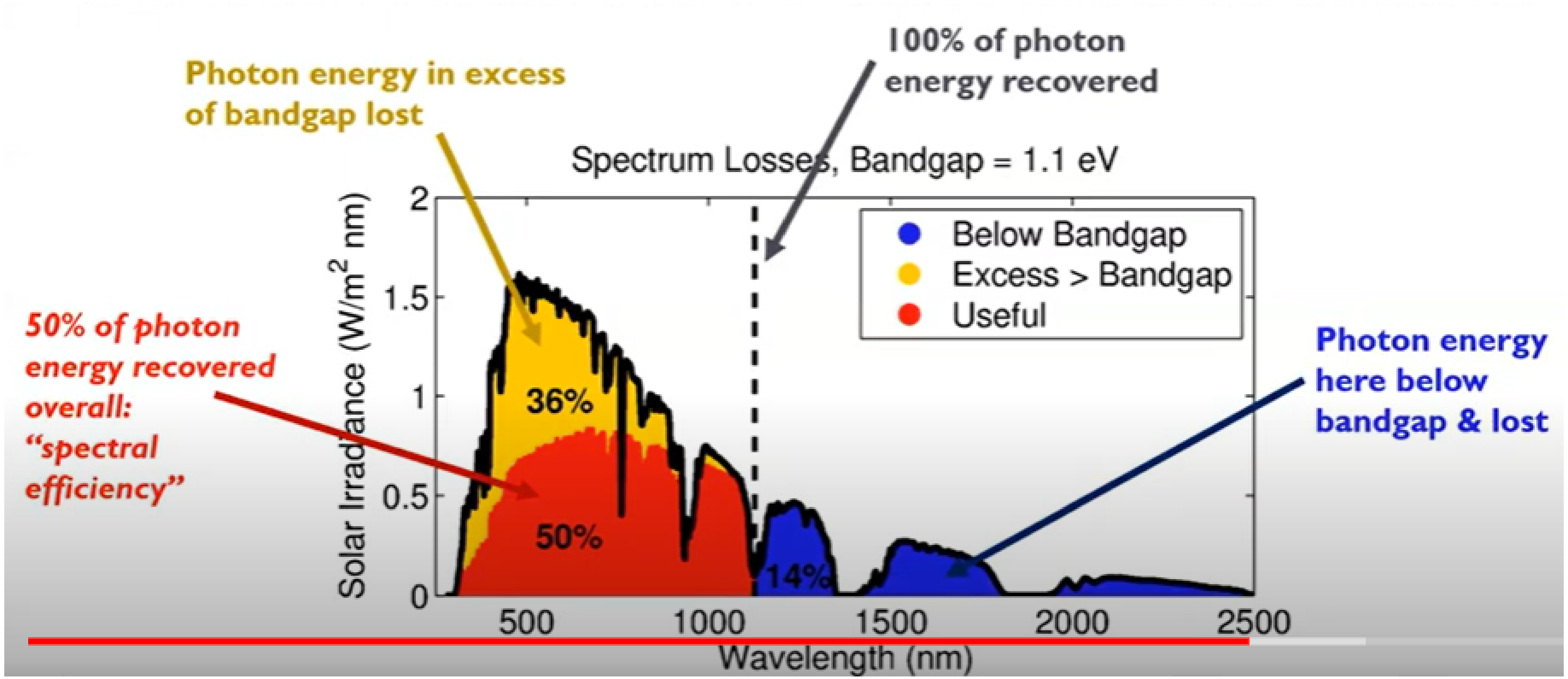

The Shockley-Queisser Limit for Solar Cell Efficiency (Steffen Eikenberry)

Temperature dependence of PV PCE

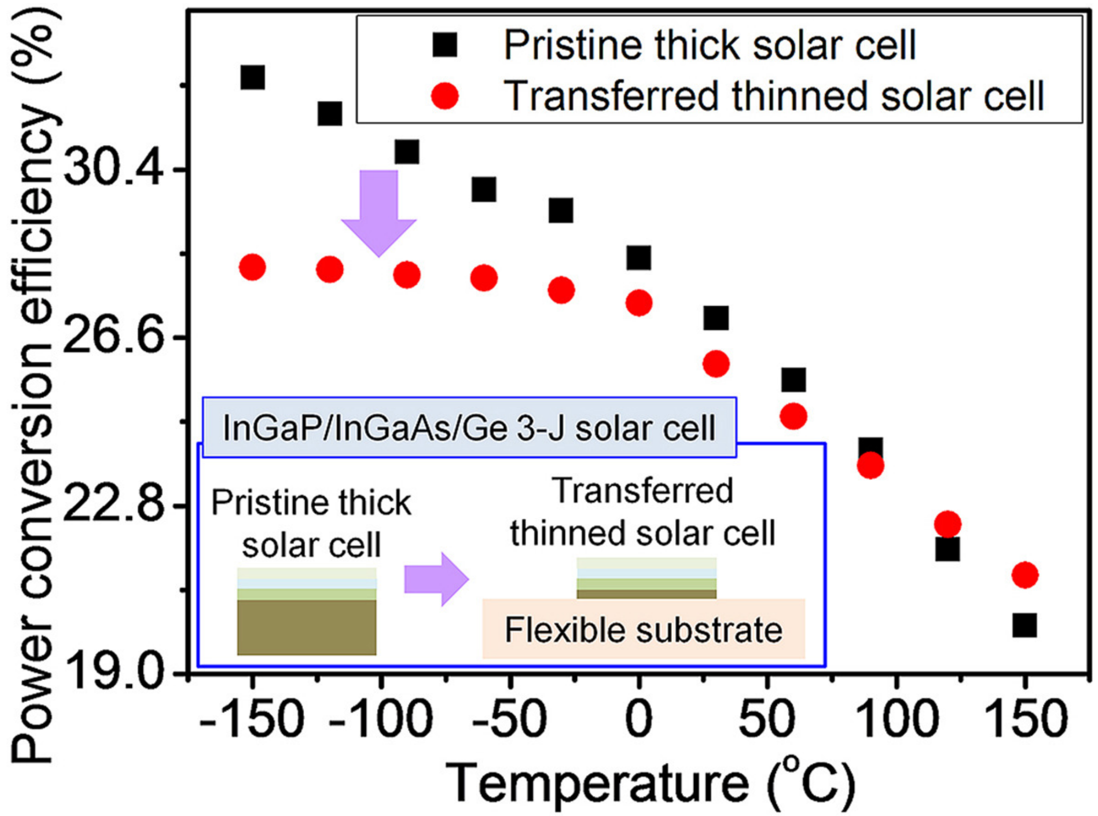

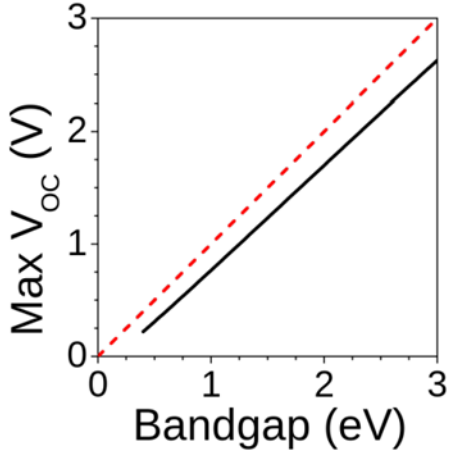

Lee et al, Current Applied Physics, Volume 16, Issue 12, December 2016, Pages 1674-1679

Increases in temperature reduce the bandgap of a semiconductor, thereby affecting most of the semiconductor material parameters. The open-circuit voltage decreases with temperature.

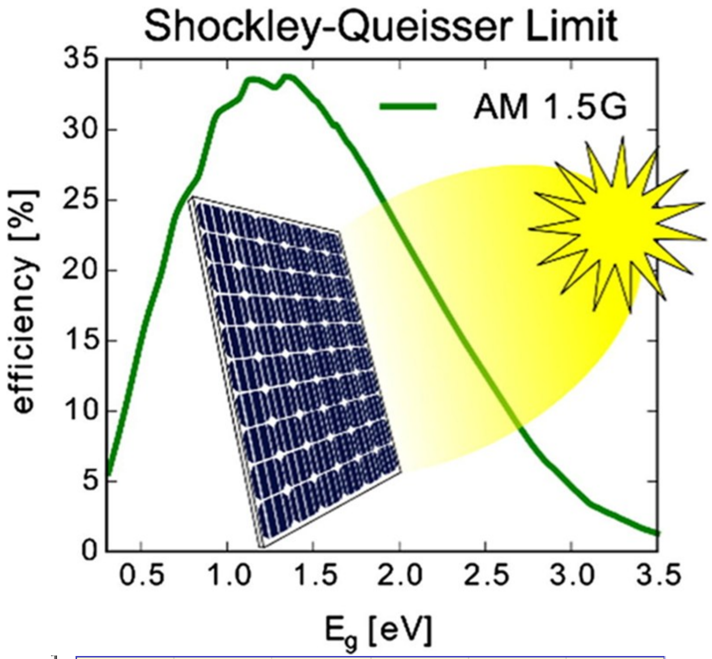

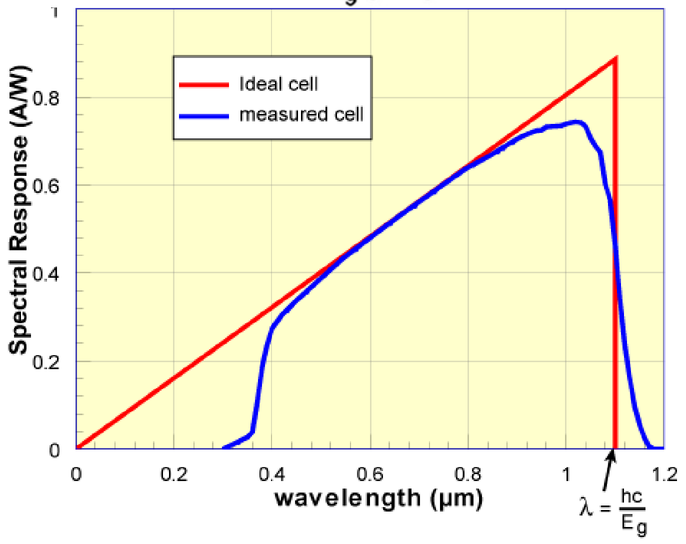

The band gap of silicon (E_g = 1.12 eV).

- The ideal spectral response is limited at long wavelengths by the inability of the semiconductor to absorb photons with energies below the band gap.
- Spectral response decreases at small photon wavelengths. Any energy above the band gap energy is not utilized by the solar cell and instead goes to heating the solar cell.
- The inability to fully utilize the incident energy at high energies, and the inability to absorb low energies of light represents a significant power loss in solar cells consisting of a single *p-n* junction.

Sven Rühle, Solar Energy, Volume 130, June 2016, Pages 139-147

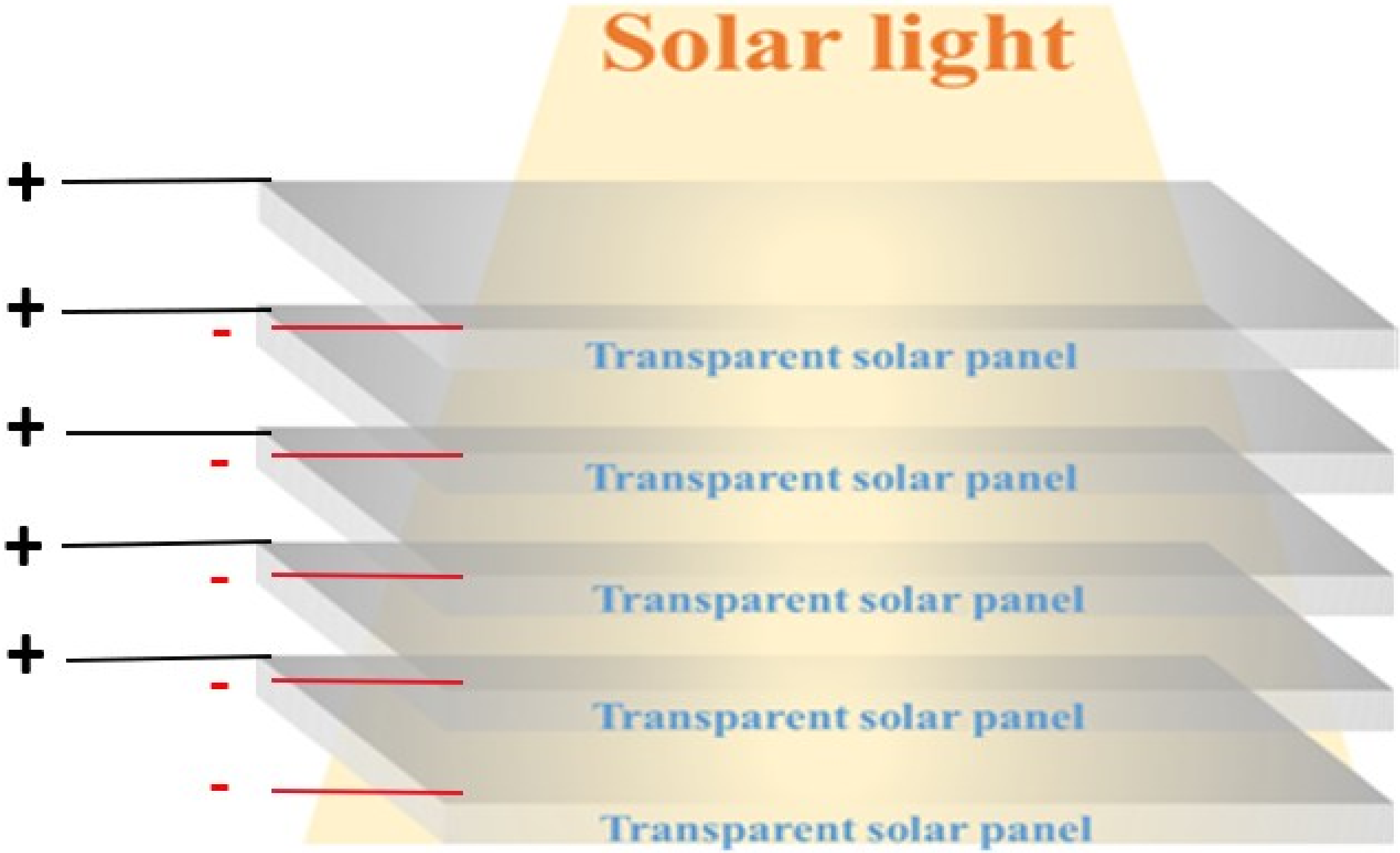

Schematic diagrams showing the concept of 3D solar light harvesting via multiple transparent solar panels.

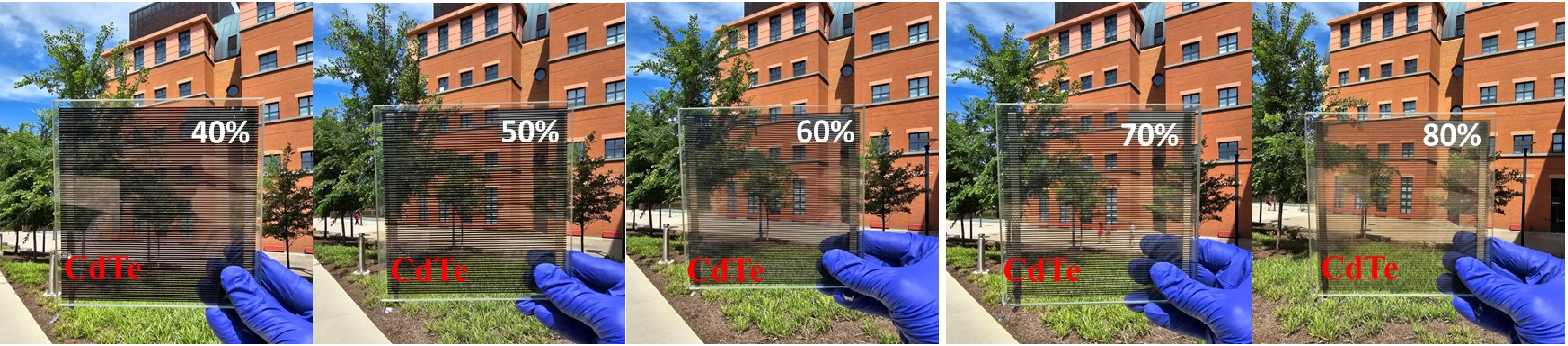

Photographs of CdTe solar photovoltaic (PV) panels with different AVTs: 40%,50%,60%,70%, 80%.

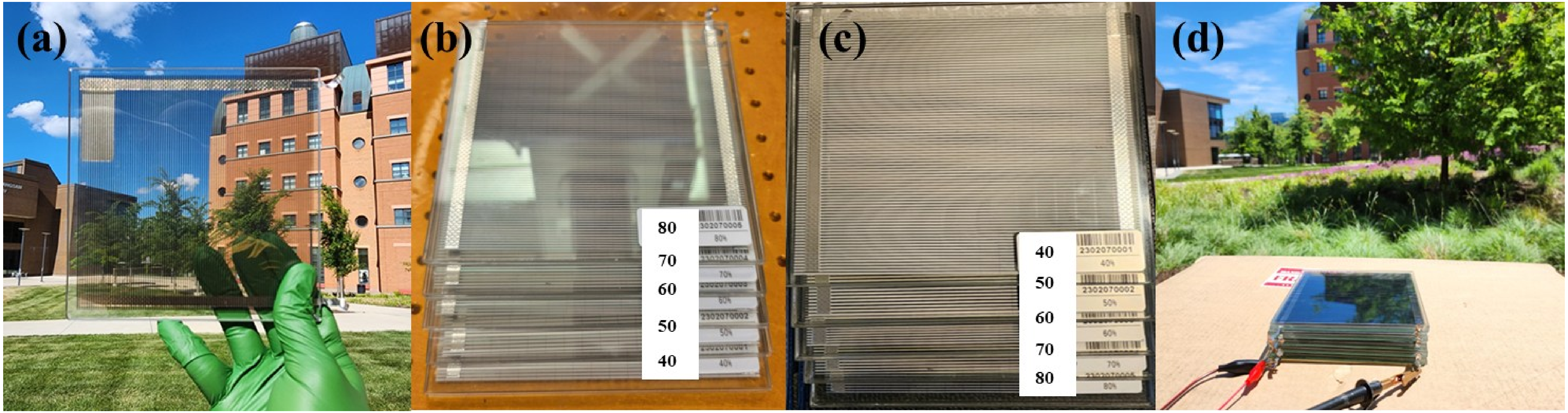

Photographs of (a) 80% CdTe solar panel on campus; (b) five CdTe solar panels stacked in parallel with descending transparency: 80%,70%,60%,50%, 40%, (c) five CdTe solar panels stacked in parallel with ascending transparency: 40%,50%,60%,70%, 80%, (d) I-V measurement set for five CdTe solar panels stacked in parallel

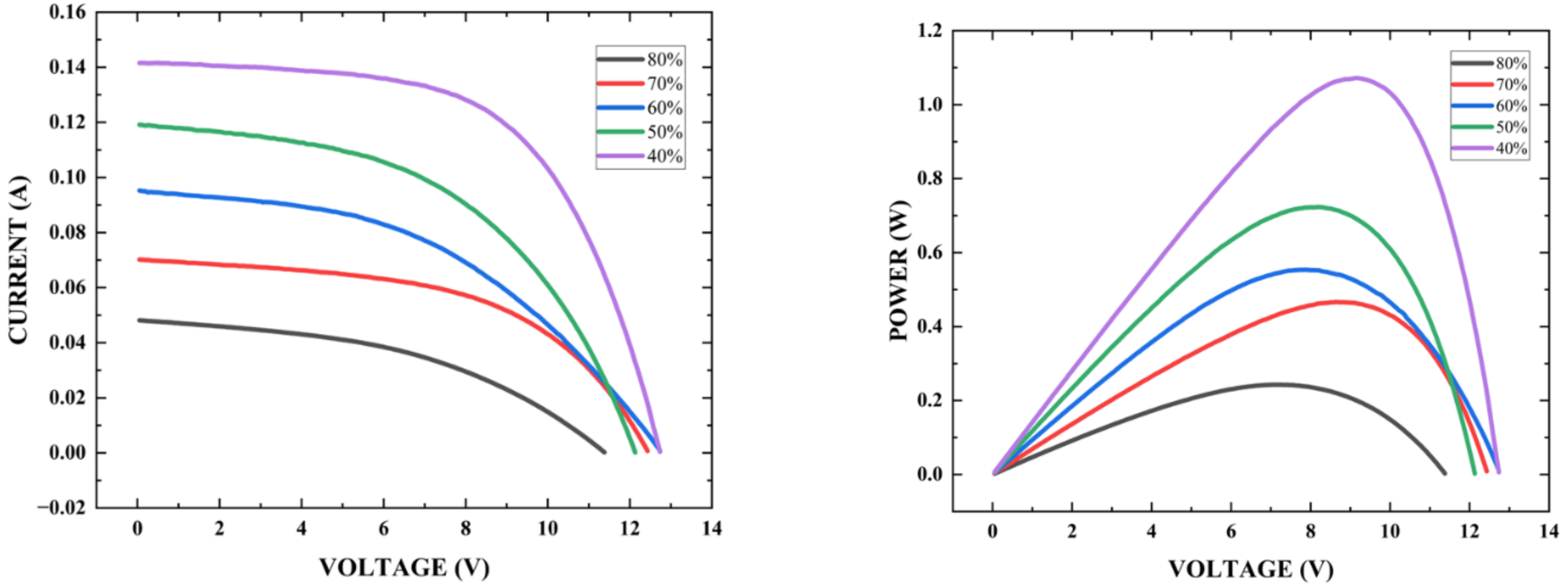

(a) I-V curves and (b) Output power of single layer CdTe solar panels with different transparencies

Solar Panel	Light Power Density (mW/cm^2)
PANEL 1 (80% AVT)	55.40
PANEL 2 (70% AVT)	44.32
PANEL 3 (60% AVT)	31.02
PANEL 4 (50% AVT)	18.61
PANEL 5 (40% AVT)	9.31

Solar Panel	Light Power Density (mW/cm^2)
PANEL 1 (40% AVT)	55.40
PANEL 2 (50% AVT)	22.16
PANEL 3 (60% AVT)	11.08
PANEL 4 (70% AVT)	6.65
PANEL 5 (80% AVT)	4.65

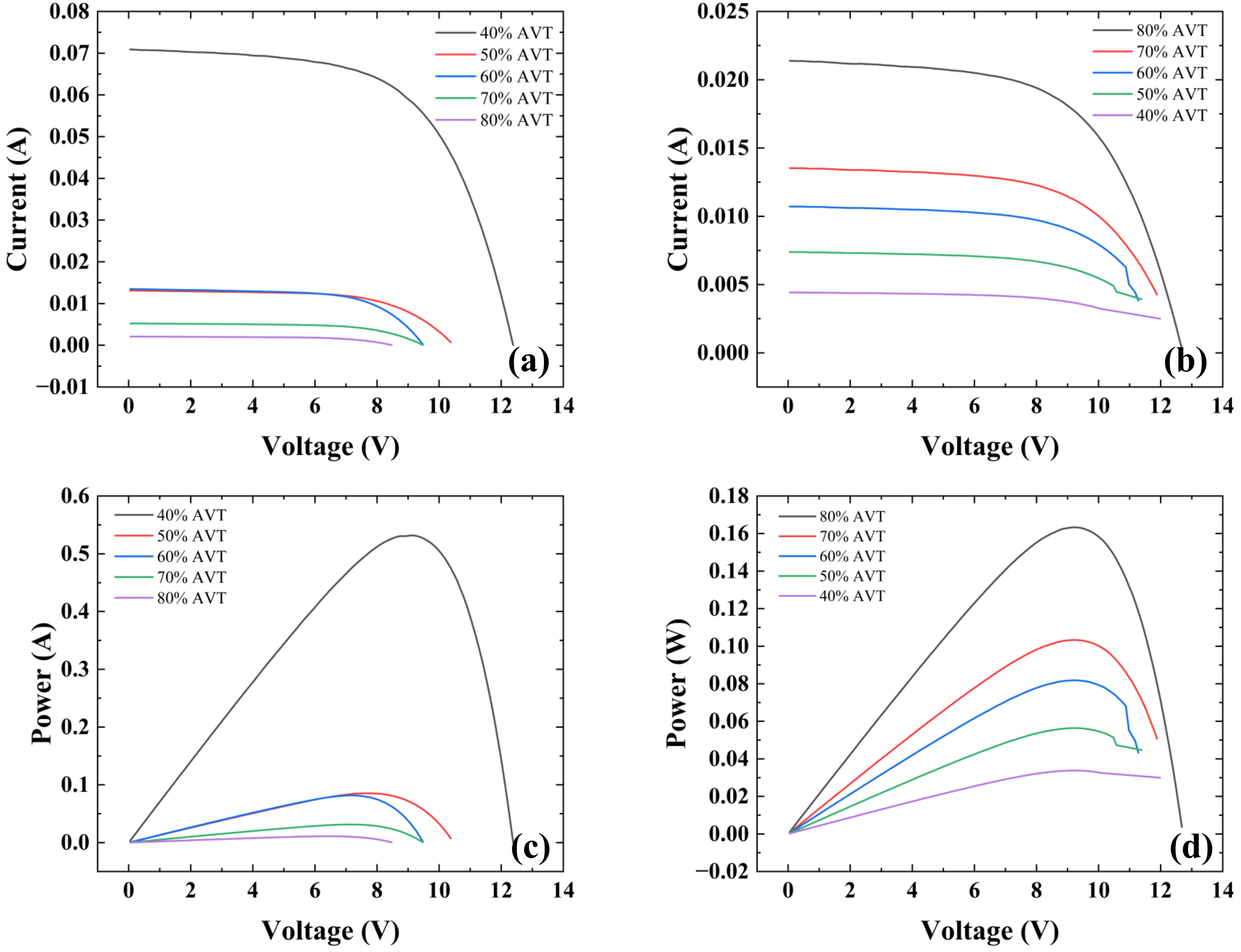

Figure 9a illustrates the I-V curves for the multi-panels arranged in ascending order; Figure 9b illustrates the I-V curves for the multi-panels arranged in descending order

PCE value of each CdTe solar panel in both descending and ascending orders. The PCE values of all five solar panels are also presented in both orders.

Solar Panel AVT	PCE Ascending	Solar Panel	PCE Descending
1st 40%	9.60%	1st 80%	1.89%
2nd 50%	3.25%	2nd 70%	3.02%
3rd 60%	1.87%	3rd 60%	1.57%
4th 70%	1.52%	4th 50%	2.16%
5th 80%	1.05%	5th 40%	2.24%
All panels	**17.29%**		**10.88%**

Harvesting Indoor Light for Continuous Electricity Generation with Semitransparent CdTe Solar Cells: Toward Energy-Neutral Buildings and Sustainable Built Environments

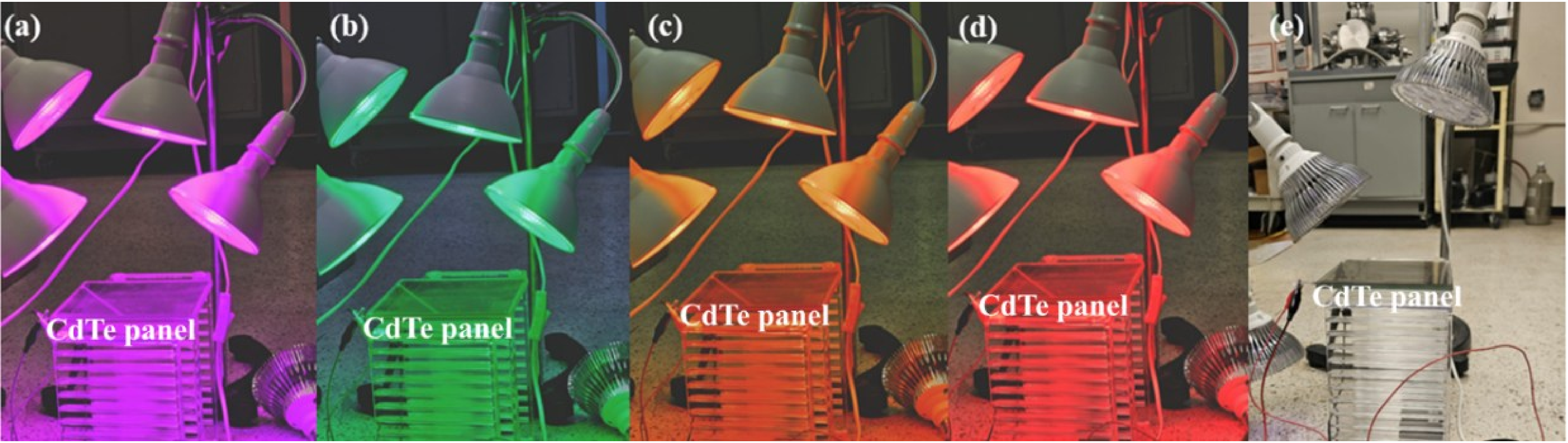

Photographs of I-V measurement set up: (a) purple lights, (b) green lights, (c) orange lights, (d) red lights, and (e) IR lights.

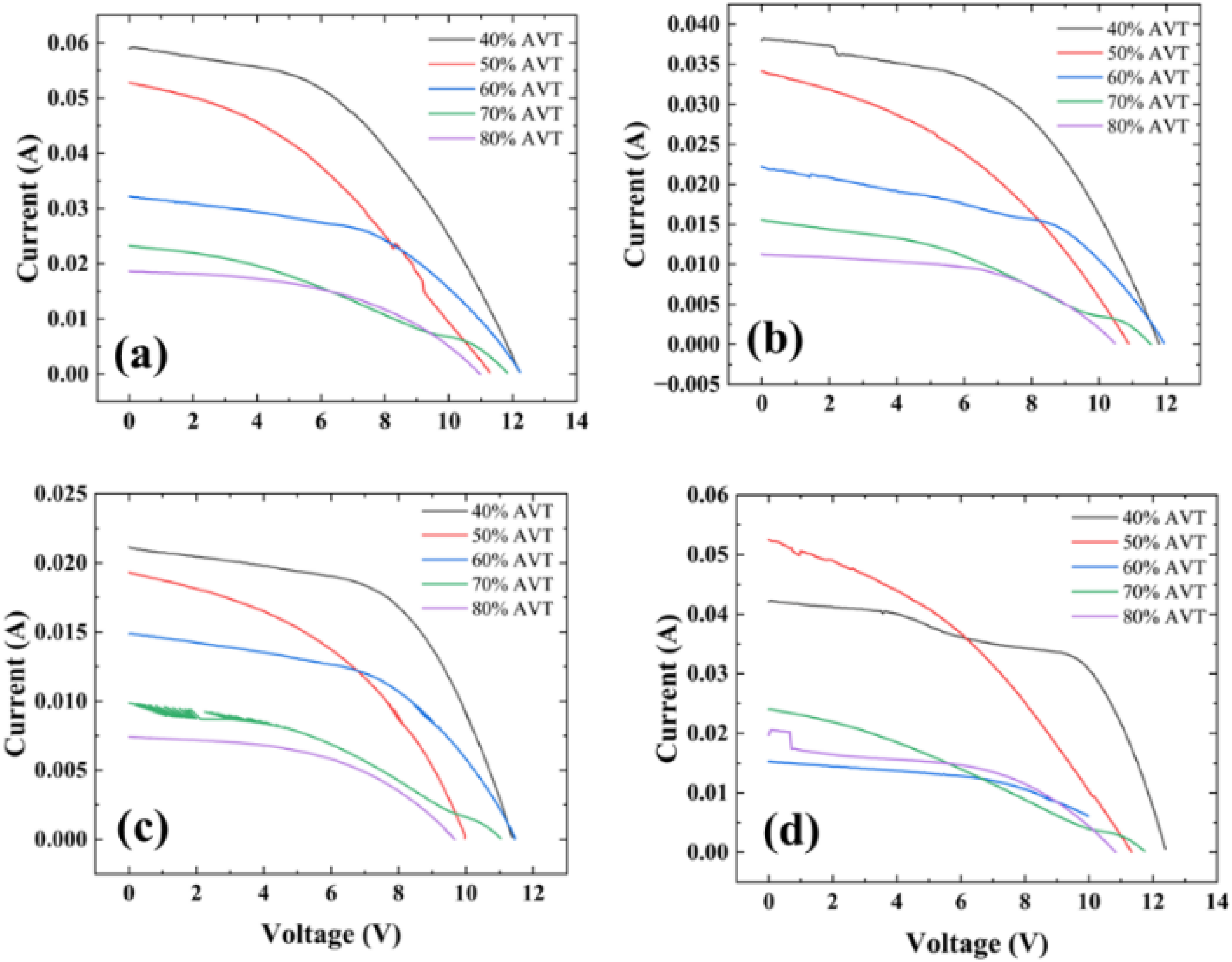

I-V curves of the CdTe solar panels of different AVTs as indicated under LEDs of different wavelengths (a) purple: 380 nm – 435 nm, (b) green: 495 nm – 570 nm, (c) orange: 585 nm – 620 nm, and (d) red: 630 nm – 750 nm.

The I-V curve parameters of the CdTe solar panels under purple light (380 nm – 435 nm).

Solar Panel AVT	$V_{OC}\,(V)$	$I_{SC}\,(A)$	$P_{MAX}\,(W)$	F.F	P.C.E	Light Power Density (mW/cm^2)
40%	12.181	0.059	0.334	0.464	4.94%	30
50%	11.278	0.053	0.227	0.379	3.36%	30
60%	12.187	0.032	0.195	0.500	2.88%	30
70%	11.830	0.023	0.094	0.345	1.39%	30
80%	10.977	0.019	0.096	0.460	1.42%	30

The I-V curve parameters of the CdTe solar panels under green light (495 nm – 570 nm)

Solar Panel AVT	$V_{OC}\,(V)$	$I_{SC}\,(A)$	$P_{MAX}\,(W)$	F.F	P.C.E	Light Power Density (mW/cm^2)
40%	11.378	0.021	0.134	0.560	1.98%	30
50%	9.969	0.019	0.083	0.438	1.22%	30
60%	11.441	0.015	0.086	0.501	1.27%	30
70%	11.027	0.009	0.041	0.413	0.60%	30
80%	9.674	0.007	0.035	0.516	0.51%	30

The I-V curve parameters of the CdTe solar panels under orange light (585 nm – 620 nm).

Solar Panel AVT	$V_{OC}\,(V)$	$I_{SC}\,(A)$	$P_{MAX}\,(W)$	F.F	P.C.E	Light Power Density (mW/cm^2)
40%	11.780	0.038	0.225	0.502	3.33%	30
50%	10.877	0.034	0.145	0.392	2.14%	30
60%	11.931	0.022	0.129	0.491	1.91%	30
70%	11.534	0.015	0.066	0.381	0.97%	30
80%	10.476	0.011	0.061	0.529	0.90%	30

Table 5 The I-V curve parameters of the CdTe solar panels under red light (620 nm – 750 nm).

Solar Panel AVT	$V_{OC}\,(V)$	$I_{SC}\,(A)$	$P_{MAX}\,(W)$	F.F	P.C.E	Light Power Density (mW/cm^2)
40%	12.381	0.042	0.312	0.599	4.66%	30
50%	11.330	0.052	0.222	0.376	3.28%	30
60%	9.975	0.015	0.085	0.568	1.27%	30
70%	11.730	0.024	0.084	0.298	1.25%	30
80%	10.83	0.019	0.094	0.456	1.40%	30

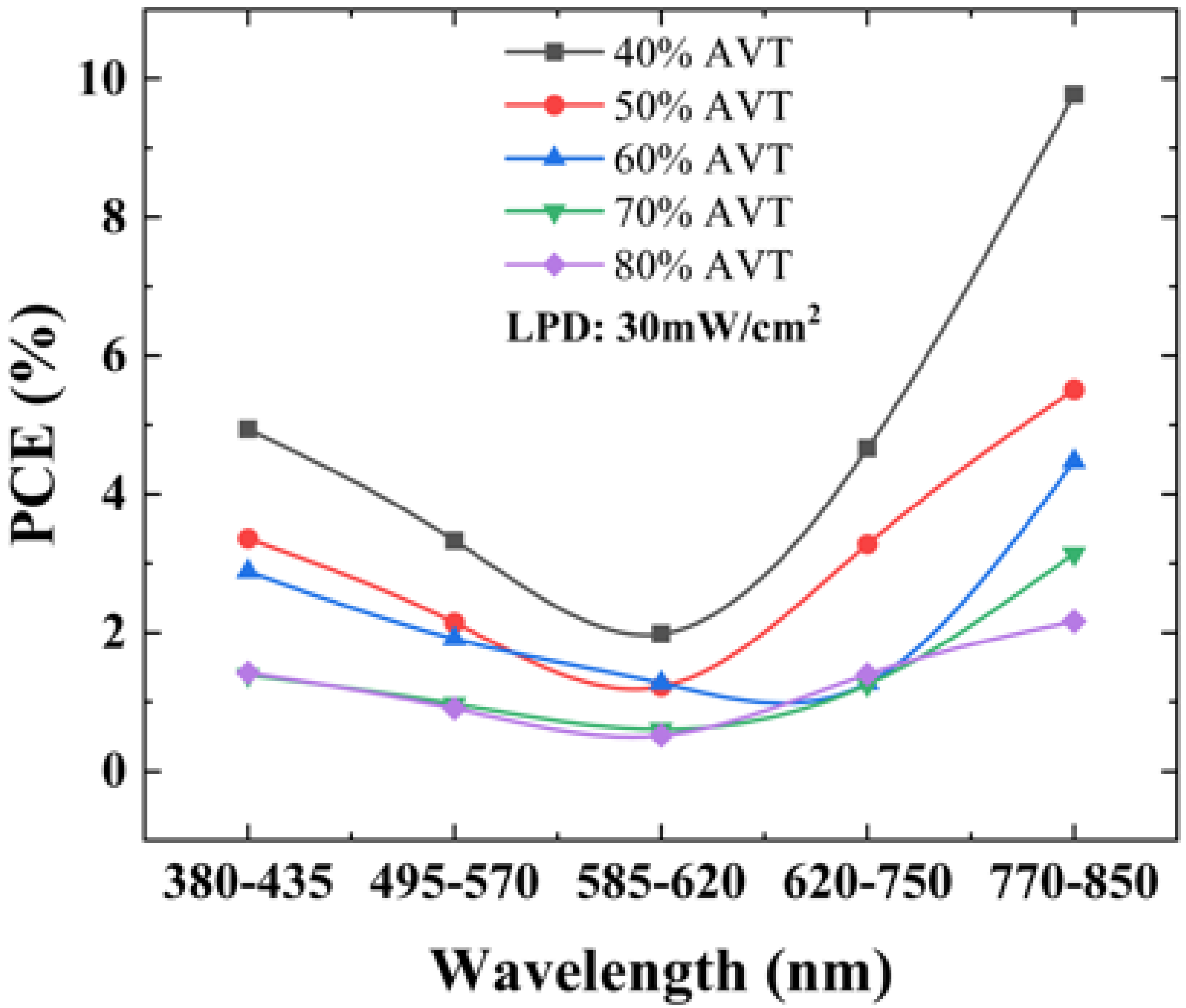

PCEs tend to increase as the LED wavelength approaches 850 nm, corresponding to the bandgap of CdTe (1.5 eV). Notably, a minimum is observed in the visible range around 585 nm to 620 nm.

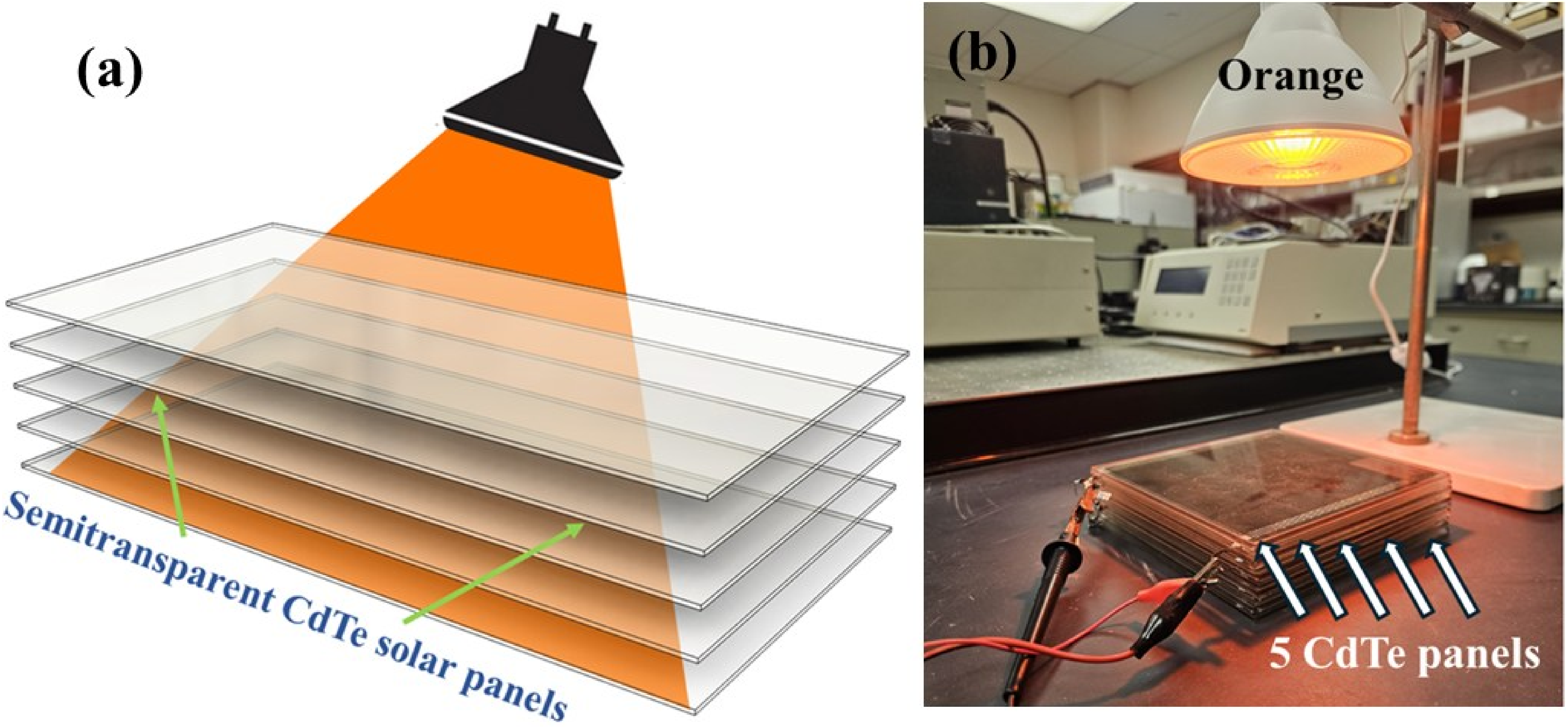

(a) Schematic diagram showing 3D light harvesting through multiple semitransparent CdTe PV panels. (b) Experimental set up with a single orange LED (585 nm – 620 nm) on the top and 5 CdTe PV panels arranged in a stack. The AVT values of the the PV panels are arranged in either descending or ascending order.

Table 9. The I-V curve parameters of a stack of multiple CdTe solar panels in ascending order.

Solar Panel AVT	V_{OC} (V)	I_{SC} (A)	P_{MAX} (W)	FF	P.C.E	Light Power Density (mW/cm^2)
40%	12.68	0.050	0.531	0.837	7.86%	30
50%	10.37	0.047	0.085	0.174	3.14%	12
60%	9.47	0.049	0.051	0.174	3.77%	6
70%	9.58	0.045	0.031	0.071	3.8%	3.6
80%	8.46	0.042	0.011	0.030	1.94%	2.52

Table 10. The I-V curve parameters of a stack of multiple CdTe solar panels in descending order.

Solar Panel AVT	V_{OC} (V)	I_{SC} (A)	P_{MAX} (W)	FF	P.C.E	Light Power Density (mW/cm^2)
80%	12.38	0.021	0.163	0.627	2.41%	30
70%	11.88	0.013	0.103	0.667	1.90%	24
60%	11.27	0.010	0.082	0.727	2.16%	16.8
50%	11.38	0.007	0.056	0.702	2.30%	10.8
40%	11.98	0.004	0.034	0.709	2.99%	5.04

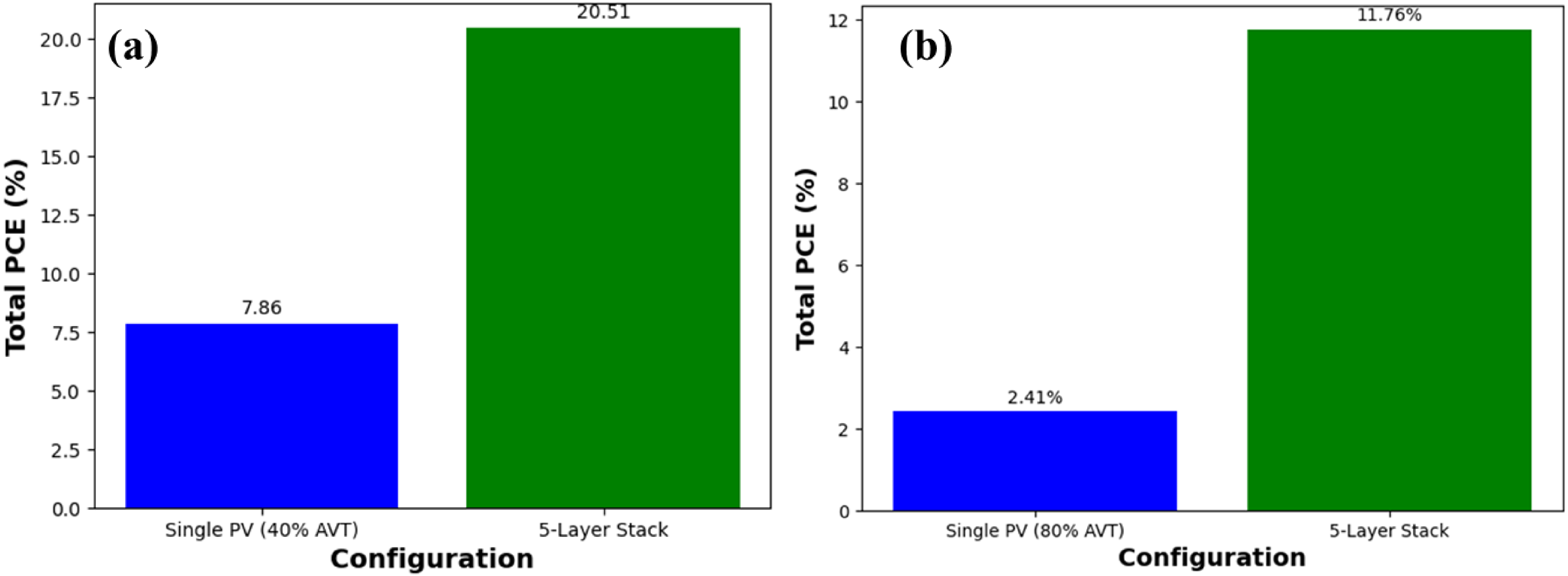

Comparison of total PCE between single PV of 40% VAT vs 5-layer stack.

Transforming Indoor LED Lighting into Continuous Energy

- **Core Breakthrough:** Semitransparent CdTe photovoltaic (PV) panels demonstrate highly efficient Power Conversion Efficiency (PCE) under standard indoor LED lighting.
- **Exponential Efficiency Gains:** Stacking multi-panel systems drastically increases output. A descending Average Visible Transmittance (AVT) configuration boosts total PCE by **387.97%** over a single panel.
- **24/7 Reliability:** Unaffected by weather, seasons, or time of day, indoor systems provide continuous, steady energy generation.
- **Operational Advantages:** Indoor deployment protects panels from environmental stressors, resulting in simpler installation, lower upfront costs, and reduced long-term maintenance.
- **Scalable Impact:** Modeling large-scale deployment (e.g., utilizing 30% of Willis Tower's floor area) proves that harvesting existing continuous lighting yields substantial annual electricity savings.
- **Strategic Vision:** Presents a viable, sustainable pathway for recycling indoor photon energy to achieve **energy-neutral buildings**.

Experimental set up for harvesting LED light with silicon PV panels.

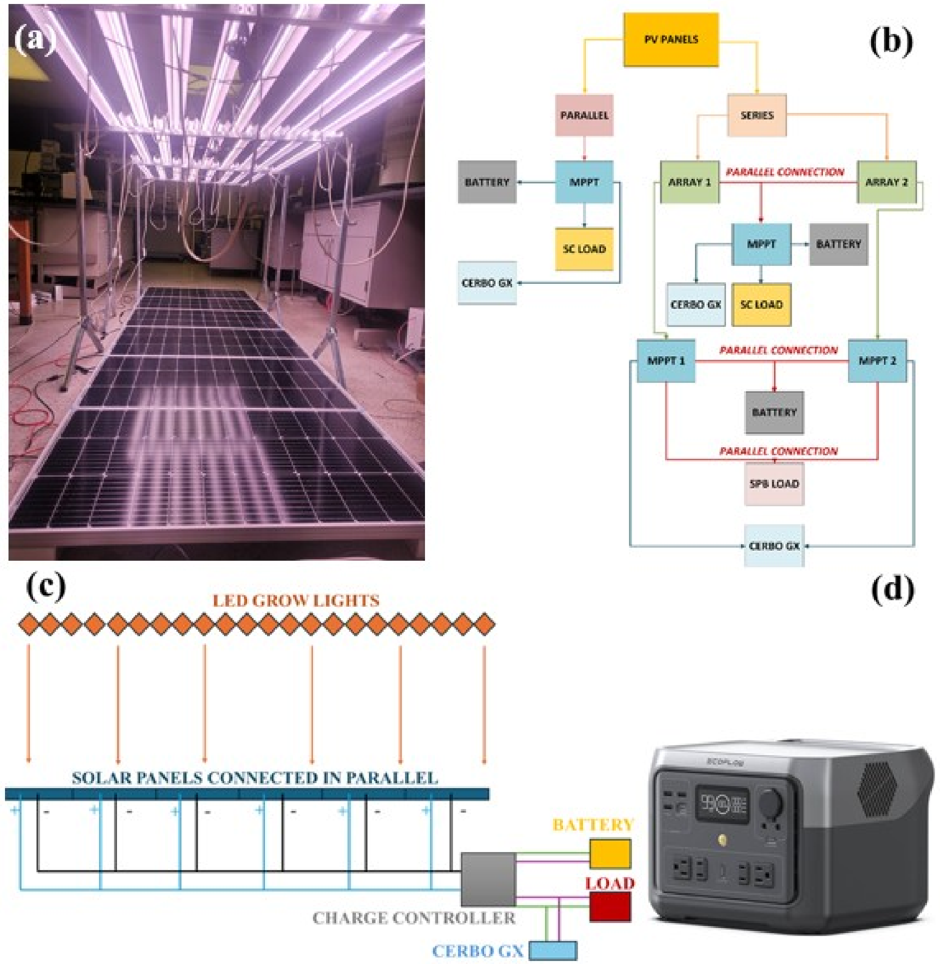

(a) Photograph showing the experimental set up of LEDs over six N-type SPV panels connected in parallel. Light Power Density: 1.4 mW/cm**2**. (b) Schematic diagram showing the PV panels connected in parallel and series. (c) Schematic diagram showing the experimental PV connections with a load. (d) An ECOFLOW Portable Power Station RIVER 2 is connected to the PV system as the load.

Table. 1 IV parameters of Silicon panels in parallel under natural light

Solar Panel Count	V_{OC} (V)	I_{SC} (A)	P_{MAX} (W)	F.F	P.C.E	Light Power Density (mW/cm^2)
1	24.27	4.94	91.66	0.764	22.85%	71.2
2	23.89	9.81	182.13	0.777	22.70%	71.2
3	24.02	14.77	274.13	0.772	22.77%	71.2
4	24.16	19.73	365.68	0.767	22.75%	71.2
5	23.96	24.60	457.70	0.776	22.79%	71.2
6	24.10	29.62	548.52	0.768	22.77%	71.2

Table. 2 IV parameters of Silicon panels in parallel under LED lights

Solar Panel Count	V_{OC} (V)	I_{SC} (A)	P_{MAX} (W)	F.F	P.C.E	Light Power Density (mW/cm^2)
1	2.97	2.13	2.91	0.459	37%	1.4
2	2.97	4.26	5.83	0.460	37%	1.4
3	2.97	6.39	8.75	0.461	37%	1.4
4	2.97	8.52	11.66	0.460	37%	1.4
5	2.97	10.65	14.58	0.460	37%	1.4
6	2.97	12.8	17.50	0.460	37%	1.4

Table. 3 IV parameters of Silicon panels in series under LED lights

Solar Panel Count	V_{OC} (V)	I_{SC} (A)	P_{MAX} (W)	F.F	P.C.E	Light Power Density (mW/cm^2)
1	9.55	0.77	3.75	0.509	47.5%	1.4
2	19.10	0.77	7.5	0.510	47.5%	1.4
3	28.65	0.77	11.25	0.509	47.5%	1.4
4	38.20	0.77	15	0.509	47.5%	1.4
5	47.75	0.77	18.75	0.510	47.5%	1.4
6	57.30	0.77	22.5	0.509	47.5%	1.4

Summary

- High efficiency: Silicon-based PV systems can achieve up to 31% PCE under indoor LED lighting, near the theoretical limit.
- Key advantages: Efficiency benefits from spectral alignment with silicon, reduced losses, and stable, directional LED sources.
- System design: Both series and parallel configurations optimize output under low-light conditions; photon recycling exceeds 37%.Reliability: Proven performance under continuous illumination, especially in urban, high-rise settings with constant lighting.
- Sustainability: Potential for decentralized, consistent, and low-carbon energy generation.
- Future focus: Mechanism studies, cost-effective integration, and synergies with smart lighting, automation, and storage.

Award Number:1953009
Project Title: Collaborative Research: Solar Energy Harvesting, Photothermal-Photovoltaic Dual Modality Building Skins towards Energy Neutral Civil Structures
PI: Donglu Shi, University of Cincinnati
Civil, Mechanical and Manufacturing Innovation (CMMI)
Program Officer: Gianluca Cusatis

Award Number:1635089
Project Title: The Photothermal Effects of Iron Oxide Nanoparticles on Energy Efficient Windows
Report Type: Annual Project Report
PI: Donglu Shi, University of Cincinnati
Civil, Mechanical and Manufacturing Innovation (CMMI)
Program Officer: Caglar Oskay

The Swiss National Science Foundation (Project No. IZSEZ0_223270) for the project titled “Photo-Thermal Coating for Energy Efficient Windows.”